CREWES

CONSORTIUM FOR RESEARCH IN ELASTIC WAVE EXPLORATION SEISMOLOGY

2014 Sponsors Meeting

Banff Park Lodge Resort Hotel and Conference Centre

December 3th - December 5th

Providing Advanced Seismic Imaging to the Geophysics Community for 26 years

UNIVERSITY OF CALGARY

CREWES

Research Report 2014
Volume 26

In this volume…

Report Summaries

On the memory stick…

Complete Reports

Student Theses

UNIVERSITY OF CALGARY

Notice of Intent to Publish

Please note that the authors of the research in this 26th Volume of the Abstract Book intend to publish or otherwise publically disseminate their full research papers in the coming calendar year. According to the contracts between the University of Calgary (CREWES) and each Sponsor, the University will make available to the Sponsor a copy of the proposed publication resulting from the CREWES Project prior to submission for publication. In the event that the Sponsor determines that Research Results within the proposed publication contain Sponsor Confidential Information, the Sponsor shall have thirty (30) days to notify the University in writing and the University shall remove Sponsor Confidential information prior to publication. This 30 day period shall be considered to have started at the end of this meeting (December 5, 2014). These full research reports are distributed on memory sticks at the CREWES annual meeting and are available on the CREWES website to all Sponsors and their employees.

CREWES Project faculty, staff and students, October 2014

Left to Right:
Front Row: Kris Innanen, Gary Margrave, Laura Baird, Kevin Hall, Peter Manning
Second Row: Bona Wu, Shahin Moradi, Winnie Ajiduah, Jessica Dongas, Penny Pan, Heather Hardeman, Tianci Cui, Roy Lindseth, Dave Henley, Michelle Montano, Helen Isaac, John Bancroft, Sergio Romahn, Wenyong Pan
Third Row: John Guo, Wenyuan Liao, Michael Lamoureux, Kevin Bertram, Rafael Asuaje, Jian Sun, Joe Wong, Raul Cova
Back Row: Tiansheng Chen, Khaled Al Dulaijan, Davood Nowroozi, Jesse Kolb, Shahpoor Moradi, Sina Esmaeili, Don Lawton, Larry Lines, Nassir Saeed, Marcelo Guarido de Andrade, Adrian Smith, Eric Rops, Scott Keating, Bobby Gunning, Junxiao Li, Adriana Gordon

CREWES in 2014

Welcome to our 26th annual Sponsors meeting. In a year of declining oil prices and crises around the globe, we hope that you will find our meeting to be a welcome technical retreat. We realize that many of you traveled great distances to be here and we are committed to making the meeting worth your while.

It has been an interesting, eventful and successful year for CREWES. Our NSERC CRD grant (NSERC is Canada's federal funding agency for science and engineering, and CRD stands for Collaborative Research and Development) which we received in 2009, and which represented 1/3 of our funding, expired in June. We have held such grants continuously since 1994 although it has always been a major effort to mount a successful application. We started the process of applying for a new grant in the summer of 2013 and submitted our proposal to NSERC in December just after last year's meeting. Our proposal set out a five year plan to develop a practical version of full waveform inversion (FWI) that emphasized land data. Furthermore we brought forward 11 Sponsor organizations with a Canadian presence and asked that their sponsor fees be matched. This initiated a 6 month process that included peer review and a site visit by a panel of respected, independent scientists. Many of you helped in this effort and we are very grateful. In June we were informed that our proposal was conditionally successful but with a condition that required an additional clause in our legal agreements with those matched sponsors. We have just now completed the signing of the 11 new CRD matching funds Agreements and so our new CRD grant funds should be released before the end of the year. We have included our 5-year research plan in this year's report and invite all of our sponsors to read and comment or otherwise become involved.

It's no secret that CREWES is facing a budget shortfall. This began about 18 months ago and continues. Last year we asked a significant number of our technical staff to drop back from full time to half time. Despite the hardship that this entailed, they all did so and are continuing to produce top quality research and to help our students. We are also looking for creative ways to stretch your sponsor dollars and one of these has been to partner with CMC Research Institutes, Inc. (CMC) on time-lapse seismology for sequestration monitoring. Our goal, and I believe we have achieved it this year, is to maintain our high standards of research output and graduate training as we adapt to new realities of life at the University of Calgary.

We welcomed 7 new students during the year and saw 5 thesis defenses (all M.Sc.'s). We now have 29 total students, divided about equally between M.Sc. and Ph.D. programs Many of these people will complete their studies soon and perhaps will become your co-workers.

We try to conduct a meaningful field experiment every year. We have just completed a major seismic survey at our test site near Priddis, Alberta. Last year we drilled two, 140m deep, observation boreholes on this site and instrumented one of these with a permanent 40-level 3C downhole array. In the recent survey we laid out a star pattern of 4 geophone lines centered on the instrumented borehole and shot into these with 140 dynamite shots and a similar number of Vibroseis source points using a special low-frequency vibrator provided courtesy of Inova. We intend for this data to be used in research associated with multicomponent data processing and inversion. We also participated in a 3C3D baseline seismic survey at a research field station being developed by CMC and the University of Calgary.

The CREWES vibrator at Priddis

We hope you enjoy our meeting and give us your feedback on the quality and effectiveness of our research. Please feel free to make suggestions or offer guidance as you see fit. If the opportunity arises, we always welcome the possibility of your direct involvement in our ongoing research.

Thank you all for your continued and generous support, and thank you for attending our annual meeting.

Calgary, Alberta
December, 2014

Gary Margrave
CREWES Director

Table of Contents

* Presenter

2014 CREWES Sponsors

Acceleware

BHP Billiton Petroleum (Americas) Inc.

CGG

Chevron Corporation

ConocoPhillips

Devon Energy Corporation

Exxon Mobil Corporation

Geokinetics Inc.

Halliburton

Husky Energy Inc.

INOVA Geophysical Equipment Ltd.

Nexen Inc.

Northwest Geology Institute, CNPC

Petrobras

Saudi Aramco

Sensor Geophysical Ltd.

Sinopec

Shell Canada Limited

Suncor Energy Inc.

Talisman Energy Inc.

Tullow Oil p.l.c.

Natural Sciences and Engineering Research Council of Canada (NSERC)
- Collaborative Research and Development Grant

CREWES Personnel

LEADERSHIP

Gary F. Margrave, Director
Professor, Department of Geoscience, University of Calgary

B.Sc. Physics, 1975, University of Utah
M.Sc. Physics, 1977, University of Utah
Ph.D. Geophysics, 1981, University of Alberta

- Work Experience: Chevron Canada Resources, Chevron Geoscience Company

Don C. Lawton, Associate Director
Professor, Department of Geoscience, University of Calgary

B.Sc. (Hons. Class I) Geology, 1973, University of Auckland
Ph.D. Geophysics, 1979, University of Auckland

- Work Experience: New Zealand Steel Mining Ltd., Amoco Minerals (N.Z.) Ltd., Carbon Management Canada

Kristopher A. Innanen, Associate Director
Associate Professor, Department of Geoscience, University of Calgary

B.Sc. Physics and Earth Science, 1996, York University
M.Sc. Physics, 1998, York University
Ph.D. Geophysics, 2003, University of British Columbia

- Work Experience: University of Houston

Laura A. Baird, Program Manager

BA, History, 1992, University of Calgary

- Work Experience: Alberta Cancer Board, Department of Geoscience at the University of Calgary

Kevin W. Hall, Technical Manager

B.Sc. Geophysics, 1992, University of Calgary
M.Sc. Geophysics, 1996, University of Calgary

- Work Experience: Lithoprobe Seismic Processing Facility at the University of Calgary

ADJUNCT DIRECTORS

Laurence R. Lines
Professor, Department of Geoscience, University of Calgary

B.Sc. Physics, 1971, University of Alberta
M.Sc. Geophysics, 1973, University of Alberta
Ph.D. Geophysics, 1976, University of B.C.

- Work Experience: Amoco Production Research, Tulsa University, Memorial University of Newfoundland

Robert R. Stewart
Cullen Chair in Exploration Geophysics, University of Houston
Adjunct Professor, Department of Geoscience, University of Calgary

B.Sc. Physics and Mathematics, 1978, University of Toronto
Ph.D. Geophysics, 1983, Massachusetts Institute of Technology

- Work Experience: Arco Exploration and Production Research Centre, Chevron Geoscience Company, Veritas Software Ltd., Gennix Technology Corp., University of Calgary.

ASSOCIATED FACULTY AND SCIENTISTS

John C. Bancroft
Senior Researcher, CREWES, University of Calgary
Instructor, Department of Geoscience, University of Calgary

B.Sc. Electrical Engineering, 1970, University of Calgary
M.Sc. Electrical Engineering, 1972, University of Calgary
Ph.D. Electrical Engineering, 1975, Brigham Young University

- Work Experience: Geo-X, Veritas Software Ltd., Ulterra Geoscience Ltd.

Michael P. Lamoureux
Professor and Department Head, Department of Mathematics and Statistics, University of Calgary
Adjunct Professor, Department of Geoscience, University of Calgary

B.Sc. Mathematics, 1982, University of Alberta
M.Sc. Mathematics, 1983, Stanford University
Ph.D. Mathematics, 1988, University of California, Berkeley

- Work Experience: Farallon Computing, NSERC Canada

Andreas Cordsen
Technical Advisor, CREWES, University of Calgary

M.Sc. Geology, 1975, Queen’s University, Kingston
M.Sc. Geophysics, 1980, Dalhousie University, Halifax

- Work Experience: BEB, Esso Resources, Norcen Energy, GEDCO, Schlumberger

Michael P. Lamoureux
Professor and Department Head, Department of Mathematics and Statistics, University of Calgary
Adjunct Professor, Department of Geoscience, University of Calgary

B.Sc. Mathematics, 1982, University of Alberta
M.Sc. Mathematics, 1983, Stanford University
Ph.D. Mathematics, 1988, University of California, Berkeley

- Work Experience: Farallon Computing, NSERC Canada

Roy O. Lindseth MC., FRSC
Technical Advisor, CREWES, University of Calgary

Doctor of Laws, Honoris Causa, 1978, University of Calgary

- Work Experience: Chevron; NSERC, Teknica Corporation; TCPL

Brian H. Russell
Adjunct Professor, Department of Geoscience, University of Calgary

B.Sc. Physics, 1972, University of Saskatchewan
Honours Certificate in Geophysics, 1975, University of Saskatchewan
M.Sc., Geophysics, 1978, University of Durham
Ph.D., Geophysics, 2004, University of Calgary

- Work Experience: Chevron Geoscience Company, Teknica Resource Development, Veritas Software Ltd., Hampson-Russell Software Ltd.

Matt Yedlin
Associate Professor, Department of Electrical and Computer Engineering, University of British Columbia

B.Sc. Honors Physics, 1971, University of Alberta
M.Sc. Physiology, 1973, University of Toronto
Ph.D. Geophysics, 1978, University of British Columbia

- Work Experience: Conoco

RESEARCH STAFF AND VISITING SCHOLARS

Kevin L. Bertram

Electronics Technician Certificate, 2005, Southern Alberta Institute of Technology

- Work Experience: Aram Systems Ltd.

Malcolm B. Bertram

B.Sc. Geology, Auckland, New Zealand

- Work Experience: GSI (Western Australia), Western Geophysics (Western Australia), Auckland University, University of Calgary.

Tiansheng Chen

B.Sc., Applied Geophysics,2001,Daqing Petroleum Institute,China
M.Sc., Geophysics,2003,China University of Petroleum
Ph.D., Geophysics,2006,China University of Petroleum

- Work Experience: Petroleum Exploration and Production Research Institute,SINOPEC,China

Patrick F. Daley

B.Sc. Mathematics, 1974, University of Alberta
M.Sc. Physics 1976, University of Alberta
Ph.D. Geophysics, 1979, University of Alberta

- Work Experience: Independent contractor associated with research centres of major oil companies

Eric V. Gallant

Journeyman Interprovincial Ticket in Electrical Construction, 1976, Cape Breton Institute of Technology

- Work Experience: IBEW, University of Calgary, MIC at the University of Calgary

David C. Henley

B.Sc. Physics, 1967, Colorado State University
M.Sc. Physics, 1968, University of Michigan

- Work Experience: Shell Oil Co., Shell Canada Ltd

Helen Isaac
B.Sc. Mathematics, 1973, Imperial College, London
M.Sc. Geophysics, 1974, Imperial College, London
Ph.D. Geophysics, 1996, University of Calgary
- Work Experience: Phillips Petroleum Company, Hudson's Bay Oil and Gas, Canterra Energy, Husky, Fold-Fault Research Project at the University of Calgary

Peter M. Manning
B.Sc. Mathematics, 1961, University of British Columbia
Ph.D. Geophysics, 2007, University of Calgary
- Work Experience: Mobil Oil Canada

Joe Wong
B.Sc. Physics/Mathematics, 1971, Queen’s University
M.Sc. Applied Geophysics, 1973, University of Toronto
Ph.D. Applied Geophysics, 1979, University of Toronto
- Work Experience: Ontario Ministry of the Environment, University of Toronto, JODEX Applied Geoscience Limited

GRADUATE STUDENTS

Winnie Ajiduah
B.Sc. Physics, University of Benin, Nigeria
M.Sc. Geophysics, University of Port Harcourt, Nigeria
- Work Experience: Shell Petroleum Development Company of Nigeria

Khaled Al Dulaijan
B.Sc. Geosciences, 2003, University of Tulsa, Oklahoma
M.Sc. Geophysics, 2008, University of Calgary
- Work Experience: Saudi Aramco

Babatunde Arenrin
B.Sc. Geophysics, 2005, University of Lagos, Nigeria.
M.Sc. Petroleum Geophysics, 2010, Imperial College London, UK.
- Work Experience: WesternGeco Norway.

Rafael Asuaje
B.Sc. Mechanical Engineering 2005, Kettering University, USA
M.Sc. Mechanical Engineering 2006, Kettering University, USA
- Work Experience: Faurecia Interior Systems.

Raúl Cova
B.Sc. Geophysical Engineering, 2004. Simon Bolivar University, Venezuela.
Graduate Diploma in Petroleum Studies, 2011. IFP School. Venezuela
- Work experience: PDVSA Intevep. Venezuela

Jean Cui
B.Sc. Geophysics, 1998, Petroleum University
M.Sc. Geophysics, 2005, China University of Mining & Technology
- Work experience: Nexen Inc.

Tianci Cui
B.Sc. Geophysics, 2013, China University of Petroleum (Beijing)

Jessica Dongas
B.Sc. Hons. Geological Sciences, 2013, Queen's University
- Work experience: Schlumberger – Carbon Services, Calgary

Sina Esmaeili
B.Sc.: Physics, 2009, Science and Research University - Iran
M.Sc.: Field Theory and Particle Physics, 2011, Science and Research University, Iran

Marcelo Guarido de Andrade
B.Sc. Physics, 2006, University of São Paulo, Brazil
M.Sc. Geophysics, 2008, University of São Paulo, Brazil
- Work Experience:Schlumberger-WesternGeco (Houston) and Georadar Leventamentos Geofísicos S.A. (Brazil)

Bobby Gunning
B.Sc. Geophysics (first class honours), 2014, University of Calgary
- Work Experience: MEG Energy, Devon Energy

Shahin Jabbari
B.Sc. Mathematics applied in Physics, 1992, University of Tehran, Iran
M.Sc. Medical Physics, 1997, Tabriz University of Medical Sciences, Iran
M.Sc. Medical Physics, 2010, University of Calgary
- Work Experience: Encana Corporation

Scott Keating
B.Sc. Honours Physics 2014, University of Alberta

Hassan Khaniani
B.Sc. Petroleum Exploration Engineering, 2003, Petroleum University of Technology
M.Sc. Petroleum Exploration Engineering, 2006, University of Calgary & Petroleum University of Technology
- Work Experience: Terras Persia Seismic Company (TPS), Nexen Inc.

Jesse Kolb
B.Sc. Physics, Minor in Geophysics, 2013, University of Maryland, USA
- Work Experience: Qeye Labs

Junxiao Li
B.Sc. Science of information and Computing (Geophysics), 2009, China University of Petroleum (Beijing)
Bachelor of Arts. English, 2009, China University of Petroleum (Beijing)
M.Sc. Geophysics, 2012, China University of Petroleum (Beijing)

Oliver Lahr
B.Sc. Pure and Applied Mathematics, 1988, University of Calgary
- Work Experience: Hampson-Russell Software Ltd.

Michelle Montano

B.Sc. Geophysics 2008, Simon Bolivar University, Venezuela

- Work experience: PDVSA Sismica Bielovenezolana, Daqing de Venezuela

Shahin Moradi

B.Sc. Applied Physics, 2006, University of Razi, Iran
M.Sc. Geophysics, 2010, University of Tehran, Iran

Shahpoor Moradi

B.Sc. Applied Physics, 2000, University of Razi, Iran
M.Sc. Theoretical Physics, 2002, University of Razi, Iran
Ph.D. Theoretical Physics, 2006, University of Razi, Iran

Davood Nowroozi

B.Sc. Mining engineering, University of Tehran, 1996
M.Sc. Mining engineering, University of Tehran, 1999

- Work Experience: Geophysicist at National Iranian Oil Company

Pan (Penny) Pan

B.Sc. Geophysics, 2012, Xi'an Shiyou University, China

Wenyong Pan

B.Sc. Computer and Software Engineering, 2009, China University of Geosciences (Beijing)
M.Sc. Geophysics, 2012, China University of Geosciences (Beijing)

Chris Petten

BSc. Physics, 2011, University of Calgary
BSc. Geophysics, 2011, University of Calgary

- Work Experience: University of Calgary Research Assistant - Stable Isotopes

Sergio Jorge Romahn Reynoso

B. Eng. Geophysics, 2004, National University of Mexico
M.Sc. Exploration Geophysics, 2012, University of Leeds. U.K.

- Work Experience: PEMEX

Eric Rops

B.Sc. Honors Geophysics, 2014, The University of Western Ontario (London Ontario)

- Work experience: Husky Energy, Sander Geophysics Ltd.

A. Nassir Saeed

B.Sc. Geology, 1991, University of Salahaddin, Iraq
M.Sc. Geophysics, 1997, University of Science, Malaysia
M.Sc. Geophysics, 2013, University of Calgary

- Work Experience: IKON Science Canada

Adrian Smith

B.Sc. Honours Geophysics 2012, University of Western Ontario

- Work Experience: Husky Energy Inc.

Jian Sun

B.Sc. Geophysics, 2009, Shandong University of Science and Technology, China
M.Sc. Geophysics, 2012, Shandong University of Science and Technology, China

Bona Wu

B.Sc., Applied Geophysics, 1999, Jianghai Petroleum Institute, China
M.Sc., Geophysics, 2006 China University of Petroleum

- Work Experience: CGGVeritas

Student Theses

The following theses are included with the CREWES 2014 Research Report:

M.Sc.	Mohammed Alarfaj	Kinematic forward modeling and interpretation of faults in 3D seismic reflection data
M.Sc.	Patricia Esperanza Gavotti	Model-based inversion of broadband seismic data
M.Sc.	Steven M. Kim	Exact, linear and nonlinear AVO modeling in poroelastic media
M.Sc.	Li Lu	Seismic Depth Imaging in Anisotropic Media East Coast of Canada Case Study
M.Sc.	Abdul-Nassir Saeed	Time-lapse AVO inversion

A modeling and migration study of fault shadows: A synthetic example

Sitamai W. Ajiduah* and Gary F. Margrave

ABSTRACT

Seismic distortions similar to salt steeps are observed in imaging of footwall reflectors. This distortion sometimes referred to as fault shadows is studied from a 2D seismic modeling and migration perspective. This study investigates shadow zones in a 2D fault model using 2D finite difference forward modeling solution and studies the capability of PSPI in imaging distorted footwall reflections. We also carried out iterated migration of the fault constrained velocity models and observed that time migration and post-stack depth migrations poorly image the reflector footwalls. The time anomalies and distorted reflection in figure 1 are a result of the truncation of the overlying stratigraphy by the fault throw causing velocity contrasts across the fault. This is caused by ray bending as it travels through the fault, it experiences traveltime distortion. The poor images in poststack time and depth migrations implies that migration with an incorrect velocities is one primary reason for fault shadows. Another limitation of time migrating faults is because the image ray bending characteristic of time migrations causes incorrect alignment of images in time. Another factor that may cause poor imaging in the poststack migration is the effect of dip dependence of normal moveout. NMO and stacking of events along hyperbolas without prior dip moveout correction of dipping data will cause apparent disruptions and smeared reflections. A better imaging solution which produced improved and continuous footwall reflection without seismic pull up artifacts is the prestack depth migration. To summarize, fault shadow is a velocity and wave propagation problem, and valid depth imaging in real cases scenario is only possible with a velocity model accurate to within a few percent.

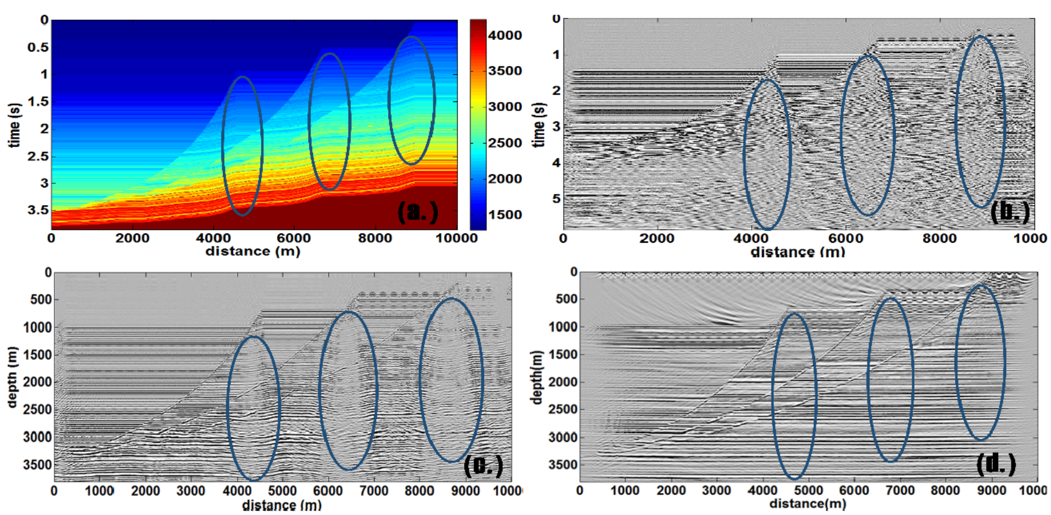

FIG.1. Fault shadow velocity anomalies (a) highlighted with blue circles as time pull up and sag. As distorted reflections in poststack time migration (b) and depth migration (c) and correctly imaged by prestack depth migration.

Azimuthal anisotropy investigations for P and S waves: a physical modelling experiment

Khaled Al Dulaijan*, Gary F. Margrave and Joe Wong

ABSTRACT

Information related to fracture orientation and intensity is vital for the development of unconventional hydrocarbons, such as tight sand gas and shale gas. Numerical modeling provides a valuable tool for geophysicists to test and validate their methodologies that provide them with information about reservoirs. Fractures make numerical modeling more complicated and introduce complexities that might even require geophysicists to validate their numerical models before using them to assess their methods. Alternatively, physical modeling provides a unique opportunity to test, validate, and develop methods for characterizing fractured reservoirs. This report utilizes seismic physical modeling for fracture characterization.

A two-layer model was built using vertically laminated Phenolic overlain by Plexiglas to represent a fractured reservoir overlaid by an isotropic overburden. The first dataset was acquired over that 2-layer model and consist of three 9-component common-receivers. P-wave first-arrival times were analyzed on all three gathers and fracture orientation was predicted. An Alford rotation was applied to the four horizontal components and successfully minimized energy on components other than those two that are related to the fast S wave and slow S wave. However, the angle between natural and acquisition coordinate systems was not predicted correctly. One possible reason could be the contact between the two media. Therefore, another dataset was acquired using a single Phenolic layer. Alford rotation was applied and the angle between natural and acquisition coordinate system was predicted correctly. That dataset was used too to measure the stiffness coefficients tensor using group velocity data.

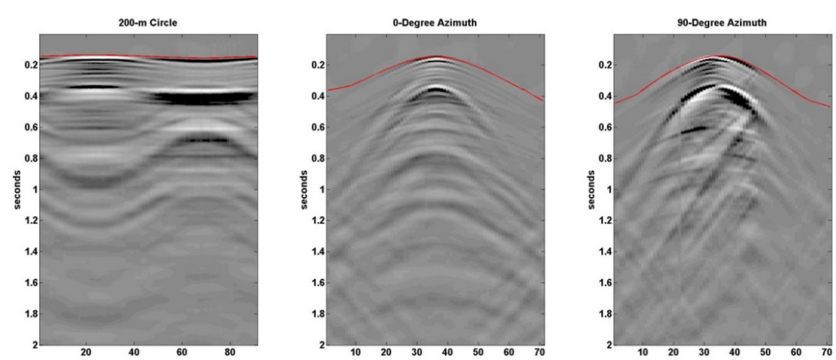

A circular gather (left) that has 200 m radius; and two linear with 0^o (middle) and 90^o (right) azimuths. First P-wave arrivaltimes are indicated by red.

V_{11}	V_{22}	V_{33}	V_{23}	V_{13}	V_{12}
3644.1	2955.1	3333.7	1451.6	1562.5	1785.7

Body wave velocities (V_{ij}) that propagates along x_i-axis and polarized along x_j-axis in (m/s).

Seismic analysis for fractured reservoirs of South Komie 3D data

Khaled Al Dulaijan and Gary F. Margrave

ABSTRACT

The South Komie 3D seismic data was acquired within the Horn River basin of northeast British Columbia. The Horn River basin has two main targets of shale gas: the Muskwa and Evie formations. Even though being an unconventional reservoir, standard seismic techniques are quite useful for such reservoirs. South Komie 3D seismic data is analyzed to identify gas sweet spots. Because the reservoirs consist of shale. Fractures are important because they can act as fluid conduits. There, the data is analyzed to identify fractures as well.

In this study, a strong channel system is observed within the near surface. The post-stack P-impedance inversion can help indicating sweet spots within Evie and Muskawa reservoirs. Also, post-stack amplitude, instantaneous frequency, and curvature attributes are useful for identifying fracture direction and intensity. Results of amplitude and instantaneous frequency correlate very well with in Evie reservoir. AVO analysis was found to help identifying top and base of Evie gas away from the well.

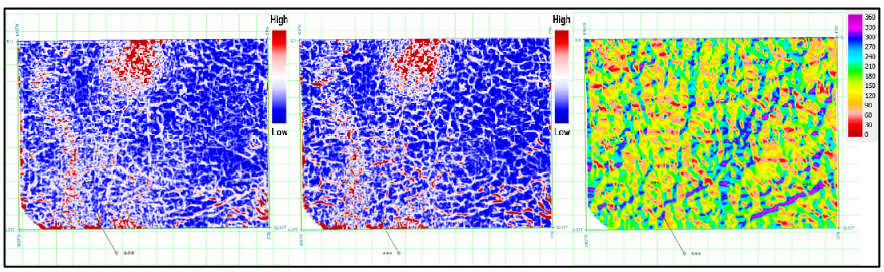

Curvature attributes of Evie reservoir: Minimum curvature (left), Maximum Curvature (Middle), Azimuth (right). High curvature values indicate fractured zones. Azimuth map indicates that the major trends are about 0^{o} and 40^{o}.

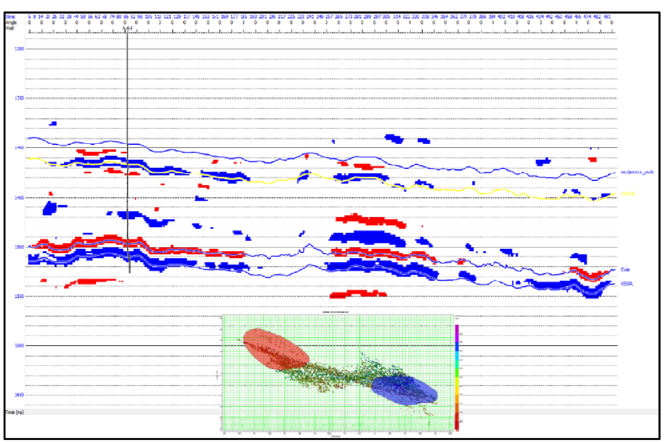

AVO cross section. Negative intercept and positive gradient is indicated by red. It represents top of class IV reservoir. Blue repents the bottom of the reservoir.

FWI with source illumination: A synthetic case study

Babatunde Arenrin*, Gary Margrave and John Bancroft

ABSTRACT

We study incorporating well log information into Full Waveform Inversion (FWI) and compare the result with a line search optimization scheme. We test this approach using a poor starting model i.e. a linear velocity v(z) model and also using smoothed version of the true velocity model. Our results show that incorporating well information into FWI saves a lot of computational time compared with a line search optimization scheme. Although the inverted model is far from convergence, we learn a few interesting things: conventional FWI cannot by itself provide good estimate for layer properties when the starting model is poor such as the case of a linear v(z) model, the information from well logs can be used to constrain the line search calculation and still save computational time, finally low frequencies are crucial for convergence.

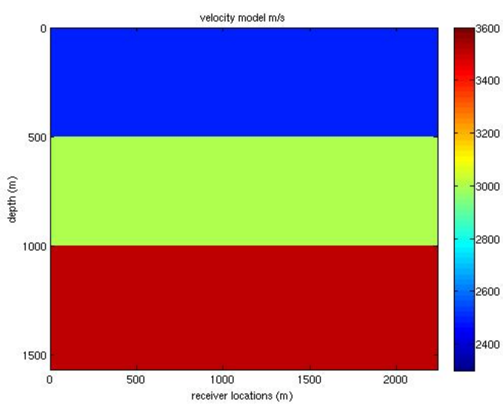

FIG 1. True velocity model.

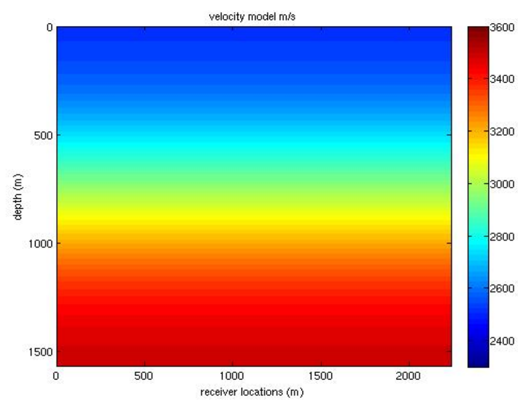

FIG 2. Initial velocity model

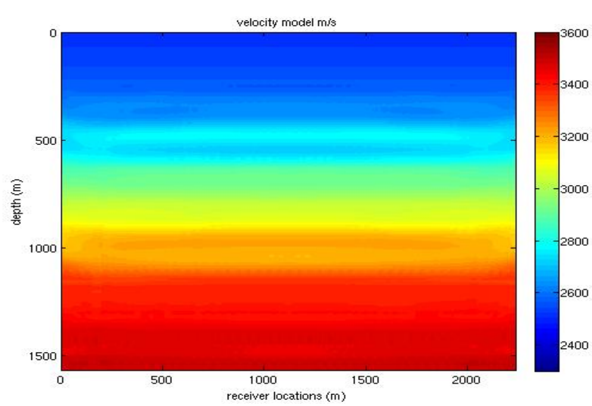

FIG 3. Inverted velocity model after 50 iterations

A turning-ray algorithm using Slotnick's equation

Babatunde Arenrin, Gary Margrave and John Bancroft

ABSTRACT

Turning-ray tomography is a good tool for estimating near surface velocity structure, especially in areas where conventional refraction statics fail such as in the case of a hidden layer. In a previous paper (Arenrin et al, 2014), we already demonstrated this by applying a tomostatics solution to Hussar 2D seismic line using Landmark's PROMAX software. In this paper we have developed a turning-ray tracing algorithm that uses Slotnick's equation. The algorithm traces turning-rays through a linear velocity v(z) medium, and has the option of specifying the top layer velocity, takeoff angles, and the subsurface velocity gradient. However not in its final product, the turning-ray traveltimes from the algorithm are in agreement with the traveltimes generated using an acoustic finite difference scheme.

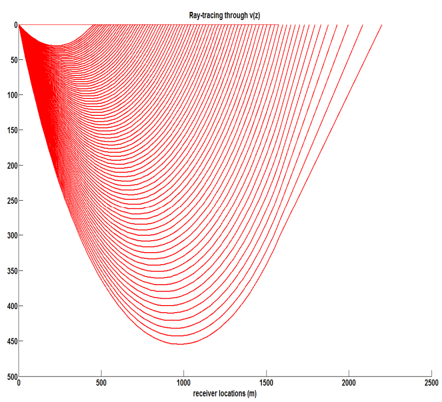

FIG 1. Modelled turning-rays.

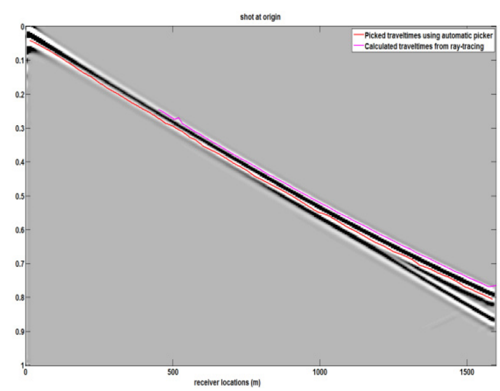

FIG 2. Picked traveltimes from finite difference modelling (red) and traveltimes calculated from turning-rays tracing (magenta).

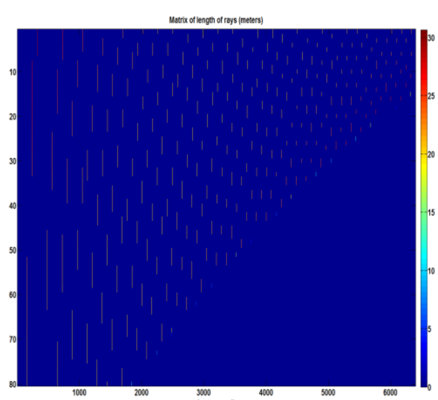

FIG 3. Matrix of length of raypaths.

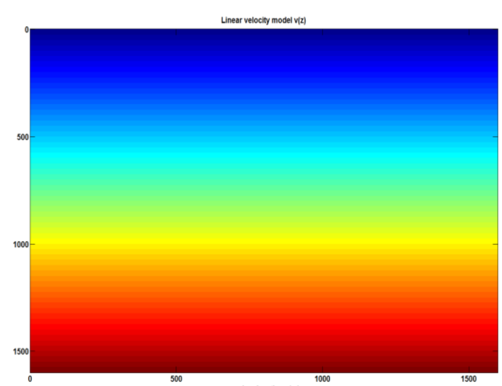

FIG 4. Linear velocity v(z) model used for shot record.

Sensitivity of interval Vp/Vs analysis of seismic data

Rafael Asuaje* and Don C. Lawton

ABSTRACT

The ratio of a compressional P wave to a shear S wave is of great importance for converted PS wave applications. Dipole sonic logs can provide accurate velocity ratio calculations but are restricted to the location of the corresponding well. Isochrons from interpreted horizons on seismic data can provide information on Vp/Vs throughout the volume that can be used for lithology and fluids studies about a particular formation. Proper interpretations of these events are necessary to avoid erroneous results. The objective of this paper is to set guidelines for an interpreter to accurately pick events and understand the error that can be expected from various isochron intervals to ultimately suggest a minimum interval time that can provide accurate Vp/Vs values.

In a study on the Hussar data set, based on the increasing observable error with respect to decrease in the time intervals, as well as taking into consideration the variability of the Vp/Vs values due to uncertainty it is suggested to use isochron intervals greater than 150ms. Interval Vp/Vs analysis for data with intervals greater than this time presented low uncertainty.

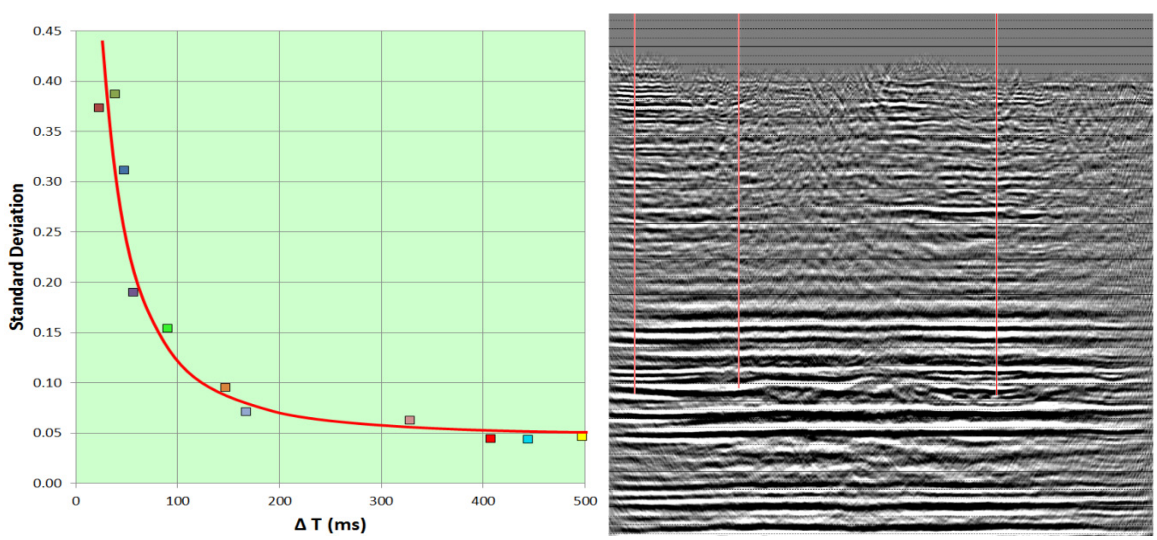

(a) (b)

FIG: Crossplot of (a) the standard deviation against delta T and (b) the PP seismic section of the Hussar data.

Comments on the imaging condition

John C. Bancroft

ABSTRACT

The processing of seismic data often uses an imaging condition where an upward propagating waveform is correlated with a downgoing waveform to estimate reflectivity. The cross correlation includes multiple energy that produces low frequency noise that contaminates a migrated imaging. This noise can be removed by a low cut filter that is counter to the requirement of low frequencies that are required for full waveform inversion. I demonstrate a simplified process that eliminates the low frequency noise.

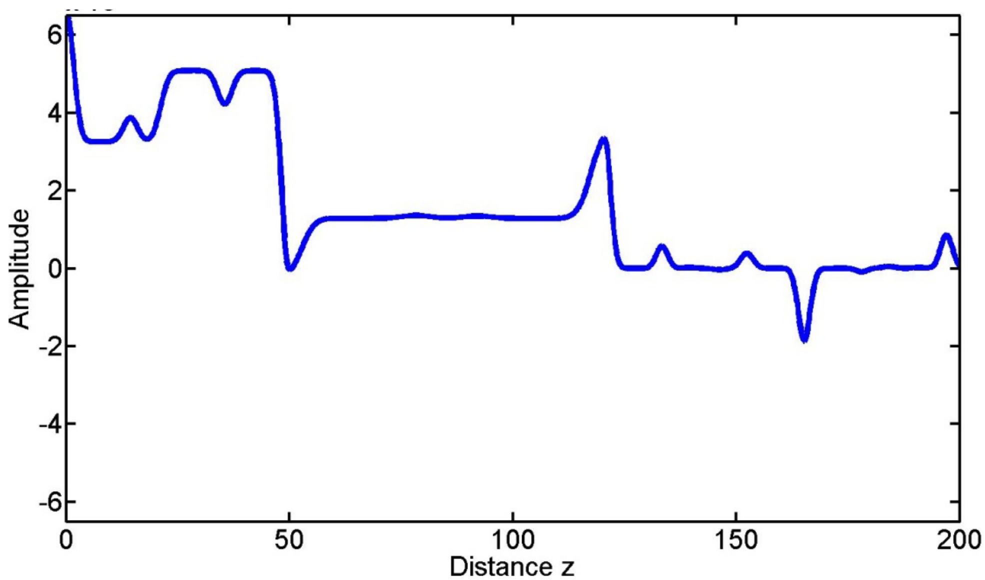

FIG. 1: Cross-correlation of the forward model using reverse time processing.

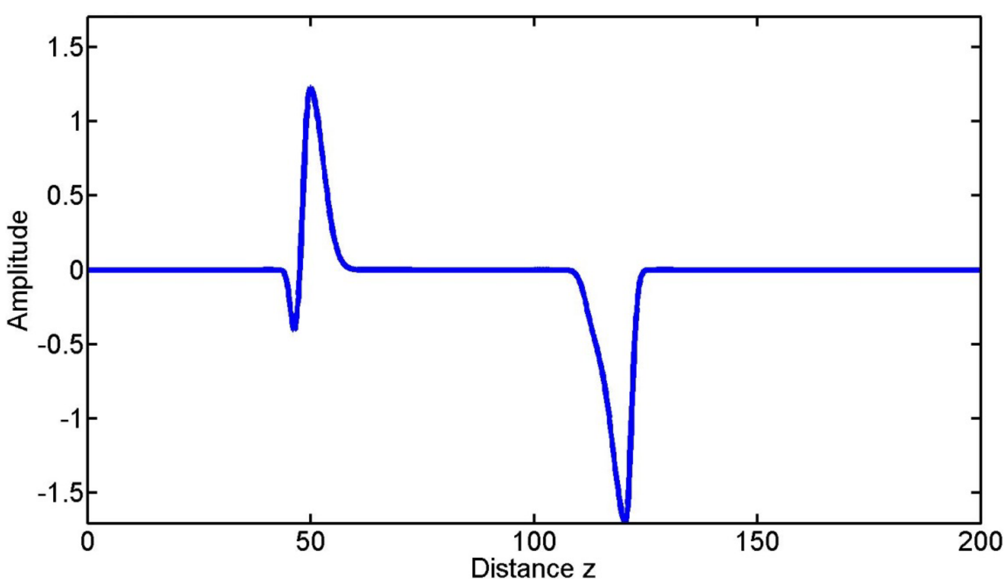

FIG. 2: Cross-correlation of the windowed forward model with the primaries.

Evaluation of one-hundred shots repeated at the same location

John C. Bancroft, Helen Isaac and Dave Henley

ABSTRACT

One-hundred shots were recorded at the same location to evaluate the repeatability of the shots, the relative amplitude of the shots, and the time repeatability of each shot. The data were recorded at the Priddis test site in Alberta. In addition to the repeatability measurements, the evaluation of random noise was also considered.

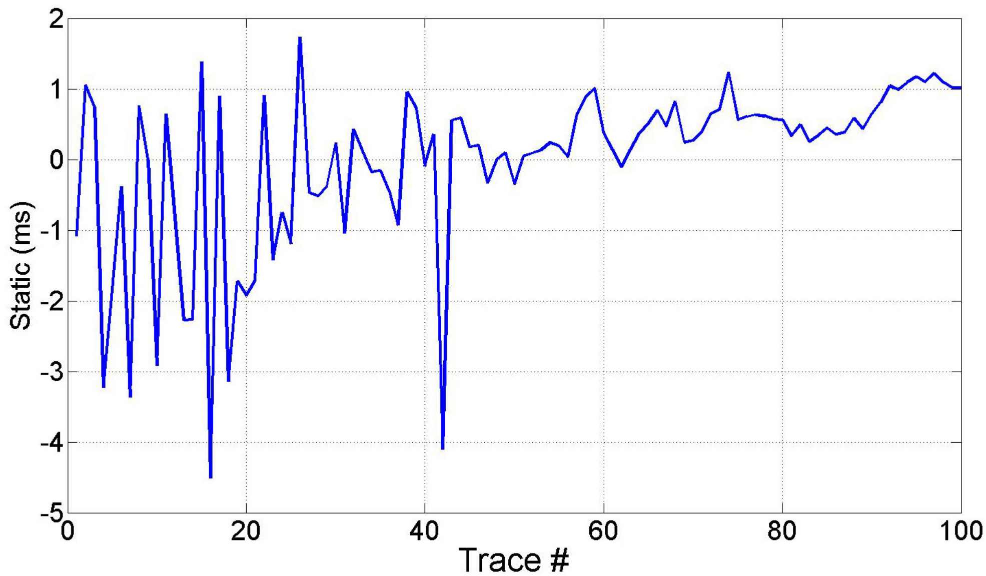

FIG. 1: Estimated static for each shot.

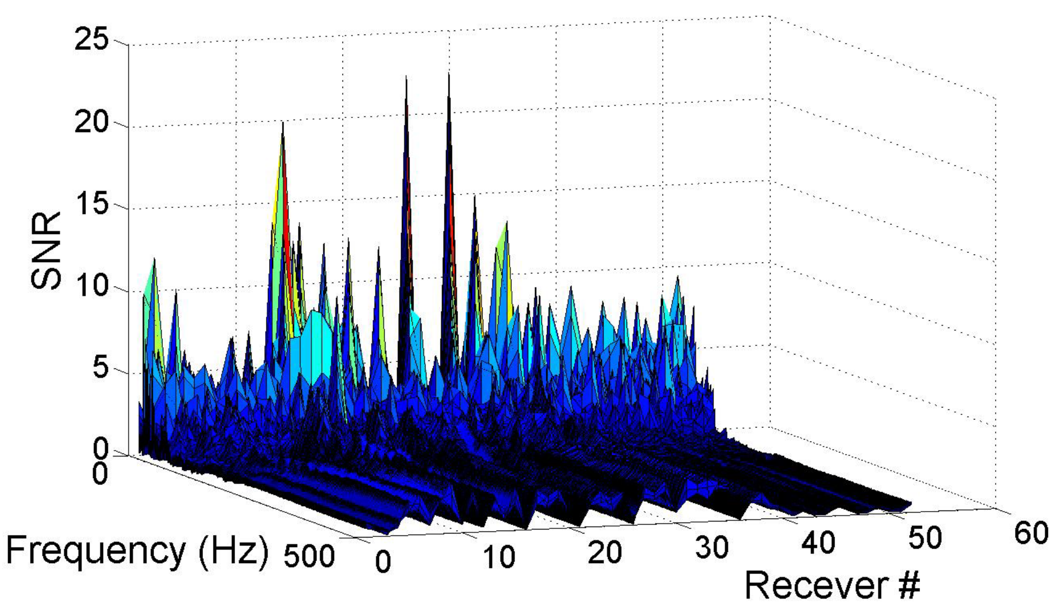

FIG. 2: SNR of the amplitude spectrum for one shot.

Modelling with finite difference approximations to the wave-equation

John C. Bancroft

ABSTRACT

Analyzing waves on a string is informative relative to the properties of various solutions to the wave-equation, and to the parameters used in finite difference approximations to those solutions. In addition, insight may be gained to various problems such as estimating the reflection coefficients from the cross-correlation imaging conditions.

Solutions are compared for a constant and variable velocity solution to the wave equations. The cross correlation imaging condition for various methods of wave-propagation is also evaluated.

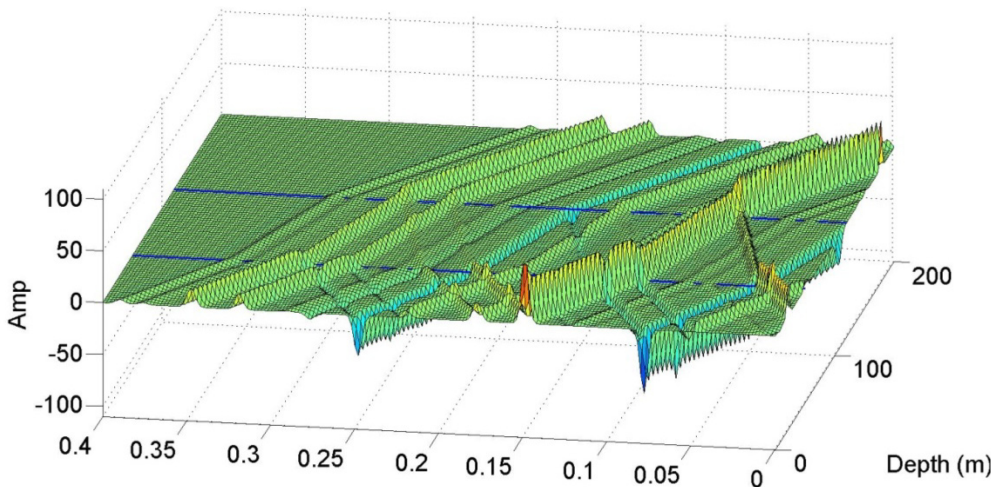

FIG. 1: Wavefield reconstruction using reverse-time.

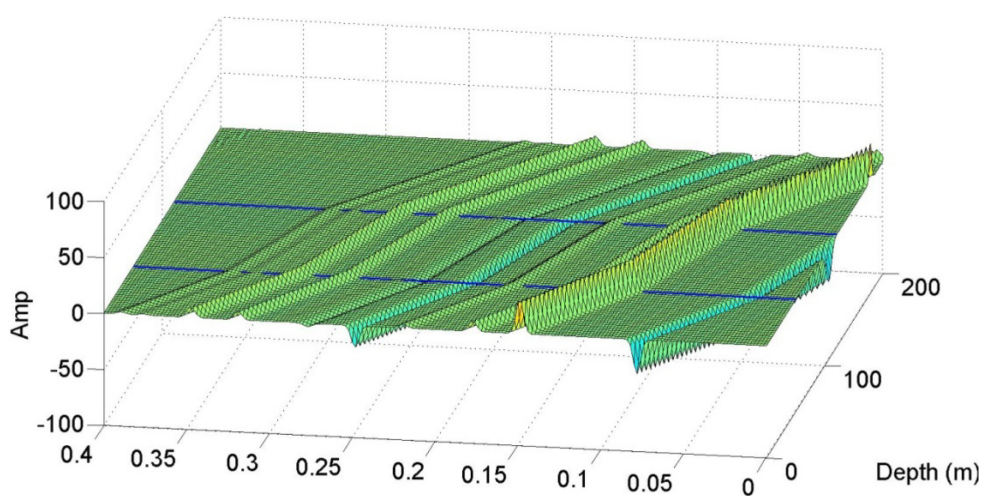

FIG. 2: Wavefield reconstruction using phase-shift.

Processing seismic data for high spatial resolution

John C. Bancroft*, Helen Isaac and Nassir Saeed

ABSTRACT

High spatial resolution has been observed on the Hussar data that shows apparent faulting. We propose that this high resolution results from processing the data with common scatterpoint gathers that allow high resolution velocity analysis, combined with velocity modifications that allow the focusing of reflections that come from reflectors that are oblique to the 2D line. To date, we have not been able to replicate this spatial resolution with conventional methods.

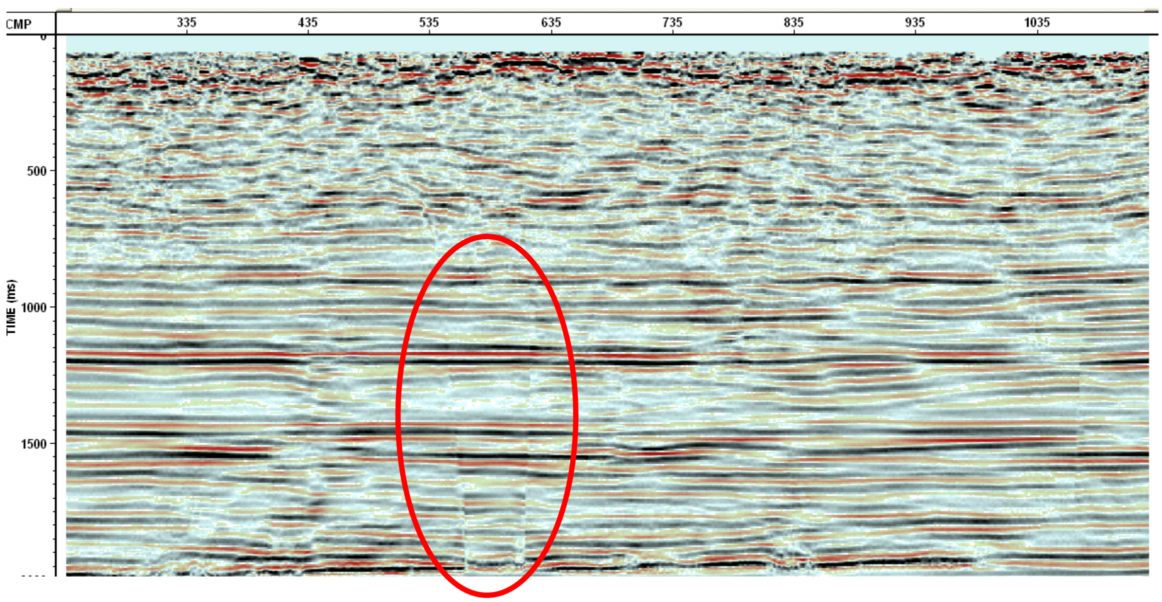

FIG. 3 Hussar data using **160%** of the picked velocities. Apparent faulting is observed in a number of areas, especially below 1500 ms within the ellipse.

The sensitivity of velocities with elevation change

John C. Bancroft

ABSTRACT

Elevation and near surface structure distort a time section. These distortions are modified by estimating the corresponding travel time (statics) that are applied to the time section. If these corrections are small enough, they have a negligible effect on the final processed image. If the static corrections are too large, the assumptions for velocity analysis and migration are violated and incorrect velocities may be estimated. These estimated velocities may not represent the structure of the subsurface. If the statics are "reasonable" then the estimated velocities may allow accurate imaging.

The effect of elevation change on RMS velocities is evaluated with the intent of understanding the velocity structure obtained when processing common scatter point (CSP) gathers on a 2D line from the Hussar data set.

Displays show the effect of the elevation change and the total static change on the velocity.

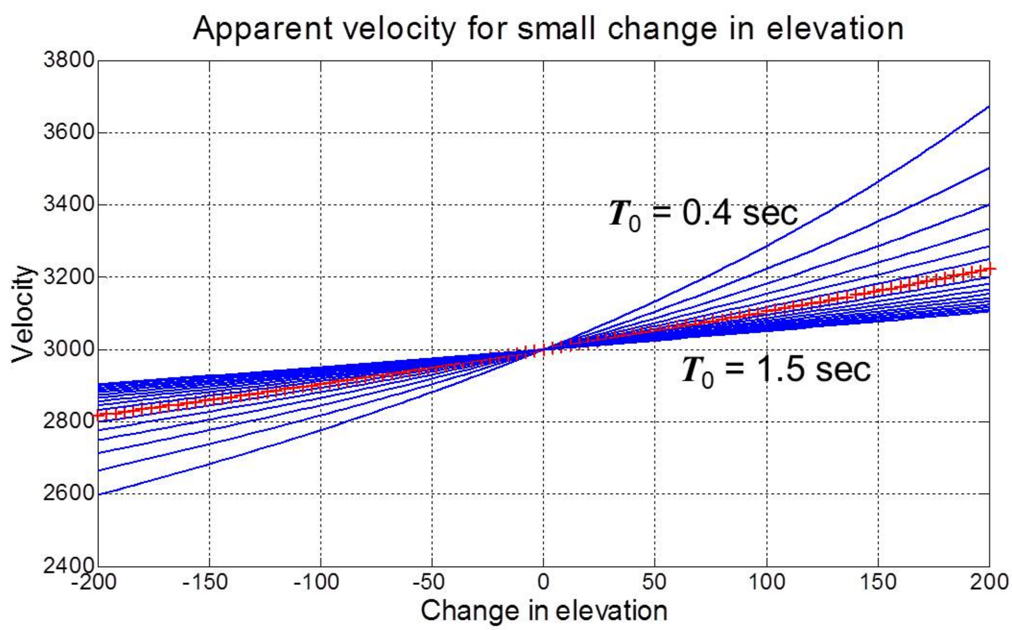

FIG. 1: New velocities plotted as a function of change in elevation. Each curve represent the time T_0 on a time section. The red curve was plotted at T_0 = 1.0 sec.

Out of the office, a brief overview of CREWES field acquisition

Kevin L. Bertram, Malcolm B. Bertram, Kevin W. Hall, Eric V. Gallant, Don C. Lawton, Gary F. Margrave and Kristopher A.H. Innanen

ABSTRACT

CREWES is proud to have access to an ever expanding collection of commercial grade seismic and survey equipment. Most CREWES staff are eager to take acquisition ideas out of the office and test them in the field. It is very beneficial for students to witness how the equipment is used to acquire data and some of the challenges that exist with acquisition. In 2014 CREWES has completed the following acquisition projects: a) a video inspection of the original observation well at the Rothney Astrophysical Observatory near Priddis, Alberta; b) an introduction of the seismic recording system and source to the new students of CREWES; c) a 3C 3D survey at a CO_2 injection test site near Brooks, Alberta; d) the 2014 GOPH549 undergraduate Field School project at the Castle Mountain Ski Resort in Alberta; e) a broadband 3C survey with VSP and a geophone coupling experiment at the Rothney Astrophysical Observatory site.

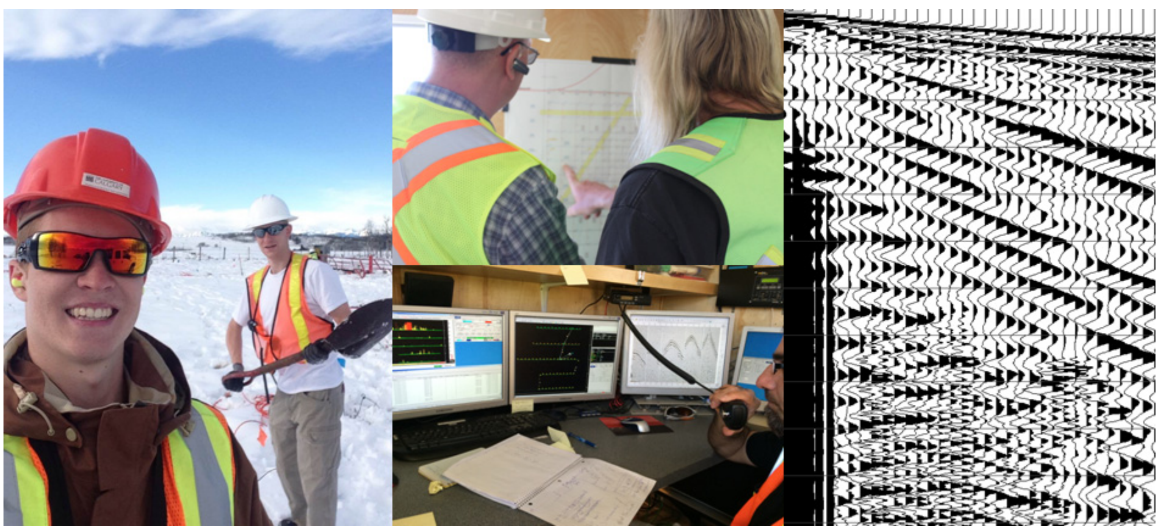

FIG. 1. Students and staff in the field collecting data.

Installation of a vertical pressure cell at the Priddis Geophysical Observatory

Malcolm B. Bertram, Kevin W. Hall and Don C. Lawton

ABSTRACT

Carbon Management Canada and CREWES are in the process of installing a vertical pressure cell in Testhole 4 at the Priddis Geophysical Observatory for the purpose of testing a prototype optical sensor from the University of Victoria that is sensitive to CO_2 concentration. Testhole 4 was drilled in 2007 and cased to a depth of 127 m with PVC casing grouted with bentonite. More recently seismic data quality obtained in the well has appeared to deteriorate in quality, possibly due to bentonite being washed away by ground water. This made it a good candidate for the installation of a vertical pressure cell. Thus far, steel coil tubing with a cap welded onto the bottom has been inserted into the well, and a bell nipple with threads for a flange has been welded onto the top of the coil tubing (Figure 1). The coil tubing will be sealed at the top with access ports for CO_2 and test instrument tubing, allowing the pressure to be taken up to 35 MPa, thereby simulating various reservoir depths. By releasing CO_2 bubbles into the bottom of the coil tubing, the new sensors can be tested and calibrated. The facility continues to be developed.

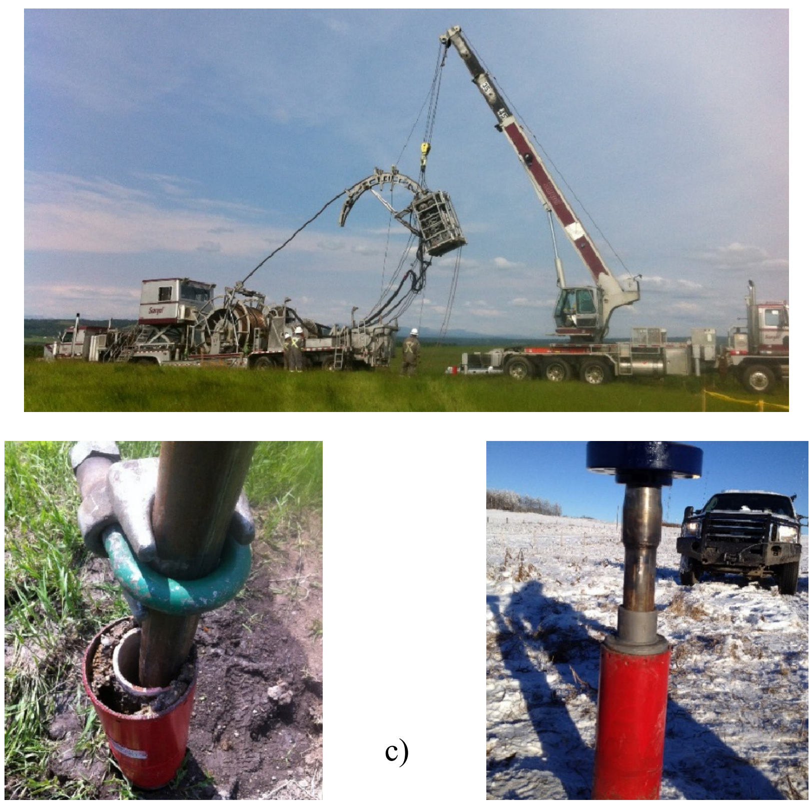

a)

b)

c)

FIG. 1. Installation of coil tubing (a), coil tubing inside PVC casing of Testhole 4 (b), and Testhole 4 finished with centralizer, bell nipple and flange (c).

Addressing non-stationary shear wave statics in the rayparameter domain

Raul Cova, David Henley and Kris Innanen

ABSTRACT

When velocity contrasts at the base of the near-surface layer are small, or when it shows some degree of structural complexity, delay times of wavefronts transmitted through this layer may become raypath dependent. Due to the low velocity of S-waves this dependency is translated into significant non-stationary delays. In order to remove this effect we transform the data to a domain in which amplitudes are a function of the raypath angle. Processing the statics in the radial trace (RT), Snell trace (ST) and *τ-p* domain achieve this goal, but with different degrees of accuracy. Since the first two domains involve only a very simple remapping of the amplitude from the original x-t domain they are free of the numerical problems experienced with the *τ-p* transform. However, the RT and ST transformations require that some assumptions about the subsurface velocity model must be made. On the other hand, the *τ-p* transform automatically scans the data in order to capture the rayparameter values that were actually recorded. The surface correction of synthetic data in a depth-varying velocity medium showed that the solutions obtained in the ST and *τ-p* domain are very similar, while common offset and RT solutions still show some unresolved problems. Further analysis was performed using real data from the Hussar experiment. Results showed that the *τ-p* solution provided a better stacking power in the deeper part of the section. In the shallow part the RT and ST solution seem to have better resolution. Further work is needed to reduce the artifacts present in the *τ-p* transformation. Trying a high resolution *τ-p* transform will be the next step in this research.

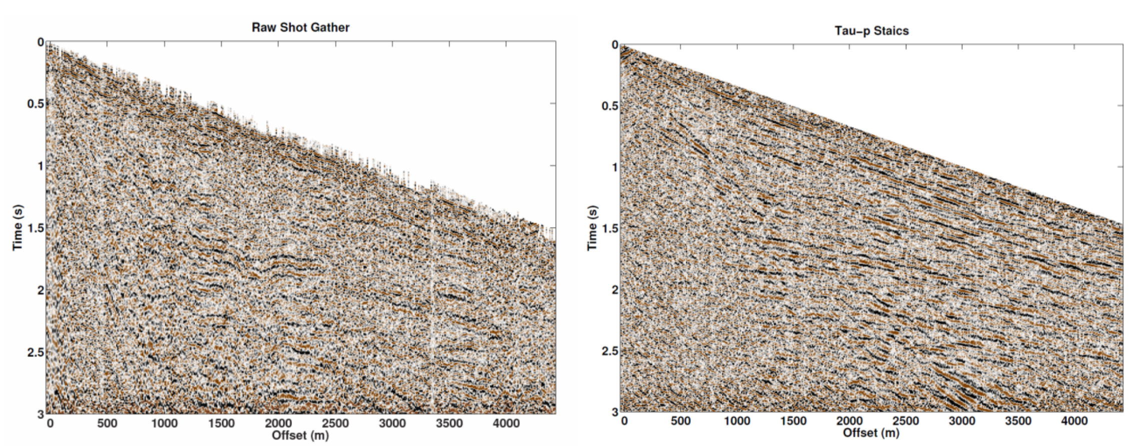

FIG. 1. Shot gather before (left) and after static corrections in the *τ-p* domain (right).

Computing pseudo-shear-wave data using PP and PS-wave traveltime interferometry in the rayparameter domain

Raul Cova and Kris Innanen

ABSTRACT

The kinematics of converted-waves is one the features that complicates the processing of multicomponent data. The asymmetry of the converted-wave raypath prevents us from using an important part of the methods developed for P-wave processing. To accommodate the issue of asymmetric raypath Grechka and Tsvankin (2002) and Grechka and Dewangan (2003) proposed what they named the PP+PS=SS method. Their goal was to generate pseudo-shear-wave data by convolution and correlation of PP and PS-wave data. By taking advantage of the shared raypath between PS and PP data in the space domain they were able to retrieve the kinematics of pure shear-wave data. Here, we propose moving the data to the plane-wave domain, where the shared features of PS and PP are more evident. Although the P and S-leg of converted-wave events may follow different raypath angles, they share the same rayparameter following Snell's law. Recently, Tao and Sen (2013) developed a mathematical framework for doing interferometry in the plane-wave domain. They showed how the cross correlation-type reciprocity equation holds for data in the rayparameter domain. Hence, data with shared rayparameters can be cross correlated to compute redatumed data. In this work I will be using seismic interferometry in the plane-wave domain to extend the PP+PS=SS method to this framework. Access to the rayparameter values will be achieved by the τ-p transform and cross correlation and convolution of PS and PP data will be performed to reconstruct the kinematics of pure S-wave data.

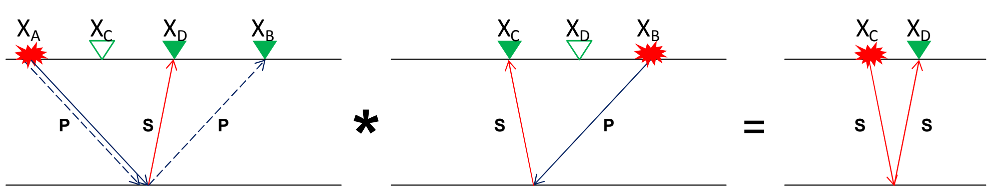

FIG. 1. Representation of the correlations and convolutions involved in the PP+PS=SS method.

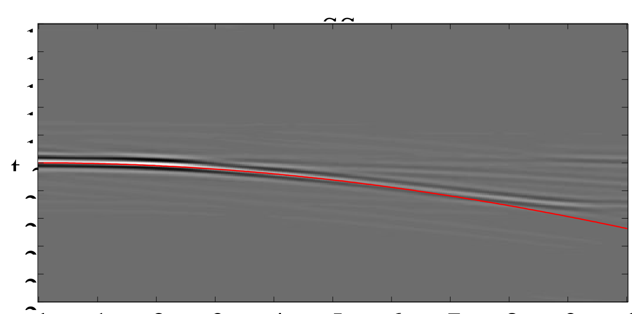

FIG. 2. Pseudo-shear-wave data after inverse transformation to the x-t domain. The red line indicates the expected SS traveltimes.

Inverting raypath-dependent delay times to compute S-wave velocities in the near surface

Raul Cova* and Kris Innanen

ABSTRACT

Characterizing the near-surface is an important part of solving seismic static problems. It is also a critical step as input for more general iterative inversion methods applied to land seismic data. In the case of converted waves this becomes even more true due to the large magnitudes of the shear-wave statics. Here we propose two solutions based on the inversion of traveltimes in the near-surface. First we address the problem of the parameterization of the inversion. Results show that performing the inversion in the rayparameter domain removes the ambiguities that exist in the raypath-angle domain. The first model we invert is based on transmission traveltimes solely in the low velocity zone. This applies to the inversion of uphole data, but introduces the requirement that multiple offsets be recorded. Secondly, a solution based on the difference in reflection traveltimes between receivers is proposed. This solution may be useful for inverting traveltimes retrieved by interferometric techniques. Due to the complexity of the partial derivatives of the forward modelling operator for this case we decided against local descent-based methods, adopting instead a simulated annealing inversion method. This is also justified by the complex topography of the objective function. Performing a representative number of iterations of the proposed algorithm successfully retrieves the true parameters of the model. Since traveltime differences were used, the inverted parameters only allowed us to compute changes in the depth of the base of the near-surface rather than its absolute value. This can be fixed through a calibration process given the depth of the low velocity zone for at least at one receiver location. Near term plans include extending the results to the full 2D problem and testing on the CREWES 2014 Priddis data set.

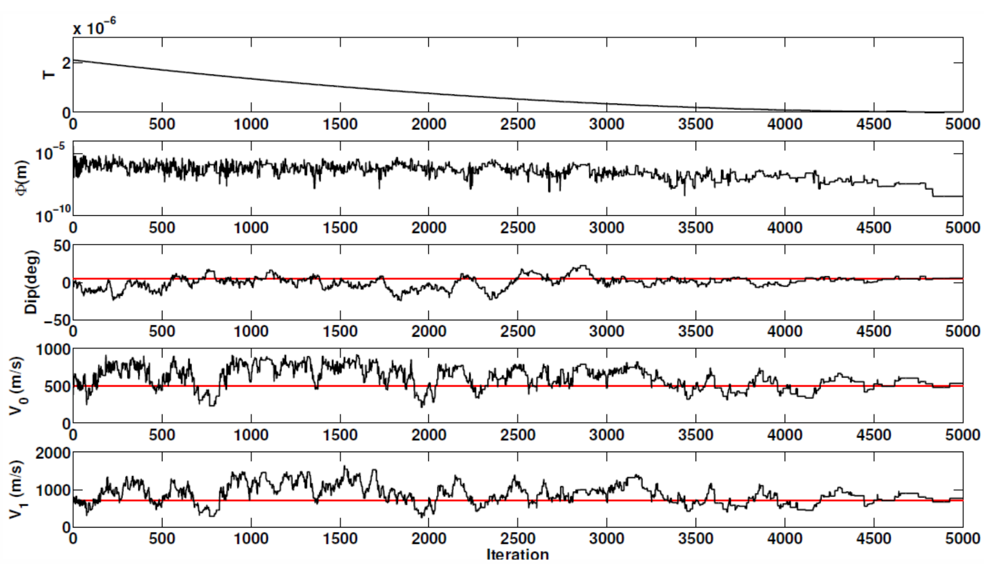

FIG. 1. Evolution of the parameters involved in a simulated annealing realization. Note how the objective function $\mathbf{\Phi}(\mathbf{m})$ shows an overall decrease while the trial parameters converge toward the true values of the model (red lines).

Drift time estimation by dynamic time warping

Tianci Cui* and Gary F. Margrave

ABSTRACT

The drift time is the difference between the event time at seismic frequencies and at sonic logging frequencies predicted by the attenuation theory. The synthetic seismogram needs drift time correction to tie the seismic trace. In this report, the drift time is estimated by dynamic time warping (DTW) method, which is based on the constrained optimization algorithm. By matching the stationary and nonstationary seismograms, DTW can estimate the drift time automatically without knowledge of Q or check-shot records. The estimated drift time is caused by apparent Q attenuation and may contain extra time shift due to the phase error in the wavelet used to construct the stationary seismogram. After applying drift time correction to the stationary seismogram, the residual phase between it and the nonstationary seismogram is almost constant in both time and frequencies. Then time-variant amplitude balancing and time-variant or time-invariant constant-phase rotation are applied to the nonstationary seismogram to perfect the matching.

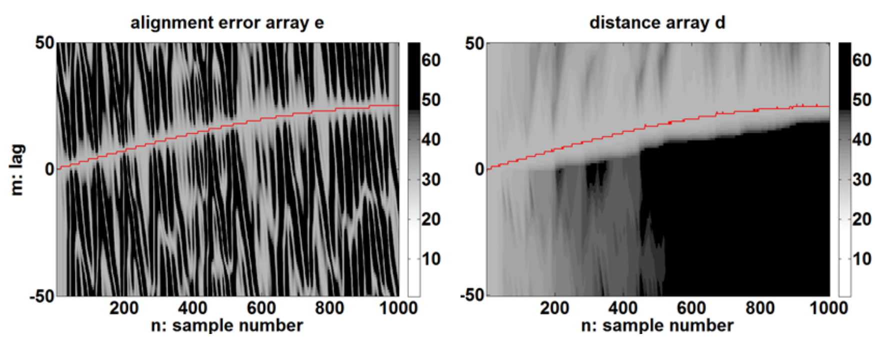

FIG 1: DTW procedure: grayscale backgrounds are alignment error array (left) and distance array (right); the red curve is the known drift time (left) and the estimated drift time by DTW (right).

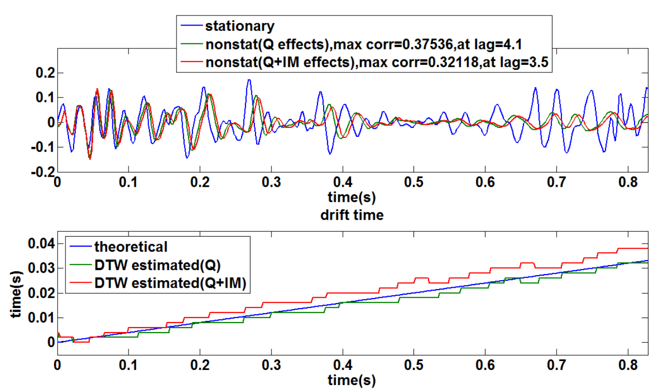

FIG 2: The drift time estimated from a nonstationary seismogram with Q and internal multiples is systematically higher than that from a nonstationary seismogram with Q effects only.

Seismic wavelet estimation

Tianci Cui and Gary F. Margrave

ABSTRACT

In this paper, four methods of seismic wavelet estimation are investigated: the statistical method, the full wavelet method, the constant phase method and the Roy White method. The influences of algorithm parameters and data types on the wavelet estimation are also analyzed. It turns out that different wavelet estimation methods may give different results. They are influenced differently by parameter values and the data used. The best method needs to be determined for the dataset at hand and different parameter values need to be tested by trial and error. What is more, a minimum-phase wavelet is modeled as a linear-phase wavelet, which may make minimum-phase wavelet estimation more simple and robust.

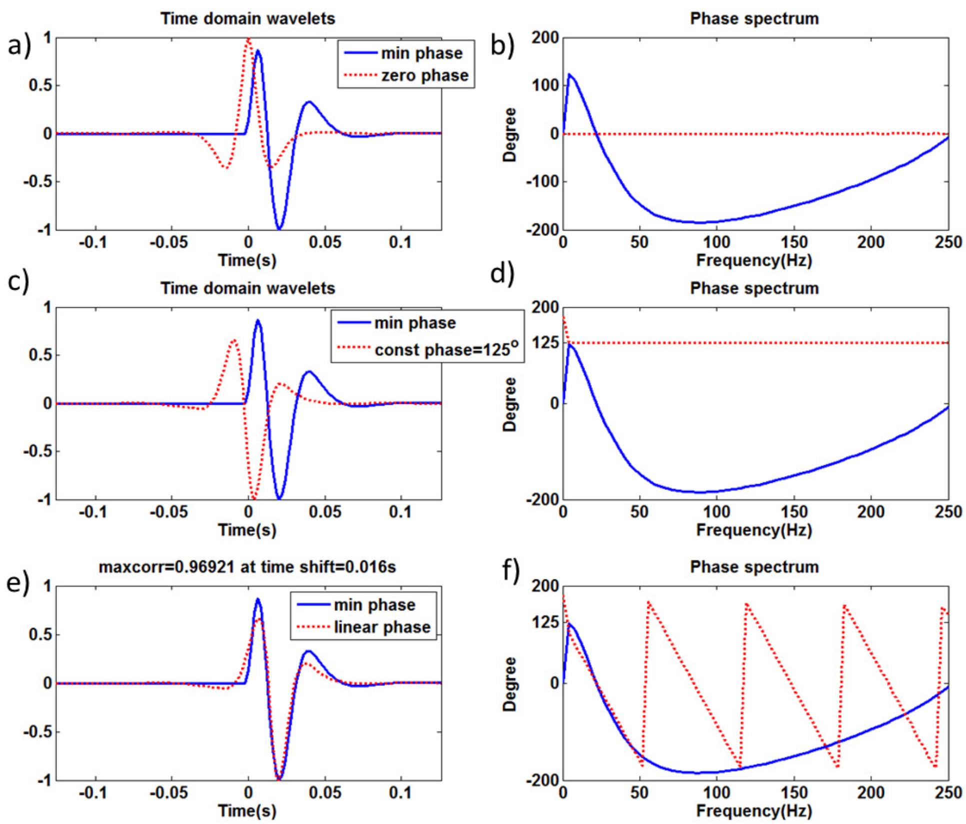

FIG 1: The procedure of modeling the minimum-phase wavelet as a linear-phase wavelet most approximate to it. Panels b), d) and f) are the phase spectra of the wavelets in panels a), c) and e) respectively. First, take find the zero-phase wavelet with the same amplitude spectrum as the minimum-phase one. Then, apply a series of constant-phase rotations to the zero-phase wavelet. For each constant-phase rotation, calculate the maximum crosscorrelation coefficient between the constant-phase and minimum-phase wavelets in the time domain. Finally, choose the maximum coefficient, about 0.97 at a time shift of 0.016 s corresponding to a constant-phase of 125 degrees. Thus, the minimum-phase wavelet in this case can be modeled as a linear-phase wavelet, whose linear-phase line is nearly tangent to the minimum-phase curve.

Absorbing Boundaries in Acoustic Wave Finite Difference Analogues

P.F. Daley

ABSTRACT

The acoustic wave equation is considered using a combination of finite integral transforms and finite differences in the solution method. This approach is known as the pseudo – spectral method or Alekseev – Mikhailenko Method (AMM) after the Russian researchers who spent decades pursuing this avenue of solution which has resulted in numerous dozens of related papers in the literature. One aspect of this solution method that is often referred to but has received little attention in the literature is the introduction of absorbing boundaries. Using the simple acoustic wave equation in this solution type, the algorithm developed by Clayton and Engquist (1977) is incorporated into the transformed wave equation to produce a manner of introducing an absorbing at the model bottom.

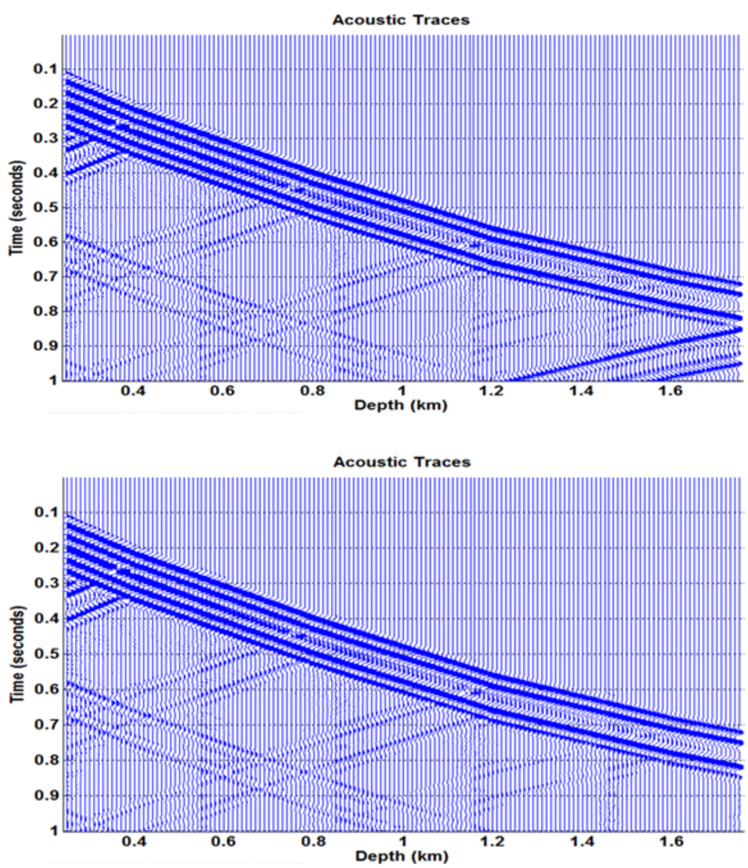

FIG. A comparison of a vertical seismic profile (VSP) without damping (upper) and with damping (lower) using blocked sonic and density logs as input.

Porous medium – the P-wave case

P.F. Daley

ABSTRACT

A subset of the general equations used to describe seismic wave propagation in a poroviscoelastic medium is investigated using finite difference methods. Theoretically for an isotropic medium of this type there are four modes a propagation: a compressional (P) wave, a shear (S_V) wave and a shear (S_H) wave as well as what in termed a slow compressional (P_S) whose actual existence has, until fairly recently, been questioned. The scaled down version of the full poroviscoelastic equation set is one which is viscoelastic and but does not contain any shear type propagation. It is the acoustic analogue of the elastic wave equation, being a set of two coupled equations in the fast and slow compressional (P) wave modes, which may be further downgraded to to a single equation in the fast compressional (P) wave mode as the slow compressional (P) wave mode is difficult to physically detect and as a consequence omitted, at least in this preliminary study. The relatively simple equation remaining was chosen so that a comparison with the seismic response of the acoustic wave could be done to ascertain the possible usefulness of pursuing this topic further. Apart from hydrocarbon related seismic applications, the use of this theory for near surface seismic or Ground Penetrating Radar (GPR) applications to locate toxic or hazardous waste sites and possibly be of assistance in delineating the extent of seepages either from actual dumping or deteriorating containers is a possibility.

TI medium – absorbing boundary conditions

P.F. Daley

ABSTRACT

When using pseudo – spectral methods to reduce to the spatial dimensionality of the 2.5D coupled $qP-qS_V$ wave propagation problem in a transversely isotropic (TI) medium to that in one spatial dimension and time, the introduction of an absorbing boundary, at least at the model bottom is useful in the removal of spurious arrivals. The top model boundary is usually wanted in the numerical calculations and reflections from the model sides may be removed by a judicious choice of model parameters, which does not significantly increase the run time. In this report, a method similar to that presented in Clayton and Engquist (1977, 1980) and is derived for the coupled $qP-qS_V$ wave propagation problem in a transversely isotropic medium. Finite Hankel transforms are used to remove the radial coordinate (r) in what is assumed to be a radially symmetric medium. The problem that remains is a coupled problem in depth (z), where the anisotropic parameters may arbitrarily vary, in depth and time (t).

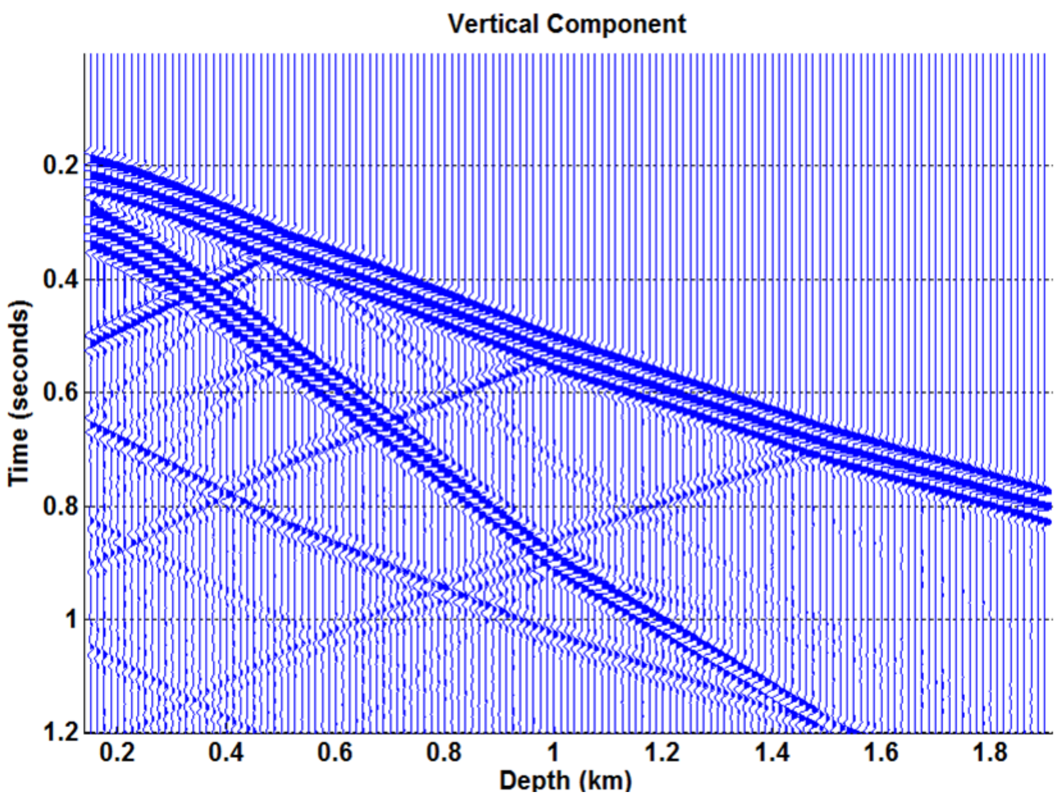

FIG. The vertical component of the VSP synthetic. In this panel the computations continued to the proper time indicating that no spurious reflections from the model are included in the traces.

Development of a geostatic model for a geoscience field research station in Alberta

Jessica M. Dongas* and Don C. Lawton

ABSTRACT

In taking action to mitigate greenhouse gases emitted into the atmosphere primarily from fossil fuel sources, carbon capture and storage is a method of sequestration to reduce CO_2 emissions. The proposed geoscience field research station will serve as a research development site of advanced technologies for monitoring subsurface fluid flow. A 5 km geostatic property model of effective porosity and permeability was constructed for both the shallow primary and deeper secondary injection interval at approximately 290 m and 480 m depths, respectively. The model incorporates existing wireline data from 75 wells and was populated using a Gaussian Random Function Simulation algorithm. The effective porosities of the primary and secondary injection intervals range from 0-27% and 0-18%, respectively (Figure 1). The primary seal interval consists of silty-sands, shales, and impermeable coal layers. The secondary seal interval consists of calcareous mudstones with bentonite layers and high illite content. The 5 km x 5 km property model was updated using two 3-D seismic reflection volumes and existing sonic log data. A time-depth relationship was configured by completing 8 well-ties. Velocity modeling was completed for depth domain conversion. Both injection intervals appear to be promising injection sites for CO_2 and have since been assessed for risk. A clipped 1 km area of the geostatic model will be tested further using Eclipse in Petrel™ 2014.1 for computerized fluid injection simulation to study the behaviour of the CO_2 in the subsurface.

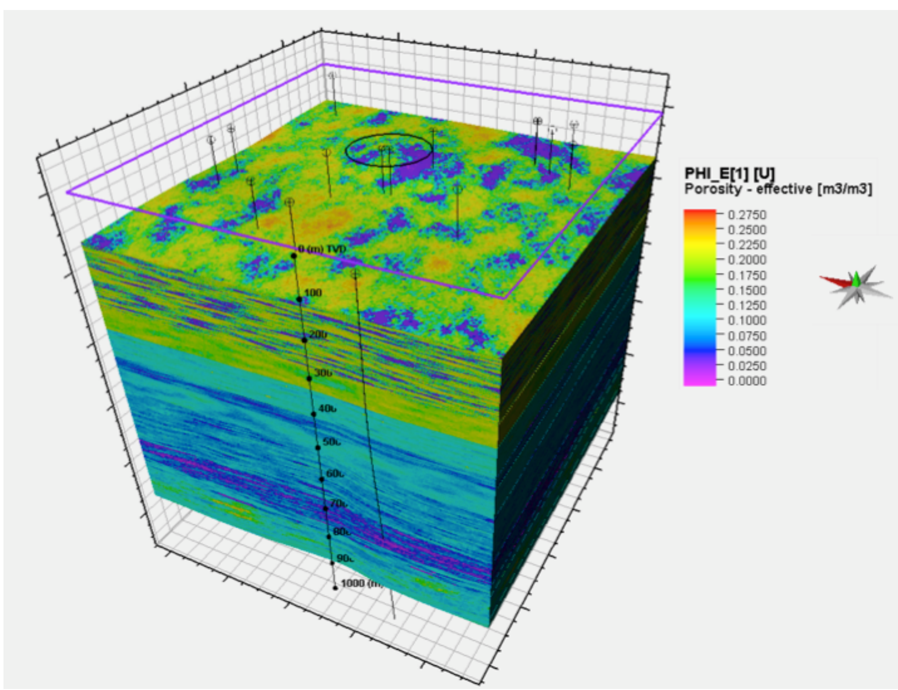

FIG. 1. Effective porosity model for the 5 km x 5 km model of the field research station

Improving frequency domain deconvolution at low frequencies

Sina Esmaeili and Gary F. Margrave

ABSTRACT

Finding the method to obtain the best reflectivity is always challenging. The accuracy of estimated reflectivity directly depends on how precise embedded wavelet is estimated. The frequency domain deconvolution algorithm, which is one of the deconvolution methods, estimates the reflectivity function via extracting wavelet from seismic data in frequency domain. This algorithm can estimate the wavelet by smoothing amplitude spectrum of data. It should be noted that the smoothing process in the deconvolution algorithm can affect the resulted reflectivity.

The purpose of this study is to investigate the performance of standard deconvolution and its ability to estimate reflection coefficient content directly from seismic data. We found that there could be different ways to smooth standard deconvolution. Three different smoothers will be used to smooth the spectrum of data to estimate the reflectivity. A synthetic zero-offset and shot gather data will be created and each of the deconvolution algorithm will be applied to them.

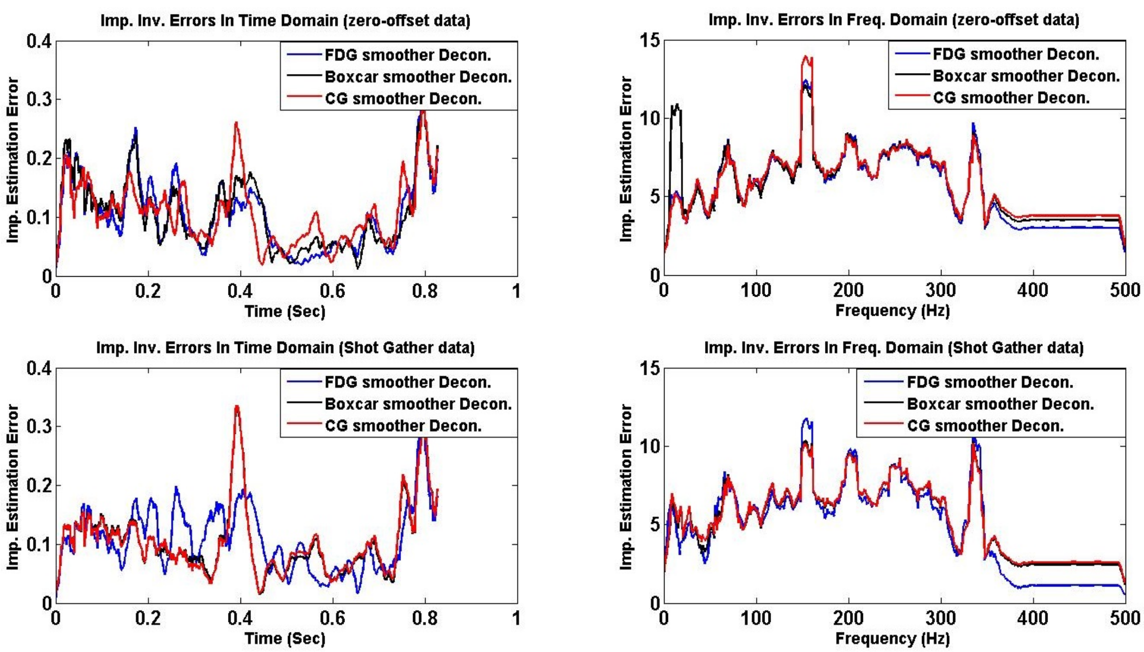

The optimum colour operator for recovering low frequencies

Sina Esmaeili* and Gary F. Margrave

ABSTRACT

Most Seismic data processing algorithms try to shape seismic data into a white spectrum during deconvolution procedure. In reality most natural occurring reflectivity sequences have coloured spectra instead of white spectra. Studying the actual earth reflectivity and its spectra's shape are showing that the effect of coloured spectra is more significant in frequencies below than 50Hz.

We study the spectral property of seismic data, and by using the well reflectivity, we introduce a new technique to shape the white spectrum of deconvolved data into the coloured spectrum of reflectivity. This leads to better recovery of the low frequency component and hence better inversion.

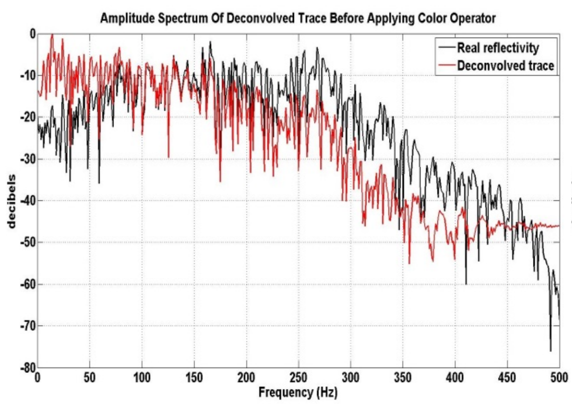

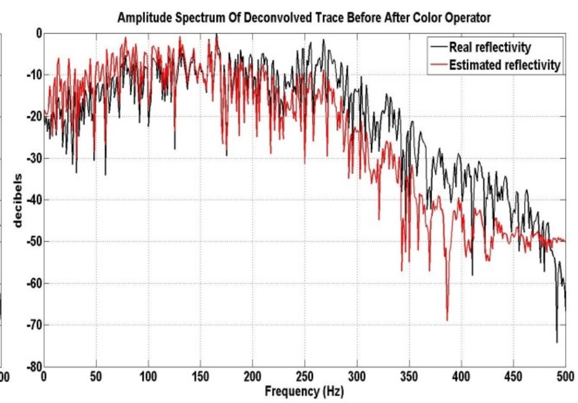

Computing pseudo-crosswell data using seismic interferometry with surface sources

Adriana Gordon, Raul Cova and Kris Innanen.

ABSTRACT

Seismic interferometry is a method based on the use of cross correlation and stacking operations to redatum seismic data. The special case of vertical seismic profile (VSP) in a cross-well configuration is the interest of this paper. We present an approach using seismic interferometry to compute pseudo-cross-well information. This study shows an analysis of the aperture effect and fold distribution for direct waves, and full wavefield interferometry at four different maximum offsets. Results indicate that where the maximum offset increases the match between raytraced traveltimes and the interferometric receiver gathers improves. Using direct arrivals it was only possible to retrieve traveltimes at receivers in a lower position on the second well. However, using reflected arrivals provided traveltimes for receiver at a shallower depth in the second well. Thus, use of the full wavefield displays a more complete result. The interferometric fold distribution showed a similar result; as the maximum offset increases the fold is improved and reaches deeper parts of the model. This type of processing may help to generate data suitable to exploit the benefits of the cross-well experiment without the risks involved in the acquisition.

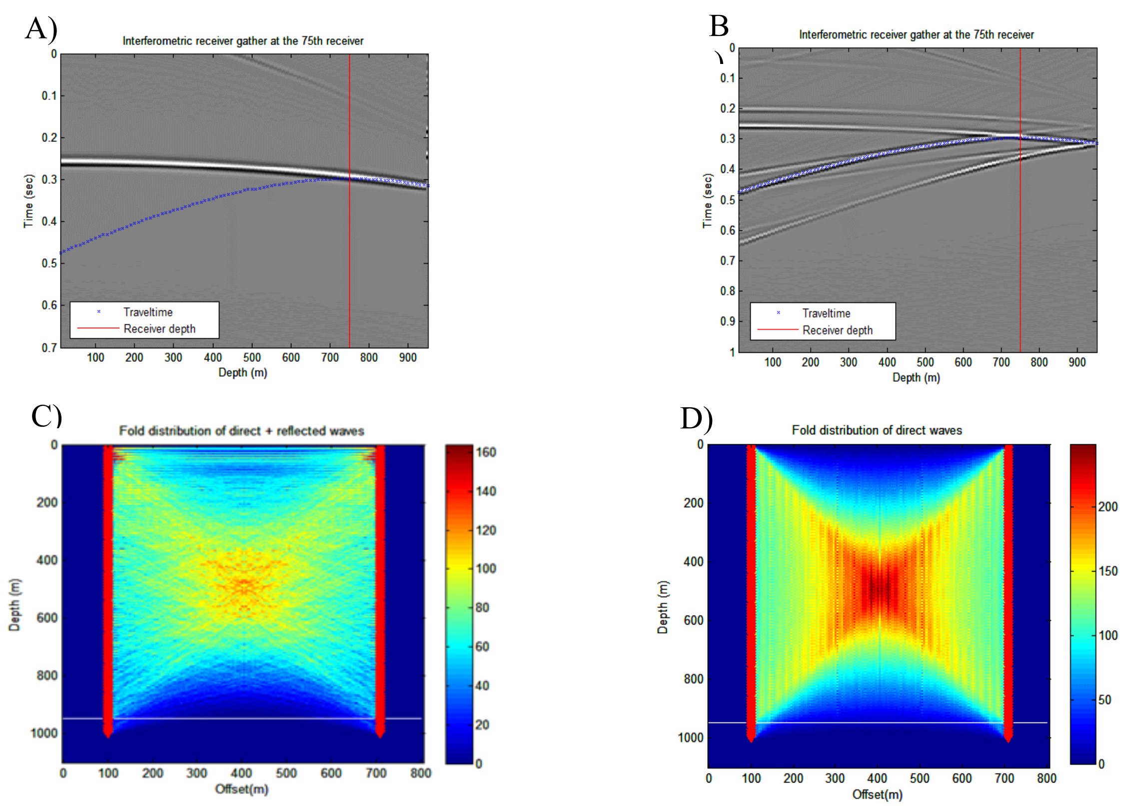

FIG. 1. Interferometric receiver gathers for receiver at 760m depth with a maximum offset of 4000m, using A) direct arrival and B) Full wavefield. C) Full wavefield interferometric fold map for a maximum offset of 4000m. D) Regular crosswell fold map of direct waves.

Full waveform inversion - a synthetic test using the PSPI migration

Marcelo Guarido*, Laurence Lines and Robert Ferguson

ABSTRACT

Full Waveform Inversion (FWI) is used to estimate subsurface parameters, such as the P-wave velocity, in an iterative process. Although having been studied for several years, practical application of the technique on real data has proven difficult. From the theory, the full update is the reverse-time migrated residuals multiplied by the full Hessian. We demonstrate for a 2D acoustic marine synthetic case that the methodology can be applied with reasonable results, using the PSPI migration with a deconvolution imaging condition and a line search to calculate the step length to invert P-wave velocity. We tested different mutes applied in the migrated residuals, resulting in higher resolution when the mute is not too narrow or wide. We present a study of the importance of the initial velocity model for the convergence we find that the best initial model gives the best inversion result. However, we obtained good responses for initial velocity models not close to the global minimum such as velocity models with smoothed flat layers based on simulated wells in the real velocity model. We showed that when using only one well to generate the initial model, our best result is when we do not sample the high velocity body. Our results suggest that we can have a higher resolution inversion if an initial model is generated by an interpolation of two or more wells.

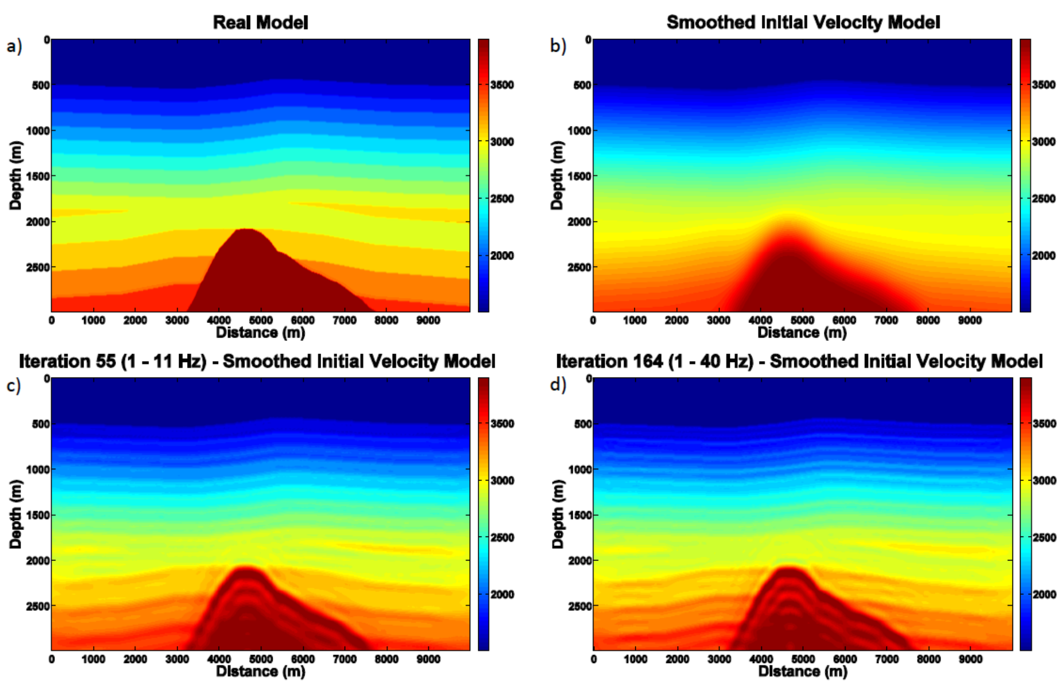

FIG. 1: FWI using PSPI migration: a) is the real model, b) is the initial velocity model c) is the iteration 55 of the process and d) is the iteration 164.

Receiver static correction of *PS*-wave using prestack data in the receiver domain

Saul E. Guevara and Gary F. Margrave

ABSTRACT

A method for receiver statics correction of the converted wave is proposed. It is based on the observation that the static time delay on PS-wave events between two adjacent receivers, after the source statics correction, should correspond mostly to the differential receiver statics. The method does not require stack or a velocity model for PS-waves. It follows the surface consistent statics model applied to Common Receiver Gathers. Cross-correlations of the corresponding traces after minimizing the NMO differential and assuming small structural component, are calculated and then stacked. The differential statics time delay should correspond to the maximum of this stack. Tests on synthetic data illustrate the resulting statics.

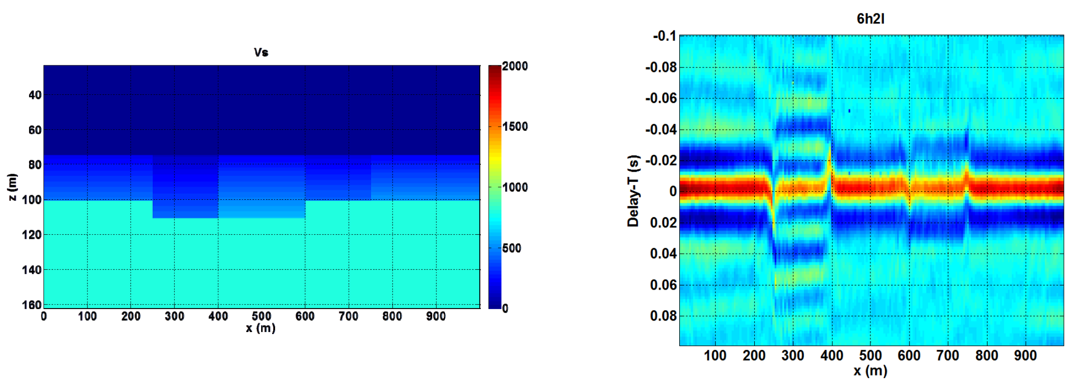

FIG 1. (a) Near surface Vs model, with lateral variation at four locations. (b) Delay time, equivalent to the differential receiver statics, after crosscorrelation of receiver gathers in the surface domain.

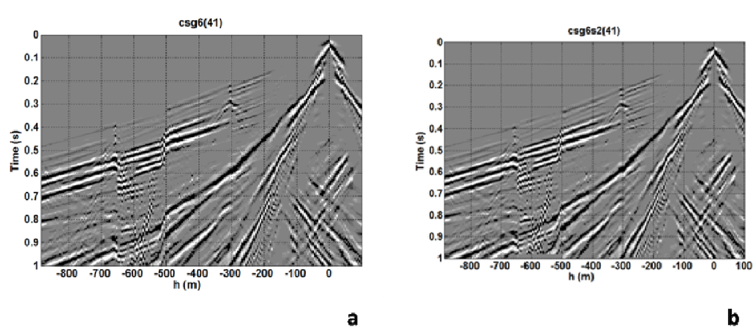

FIG 2. Shot gathers of the horizontal component (PS-waves) (a) before the receiver statics correction, (b) After the receiver statics correction. Notice increase in the continuity of the events.

Processing and interpretation of 2D seismic data from Inglewood Park, Calgary, Alberta

Bobby J. Gunning and Don C. Lawton

ABSTRACT

Significant rainfall and rapid snowmelt occurred in June of 2013 in Southern Alberta. The largest flood, on record, of the Bow River and its tributaries was triggered from the heavy rainfall and snowmelt. Following the flooding event, several 2D seismic lines were recorded on a point bar near the intersections of the Bow and Elbow Rivers in Calgary Alberta (Figure 1, left). Several seismic data processing steps were used to attempt to create an image, representative of geology, of the subsurface beneath Calgary. The near surface was searched for signs of fluvial geomorphology and two major drape structures were identified from the seismic. The seismic line processed for this paper shows a complex near-surface geomorphology (Figure 1, right).

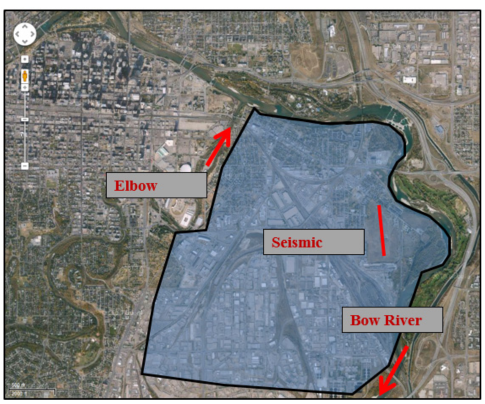

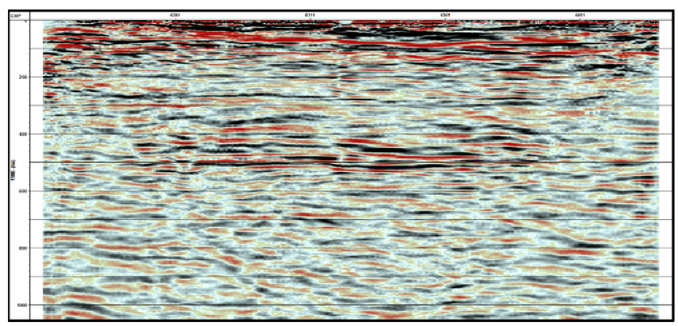

FIG. 1. (Left) The Bow and Elbow rivers, the seismic line, and a flood risk area between the two rivers. Arrows indicate river flow direction. Image courtesy of Google Maps 2014. (Right) The processed seismic line.

Arbitrarily sampled Fourier transform (ASFT) for 5D interpolation

John Guo, Ye Zheng and Wenyuan Liao

ABSTRACT

Seismic trace interpolation, which spatially transforms irregularly sampled acquired data to regularly sampled data or to any desired grid in general, is an important step in seismic data processing. A class of algorithms, such as Minimum Weighted Norm Interpolation (MWNI), Anti-Leakage Fourier Transform (ALFT), and Matching Pursuit (MP), are based on the Fourier theory in the f-k domain by computing the estimated spatial frequency content of irregularly sampled data. However, a key limitation of current algorithms is that the spatial frequency content is always restricted to a regularized grid in the f-k domain, therefore, they cannot achieve the optimal sparsity in the f-k domain, and consequently this may reduce interpolation accuracy.

We present the Arbitrarily Sampled Fourier Transform (ASFT) method for 5D interpolation, which incorporates several enhancements. First, true positions of the input data are used for computation; second, the spatial frequency content is allowed to be at an arbitrary point in the f-k domain. As a result, ASFT is able to obtain better sparsity in the f-k domain. ASFT was tested on Western Canadian Sedimentary Basin data and produced excellent interpolation results.

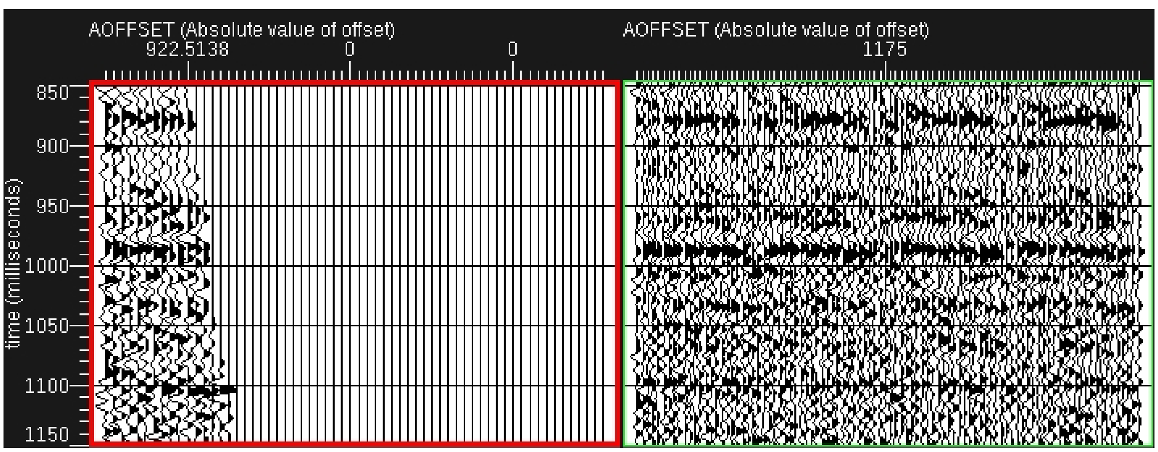

Comparison of gather data before (left) and after 4-azimuth ASFT interpolation (right).

Priddis 2014 broadband surface and walkaway VSP seismic experiment

Kevin W. Hall*, Kevin L. Bertram, Malcolm B. Bertram, Joe Wong, Peter M. Manning, Eric V. Gallant and Gary F. Margrave

ABSTRACT

CREWES and INOVA conducted a high-resolution broadband multi-component seismic surface and borehole test survey at the Priddis Geophysical Observatory in late October and early November of 2014. Two types of sources were used; 0.125 kg of dynamite at 5 m depth with source points every 6 m, and an INOVA UNIVIB using a linear 1.5-150 Hz sweep with two sweeps per vibe point.

Four source and receiver lines were laid out in a star pattern centred on Testhole 1, which is an instrumented borehole installed by CREWES in 2013. All four receiver lines had SM7 10Hz three-component geophones at a 3 m receiver spacing. In addition, one of the receiver lines also had twelve SM7 geophones in groundscrews as well as single-component SL11 accelerometers and SM24 10 Hz high-sensitivity geophones, all at a 6 m receiver spacing.

The forty-five three-component 28 Hz geophones permanently installed in Testhole 1 at a nominal 3 m spacing were also used for this survey. Prior to beginning the seismic survey, natural gamma-ray and full waveform sonic logs were acquired in Testhole 2, 50m away from Testhole 1, which was then instrumented with a USSI retrievable clamping three-component fibre-optic system with six nodes spaced 20 m apart.

FIG. 1. Dynamite shotholes being drilled and loaded.

Projections: an old diagnostic tool revisited

David C. Henley

ABSTRACT

Many kinds of projections have been used to help analyze seismic data over the history of seismic exploration, probably the most familiar being the CMP stack. We explore here various projections with an eye to adapting them for particular kinds of analysis. We present, as an example, several different projections applied to a 4D (time-lapse) seismic experiment in central Alberta and discuss the diagnostic possibilities of projections in this setting.

While we draw no conclusions in this work, we review the topic of projections in order to stimulate thinking about new ways in which to summarize and analyze multi-dimensional data volumes. In the figure below, from the time-lapse experiment, only projection (a) is a function of surface location; the other projections are raypath-dependent. In projections (b), (c), and (d), anomalies seem slightly more visible than when they are projected along surface location (better seen at higher magnification).

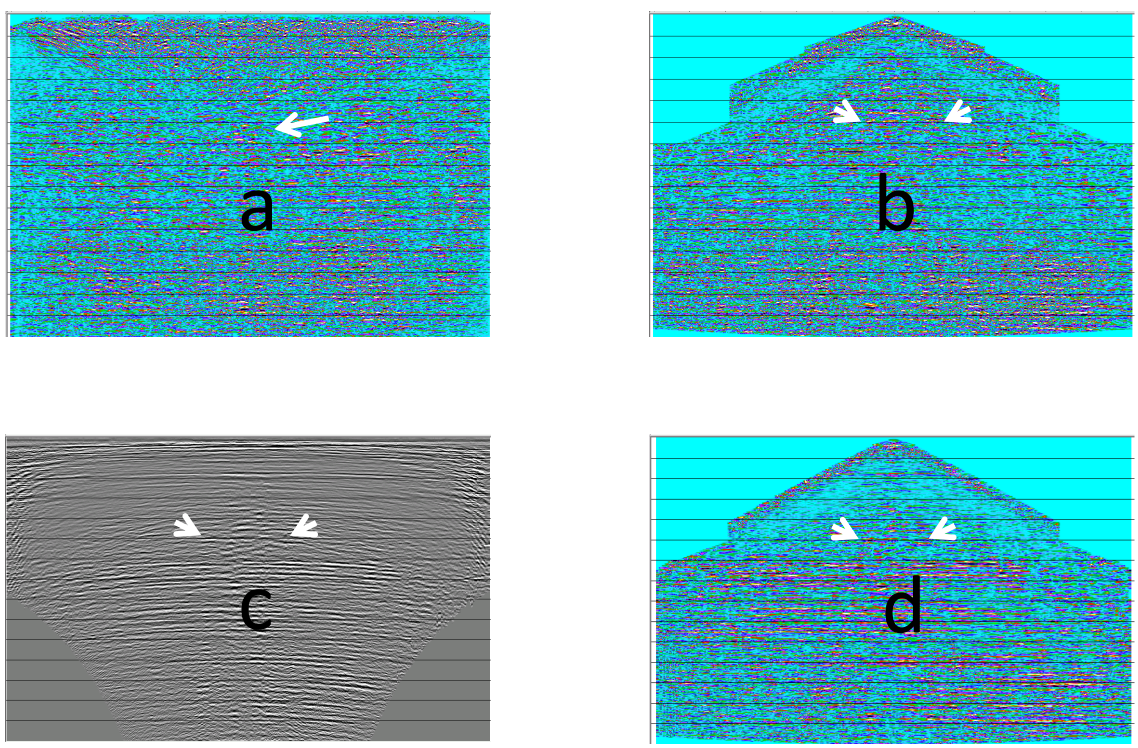

FIG. 1. 4D Violet Grove time-lapse anomaly highlighted using four different projections. (a)—CMP stack difference; (b)—common-offset stack difference; (c)—common-raypath stack difference; (d)—Inverse RT Transform of common-raypath stack difference. White arrows indicate locations of possible anomalous amplitudes marking the time-lapse differences. Anomalies may be more visible in (c) and (d).

Reversing entropy: deblending and imaging physical modeling data

David C. Henley and Joe Wong

ABSTRACT

Physical modeling has become one of the key activities pursued by students and staff at CREWES. It is an important technology for verifying the theory of elastic wave propagation, as well as for developing and testing acquisition and processing techniques which are directly applicable to full scale field seismic operations. Many of the problems which afflict full-scale seismic exploration are present in the physical modeling environment as well. One of these, the acquisition time required by a massive 3D seismic survey, has found a partial solution in the use of multiple simultaneous sources during the acquisition. Here, we analyze a small portion of a large 3D data set acquired in the CREWES physical modeling facility using 8 simultaneous sources (to decrease acquisition time by a factor of 8). We show that with suitably selected acquisition geometry, the simultaneously acquired source 'supergathers' can be untangled or 'deblended' and subsequently imaged with no significant crosstalk from the wavefields of the simultaneous sources. While this achievement in itself is not unique, we demonstrate a new implementation based on previous wavefield separation work. We document here our increasingly sophisticated ability to acquire and process complex physical model data in a way that can emulate actual field seismic surveys.

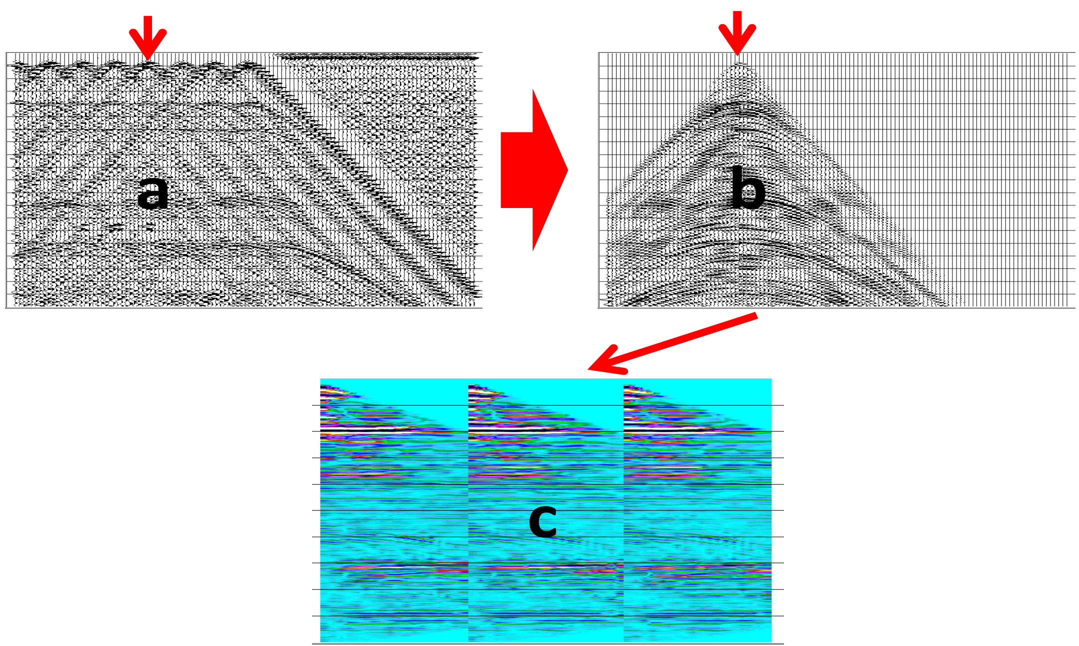

FIG. 1. Blended supergather (a) can be deblended using wavefield separation techniques based on NMO corrections and radial trace (RT) filtering (b). Deblended source gathers can then be imaged. Three individual 2.5D "Cross-stacks", created by stacking selected traces from the deblended shot gathers, shown in (c).

Through a glass darkly: improving raypath interferometry

David C. Henley*

ABSTRACT

The processing technique known as raypath interferometry has been successfully applied to several different sets of 3C model and field seismic data, to correct their images for the degradation caused by irregularities in the near-surface layer. We continue to refine and improve the technique. In this report, we demonstrate an alternative scheme for creating the reference wavefield, or 'pilot traces' used in the interferometry, and we demonstrate the use of the Snell Transform, a modified Radial Trace Transform, for mapping the raw seismic data into the common-raypath domain required by raypath interferometry.

For pilot trace creation from raw data gathers, we find that singular value decomposition (SVD) methods can be used as an alternate or supplement to lateral smoothing, but that this method, like lateral smoothing, works best when lateral structure and discontinuities are first reduced by 'brute force' techniques like horizon flattening and 'trim' statics.

The Snell Transform, because its sampling trajectories are more likely to map seismic data at all depths onto common raypaths, appears to lead to slightly better interferometric images, especially at shallow depths, than the Radial Trace Transform; but trial and error are needed to set parameters appropriately.

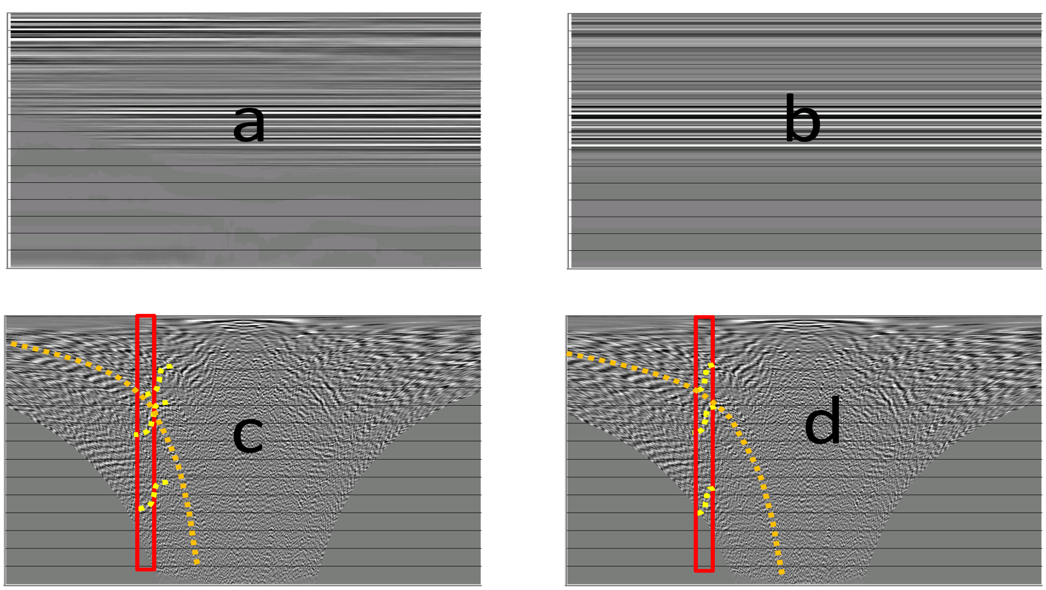

FIG. 1. Reference wavefield estimate using lateral smoothing (trace mixing), (a), and SVD (b). RT Transform in (c) does not completely align raypath-consistent statics. The Snell Transform in (d), however, with smoothly increasing velocity function, improves the alignment.

Estimating anelastic dispersion from uncorrelated vibe data

Kris Innanen

ABSTRACT

A vibroseis sweep and a dispersive geological volume act to negate each other: the sweep delays the arrival of higher frequencies and the dispersive medium hurries them along. We derive a simple analysis procedure in which the time-frequency spectra of a programmed sweep and the uncorrelated measurement are compared in order to estimate the frequency-dependence of the phase velocity. The approach is developed with a synthetic example and applied to a 3C VSP data set.

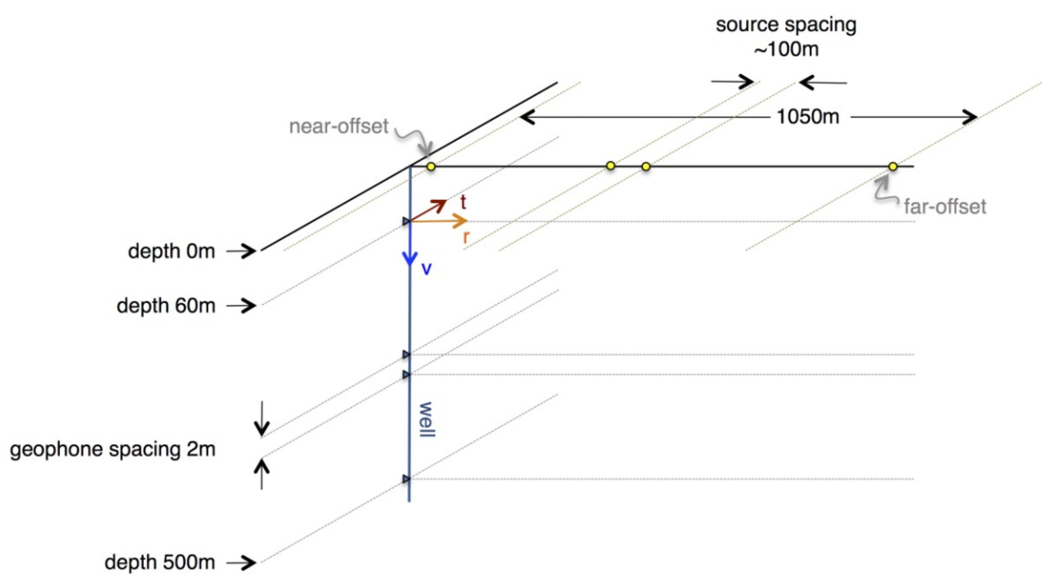

FIG. 1. Configuration of the 3C VSP data set.

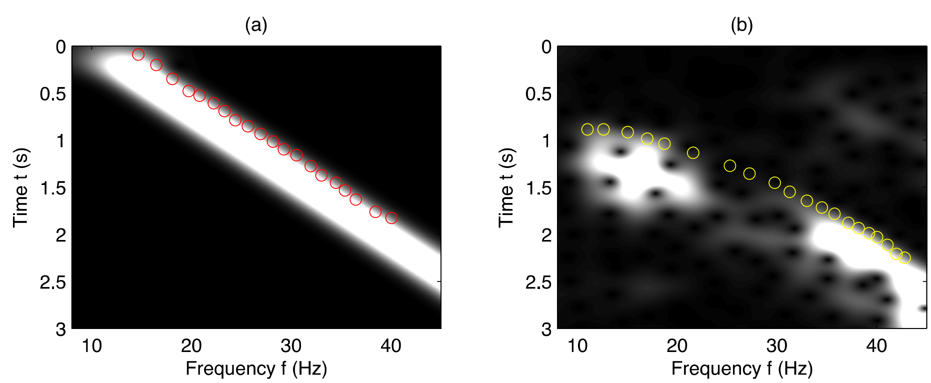

FIG. 2. Comparison of Gabor spectra associated with (a) the linear sweep program used in the 3C VSP experiment and (b) the uncorrelated direct wave measurement at a geophone at depth 120m and offset 320m from the surface source. The difference between sweep picks (red) and data picks (yellow) drive estimation of c(*f*).

Formulas for time-lapse seismic refraction data analysis

Kris Innanen

ABSTRACT

Formulas for the analysis of time lapse seismic refraction difference data are derived, motivated by indications that during the 2014 University of Calgary Geophysics Field School a significant rain event produced detectable changes in the depth of the water table. The formulas are extensions of Hagedoorn's plus-minus method, wherein forward- and reverse-shot baseline and monitoring refraction travel times are mixed in several ways to extract differential depth-to-interface and jump in subsurface velocity values.

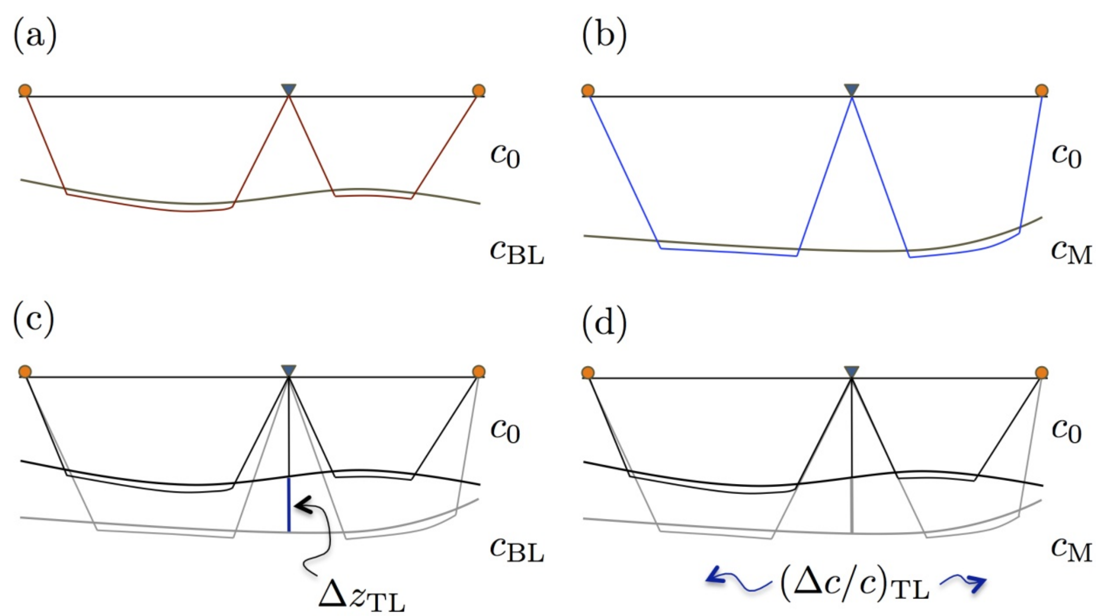

FIG. 1. Forward and reverse shots for (a) baseline and (b) monitoring surveys. Time lapse formulas mix baseline forward, monitoring reverse, and vice versa to characterize (c) the time-lapse jump in interface depth below the geophone and (d) the time-lapse jump in refraction velocity.

Large dip artifacts in 1.5D internal multiple prediction and their mitigation

Kris Innanen and Pan Pan

ABSTRACT

In this short note we point out that large-dip artifacts noticeable in k_g dependent integration limiting parameter ε. The results are largely consistent with those obtainable by post-prediction filtering, but the $\varepsilon(k_g)$ approach is preferable in that it is tied to our interpretation of the origins of the artifacts.

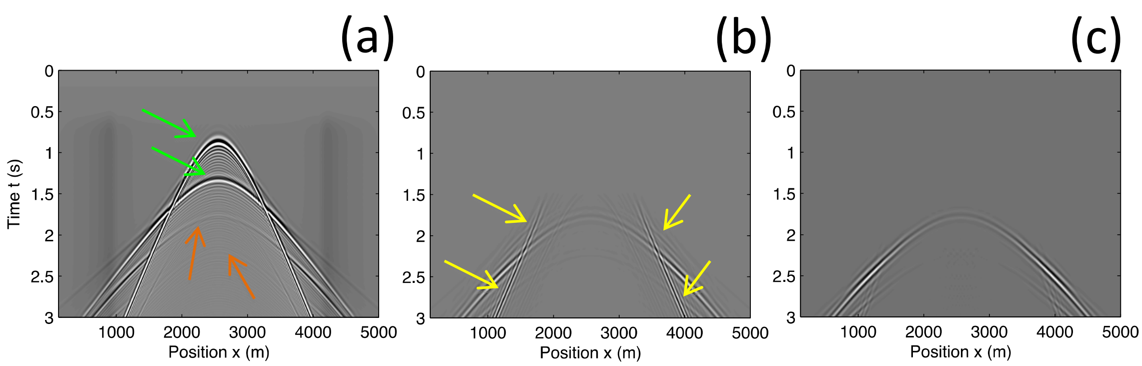

FIG. 1. Predictions from a multiple-bearing synthetic (a), with two primaries (green) and two multiples (orange), if constructed with constant ε, can exhibit artifacts (yellow) tied to large k_g values (b); a simple linear prediction parameter $\varepsilon(k_g)$ provides a clean fix.

Multicomponent elastic reflection full waveform inversion

Kris Innanen*

ABSTRACT

Full waveform inversion applied to reflection mode, multicomponent land data is considered, in the context of the iterated recovery of a range of parameters, ranging from standard elastic λ, μ and ρ, through to petrophysically relevant parameters such as the fluid term *f* of Russell and Gray. Much of the effort lies in constructing a flexible framework for elastic multicomponent sensitivities, which we address with a two-stage integration by parts regimen. Matrix forms for a multicomponent objective function and three term gradient and nine term Hessian are then determined, and the reductions necessary to invert PP, PS, SP, and SS modes independently or jointly are formed.

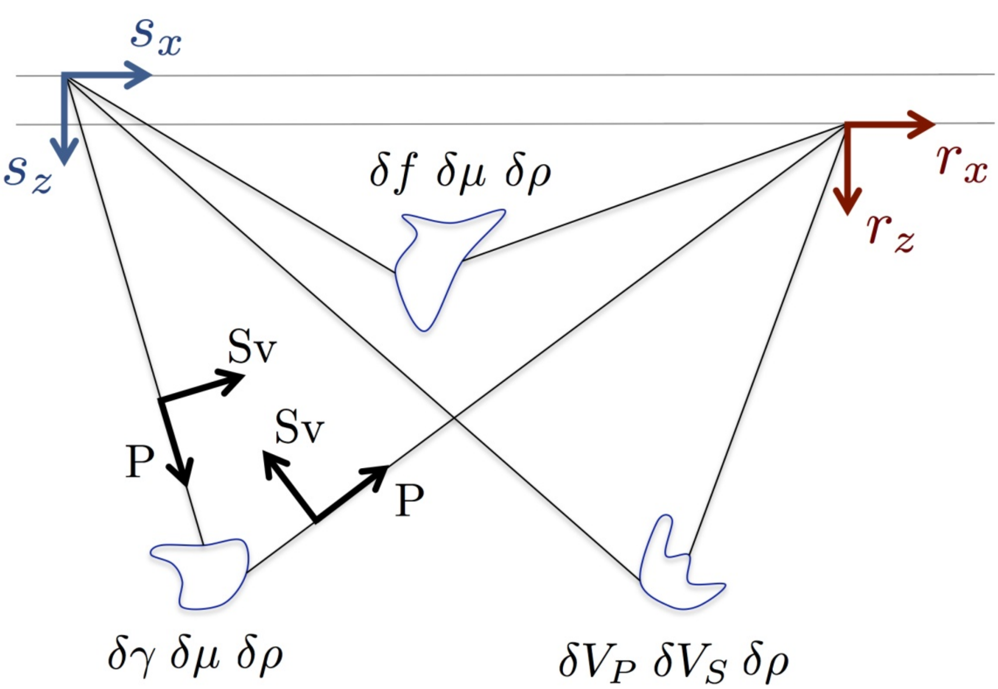

FIG. 1. 2D multicomponent FWI configuration, involving P and S components of the source field (blue) into P and S components of the receiver field (red). Sensitivities in a wide range of parameters are derived from a scattering formulation.

Particle model of walkaway VSP data

Kris Innanen

ABSTRACT

Earlier treatment of zero-offset VSP data arrival times in terms of perfectly inelastic particle interactions is extended to include walkaway modes. The space-time tracks of particles moving under the influence of a uniform force field accelerate in such a way that they capture approximately the moveout in the VSP gather. In zero offset data and walkaway modes NMO correction is realized through transformations from the laboratory reference frame of the collisions to rest frames of individual particles before and after colliding. Galilean transformations suffice for zero-offset data, whereas something akin to relativistic transformations are needed for walkaway modes.

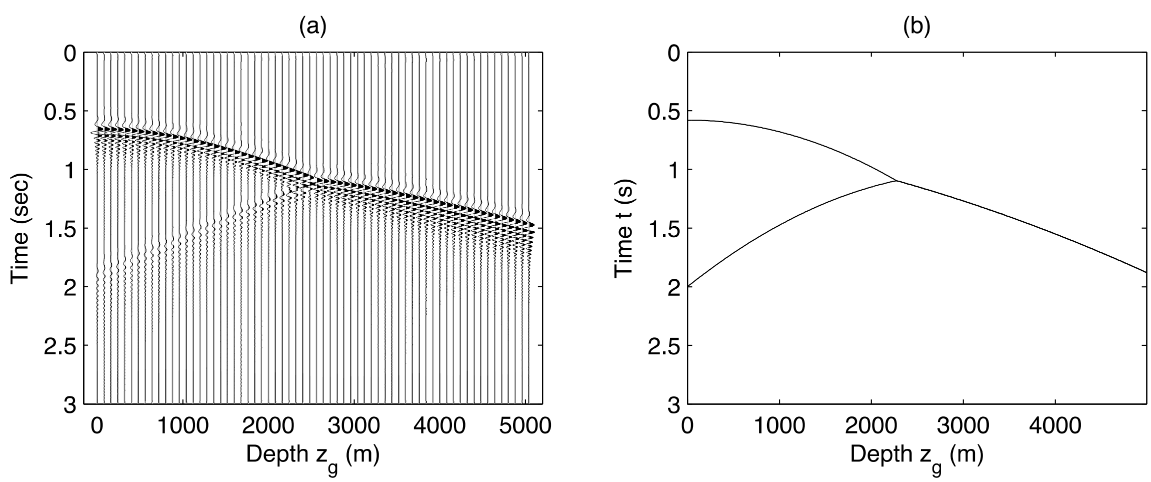

FIG. 1. The arrival times and amplitudes in a walkaway VSP data set (a) are predictable by viewing each event as a particle, with a well-defined but notional mass and momentum, and allowing these particles to interact inelastically in a uniform acceleration field.

Quantifying the incompleteness of the physics model in seismic inversion

Kris Innanen

ABSTRACT

At each stage of seismic processing we adopt an underlying physical or mathematical model, and rely on its degree of incompleteness (relative to what is actually experienced by a seismic wave) being either negligible, or irrelevant to the processing task in question. For some tasks we can proceed with remarkably simplistic approximations, but in seismic inversion, our choices are few: any parameter or process affecting the seismic wave has to be included. The geophysical literature reflects the broad range of possible responses to this issue: suppressing elastic conversions in order to use acoustic physics; selecting analysis domains which boost P-wave influences over S-wave, etc. A smaller number of researchers have grappled directly with incompleteness, through probabilistic and numerical schemes. We may be able to come to grips with this problem more deterministically, if we learn to view complex physical models as being perturbations of simple physical models. This will be an important part of a meaningful attempt to apply full waveform inversion / IMMI to multicomponent land data.

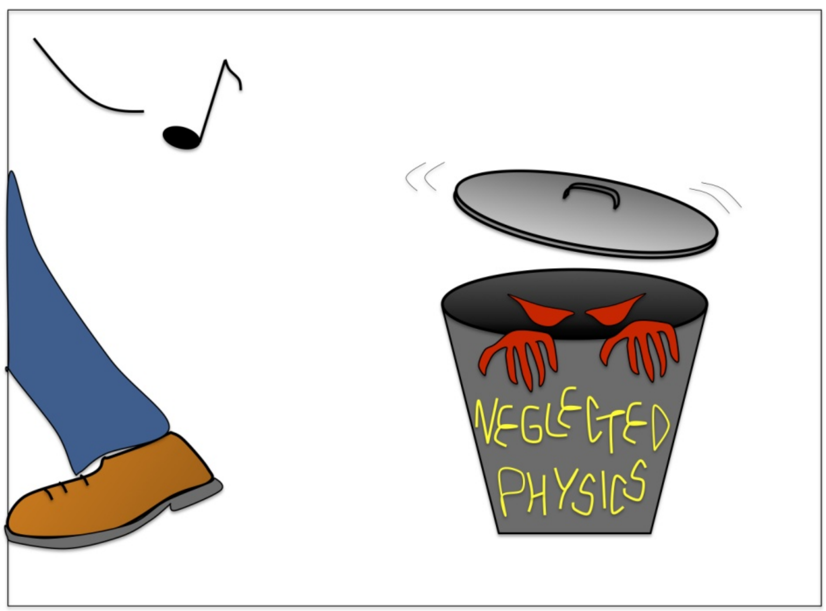

FIG. 1. Just don't forget the little fellow's in there.

A second-order preconditioner for Newton updates in seismic full waveform inversion

Kris Innanen

ABSTRACT

Newton updates (i.e., the updates invoked in the most general forms of seismic full waveform inversion) are intrinsically nonlinear, in the sense that they invoke the data twice, once in the gradient and once in the inverse Hessian. However, a simple univariate example demonstrates that its nonlinear nature is not used advantageously in inversion. This can be fixed by introducing a formal parameter λ to the nonlinear part of the inverse Hessian, and determining a value for it which correctly implements second order nonlinearity. The approach extends without requiring any additional conceptual leaps to a multidimensional scalar full waveform inversion problem, provided that development makes use of a nonlinear sensitivity expression such as that developed in a companion report.

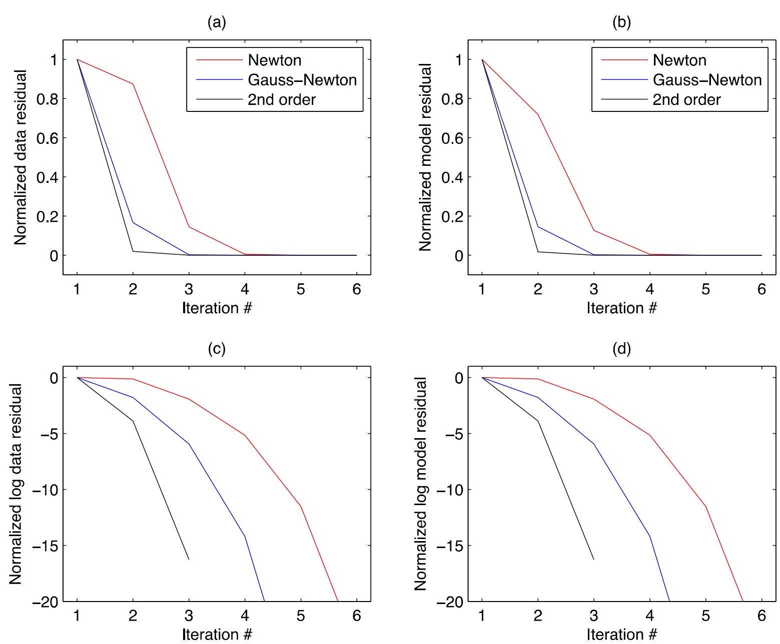

FIG. 1. Newton, Gauss-Newton, and the second order preconditioner enacted on a univariate minimization problem.

Seismic full waveform inversion with nonlinear sensitivities

Kris Innanen

ABSTRACT

Convergence and physical interpretability of full waveform inversion updates are key issues as we contemplate practical FWI. One aspect of standard FWI updates that has been only superficially broached thus far is the idea that the sensitivity or Frechet kernel used in the gradient calculation could be re-tuned to increase convergency by accommodating more than the first order model/field variations. We present and analyze an approach to the construction of a second order sensitivity, and demonstrate its natural accommodation of for instance nonlinear reflection amplitudes, of the type encountered when contrasts causing reflections are large. In a companion paper we show how second order data-model interactions are properly incorporated in the inverse Hessian, but those do not appear in the updates we study here, and evidently do not adversely affect the treatment of second-order reflectivity.

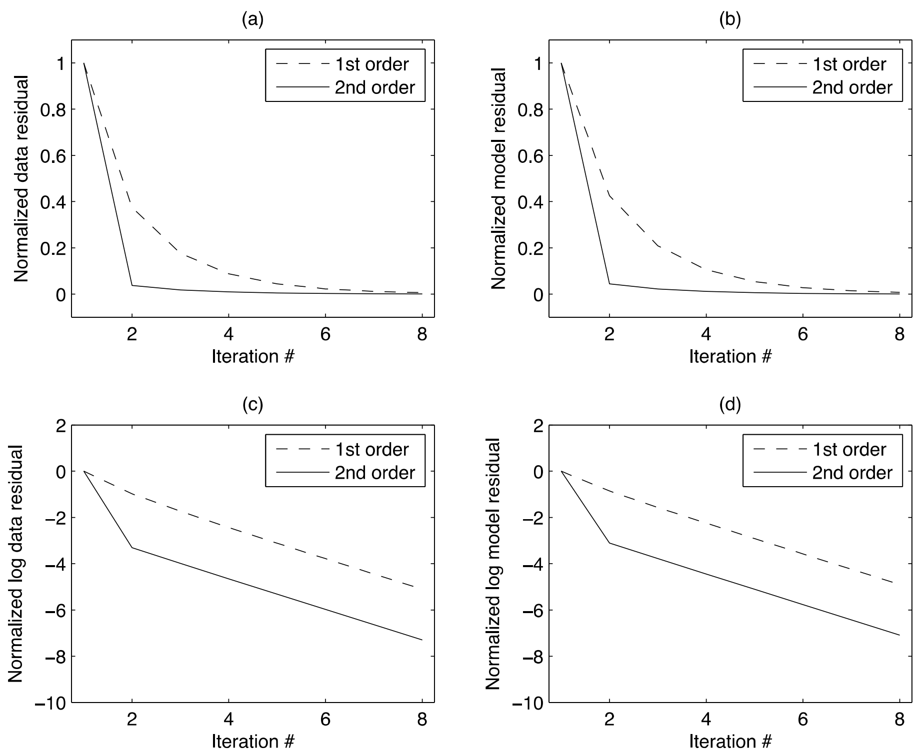

FIG. 1. Convergence of linear (dashed) vs. nonlinear (solid) data/models over <10 iterations.

Preparing for experimental CO_2 injection: Geology of the site

J. Helen Isaac and Don C. Lawton

ABSTRACT

We studied the geological properties of three prospective experimental CO_2 injection zones in the study area in Southern Alberta. The primary target is the Basal Belly River Formation, with secondary targets in the Medicine Hat and Second White Speckled Shale formations, which are at depths of about 285 m, 475 m and 710 m, respectively, below the surface.

We correlated well logs in the immediate area of interest with well logs from a well having a lithology log and from wells with Basal Belly River production. We calibrated the gamma ray logs in the top of the Pakowki Formation so that the average values were consistent in all of the well logs. We then used the gamma ray logs to assess reservoir continuity and sand/shale content in the Belly River Formation above the proposed injection zone and to estimate the sealing properties of this formation (Figure 1).

Based upon our interpretation of the gamma ray logs, it seems probable that the Belly River Formation will have sufficient shale content to be a seal in the area of interest.

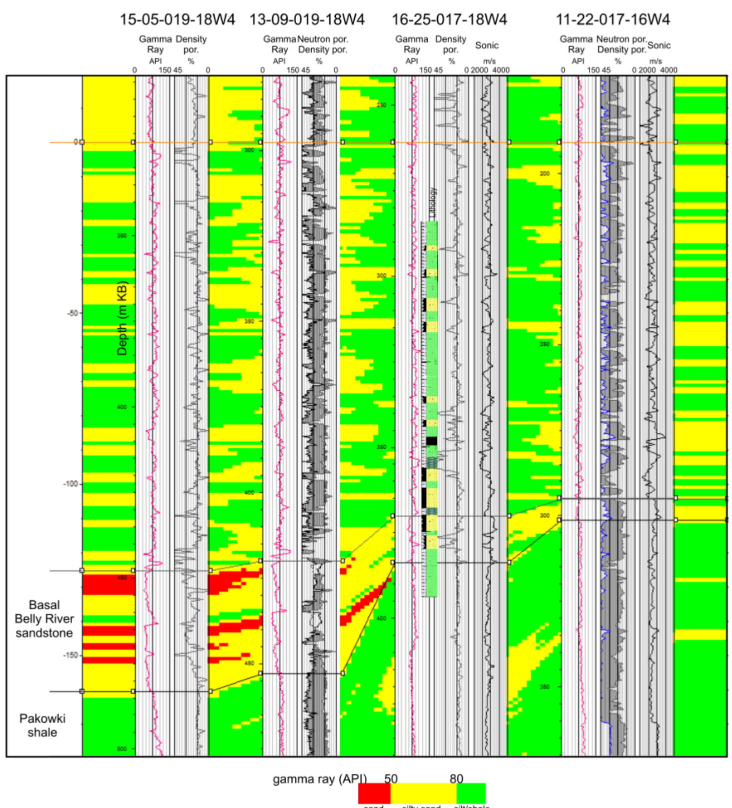

FIG. 1: Correlation of gamma ray logs from well 11-22-017-16W4M with well 16-25-017-18W4M, which has a lithology log, and wells 15-05-019-18W4M and13-09-019-18W4M, which are producing from a thick Basal Belly River sandstone. The logs are flattened on an event in the Belly River Formation, approximately at the top of the Foremost Formation.

Preparing for experimental CO_2 injection: Seismic data analysis

J. Helen Isaac and Don C. Lawton

ABSTRACT

We processed and interpreted a small new 1 km x 1 km 3D seismic survey in the study area in Southern Alberta. This area is of interest for planned experimental CO_2 injection into sandstones in three formations; the Basal Belly River at about 285 m, the Medicine Hat at 475 m and the Second White Speckled Shale, at 710 m. An example of cross-line data is shown in Figure 1.

The processing included noise attenuation, Gabor deconvolution and post-stack time migration. We also filtered the data after NMO to remove strongly dipping events.

We interpreted the data and made time and depth structure maps. We also mapped the formation tops from wells. In general there is gentle geological dip to the northwest. In the immediate area of interest (section 22, R017 T18W4M) the surface elevations vary by only about 7 m.

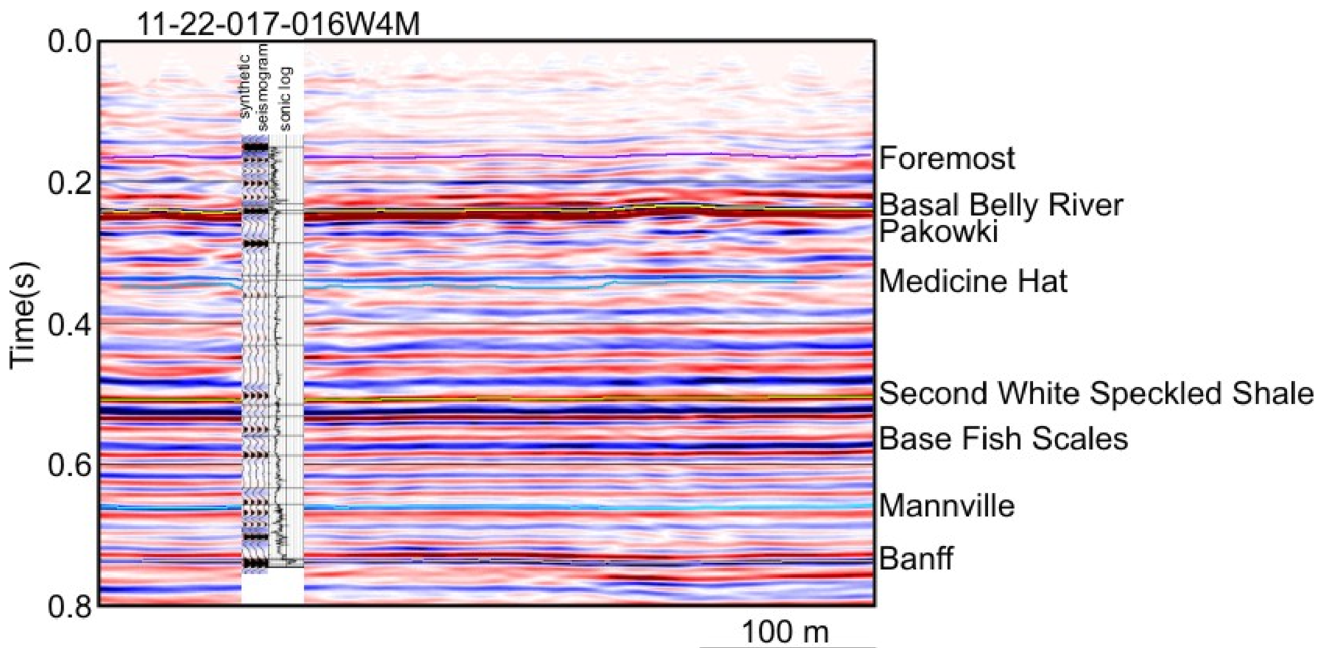

FIG. 1: Synthetic seismogram for well 11-22-017-16W4M and a crossline from the new 3D survey with interpreted horizons.

Towards application of nonlinear time-lapse AVO to the Pouce Coupe data set

Shahin Jabbari, Jeff Grossman, Helen Isaac and Kris Innanen

ABSTRACT

A multicomponent time-lapse seismic data set was acquired during hydraulic fracturing of two horizontal wells in the unconventional Montney Reservoir at Pouce Coupe Field in the Peace River area by Talisman Energy Inc. An increase in pore pressure has been induced following the hydraulic fracture operations in the unconventional Montney shale reservoir. This will affect the seismic parameters including P-wave and S-wave velocities and density of the subsurface, which can be approximated by applying time-lapse AVO (amplitude variation with offset) analysis methods. In this study, we are analyzing this data to validate our linear and nonlinear theoretical results for the difference data during the change in a reservoir from the baseline survey relative to the monitor survey. Prestack time migrated common depth point gathers (PSTM CDP) for the baseline and two monitor surveys are used. Due to the tight nature and low permeability of the Montney reservoir, the injection of fluid into the reservoir during the fracture operations will affect only the close vicinity of the fractures. For this reason, the change in P-wave velocity should be investigated in the vicinity of the hydraulic fractures in the horizontal wells. We have initiated the investigation and are analyzing methods to quantify the P-wave time-lapse difference AVO, and now well-positioned to pick events whose time-lapse AVO signatures may be analyzed for nonlinearity. Also monitoring any converted wave time-lapse changes can lead to modeling the hydraulic fracture stimulation. Data analysis is still under review pending more well data information.

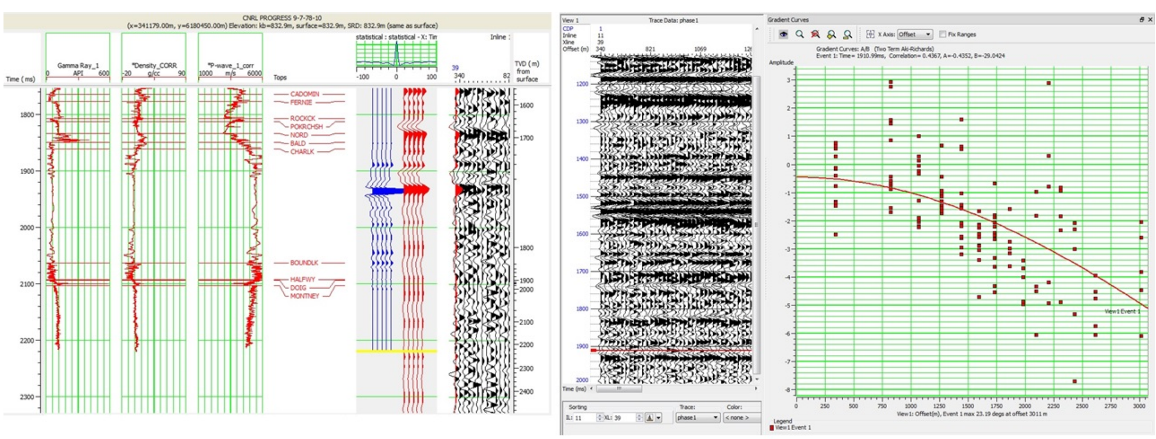

A B

FIG 1. AVO analyzing the Montney reservoir in Pouce Coupe area: (A) Vertical well tie with baseline P-wave seismic and (B) Amplitude versus offset for offset and azimuth ranged from 340-3011 meters and 0-360 degrees respectively.

Azimuthal AVO and curvature

Jesse M. Kolb*, David Cho[1] and Kris Innanen

ABSTRACT

Azimuthal AVO can be used to determine anisotropic elastic parameters in the subsurface. AVO methods often separate the effects of elastic parameters on the reflection coefficient into three terms: intercept, gradient, and curvature. In this paper we show that the gradient is characterized by multiple independent terms that change with azimuth, leading to nonuniqueness when used to characterize anisotropy, while the curvature term is only influenced by a single term proportional to the change in horizontal P-wave velocity across the interface along an azimuth. This gives the curvature the capability of determining anisotropy without ambiguity and makes it a useful quantity to estimate, especially when it is combined with the gradient.

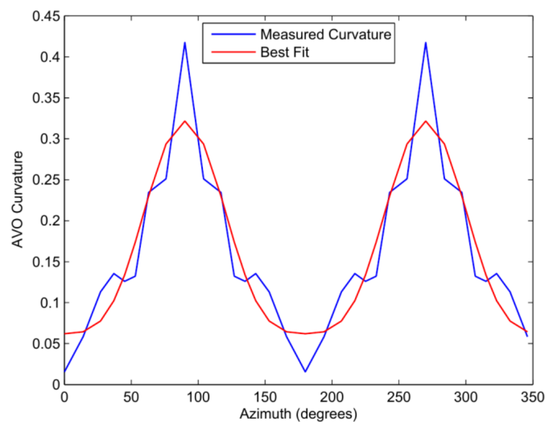

Fitting the AVO curvature measured from physical modeling data from Mahmoudian (2013).

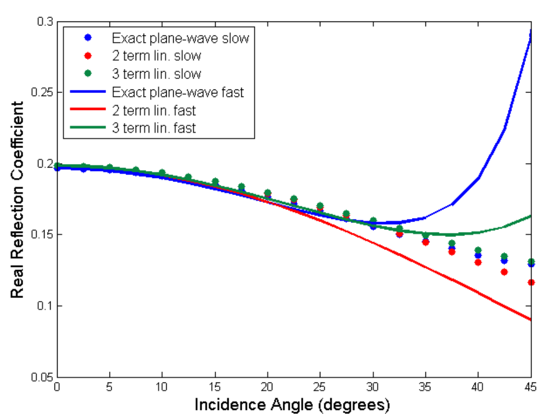

Error in linearized approximations at large angles for large contrasts. This error propagates to the magnitude of the estimated curvature.

[1] Qeye Labs Canada

Series analysis of anisotropic reflection coefficients for inversion

Jesse M. Kolb, Kris Innanen and David Cho[1]

ABSTRACT

Azimuthal AVO analysis is typically performed using linearizations of the exact formula for anisotropic reflection coefficients. These approximations often make simplifying assumptions about the types of media on each side of an interface and fail at large angles, especially when there is a large contrast in elastic parameters across the interface. Since the larger angles of incidence are more sensitive to azimuthal anisotropy, this failure can cause poor estimates of azimuthal anisotropy. In order to better understand and reduce the nonlinearity that can adversely affect inversions using linearizations, we analyze higher-order terms of the reflection coefficients. We show that the nonlinearity for large contrasts and long offsets is significant, indicating the need to use exact reflection coefficients in many situations.

$$R_{PP} = \frac{1}{4}(\delta a_{33} + 2\delta\rho) + \frac{(a_{13}^{(1)}(a_{13}^{(1)} + a_{55}^{(1)})}{2(a_{33}^{(1)} - a_{55}^{(1)})}p^2\delta a_{13} - \frac{a_{33}^{(1)}(a_{13}^{(1)} + a_{55}^{(1)})^2}{4(a_{33}^{(1)} - a_{55}^{(1)})^2}p^2\delta a_{33} + \frac{1}{8}(\delta a_{33})^2$$
$$- \frac{(a_{13}^{(1)} + a_{33}^{(1)})^2 a_{55}^{(1)}}{4(a_{33}^{(1)} - a_{55}^{(1)})^2}p^2\delta a_{55} - \frac{a_{55}^{(1)}(a_{13}^{(1)} + a_{33}^{(1)})(a_{13}^{(1)} + a_{55}^{(1)})}{(a_{33}^{(1)} - a_{55}^{(1)})^2}p^2\delta\rho + \frac{1}{4}(\delta\rho)^2 + \cdots$$

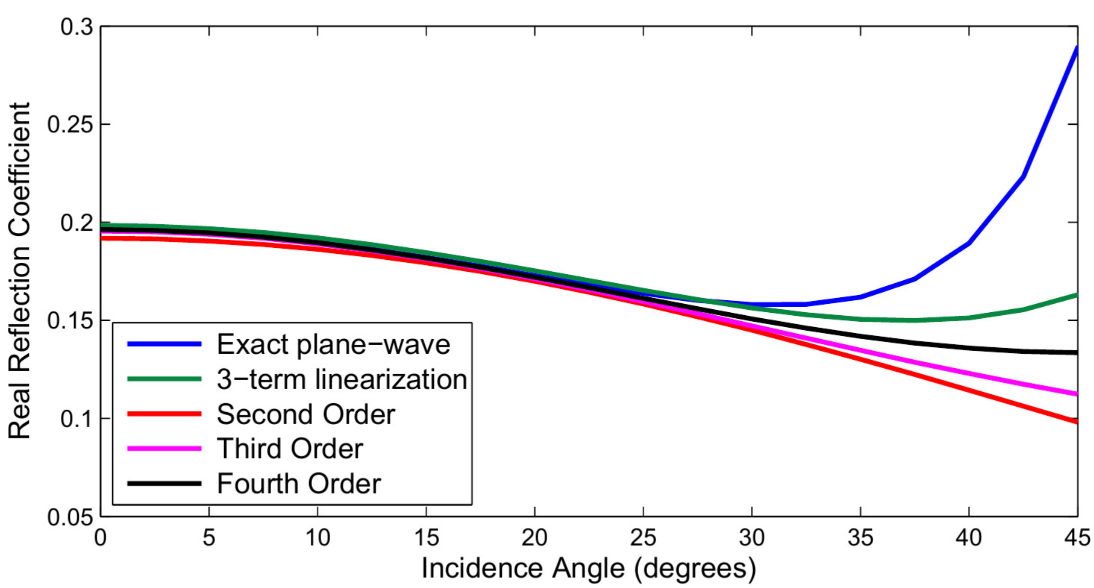

Comparison of higher order terms from a series expansion using only top-layer elastic parameters and counting angle terms as orders vs. a 3-term linearization using average-medium elastic parameters.

---

[1]Qeye Labs Canada

Non-linear Vibroseis models for generating harmonics

Michael P. Lamoureux

ABSTRACT

Vibroseis devices are a convenient seismic source for generating energy to propagate into the earth, driving a spot on surface of the earth with a controlled force that sets up a seismic wave used in the seismic imaging experiment. For a variety of reasons, harmonics are generated when a pure frequency drives the Vibroseis device – these harmonics may be considered as noise, or as extra correlated data that might be used in the imaging algorithms.

In this short project, we build several simple mathematical models for the Vibroseis device, to help to understand where these harmonics come from. The simplest models are one-dimensional non-linear oscillators, where the response of the oscillator includes non-linear effects of the earth, limiting devices on the motion, and other mechanisms that may introduce harmonics. Better models include more physical details of the Vibroseis device – the motion of the reaction mass, the baseplate, the control machinery, and so on. These require a system of ordinary differential equations to represent the mathematics. Not all models are able to capture all the harmonic details of the Vibroseis device.

We make use of the Gabor transform to view the time-frequency characteristics of the seismic signal generated in these Vibroseis models. This provides a simple test to verify the presence and behavior of the harmonics in these signals.

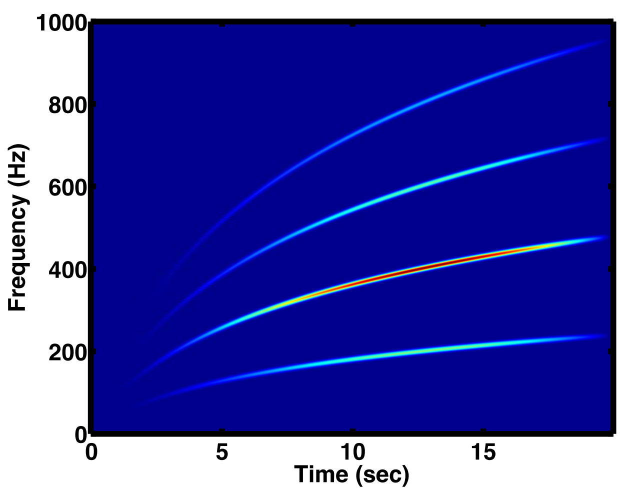

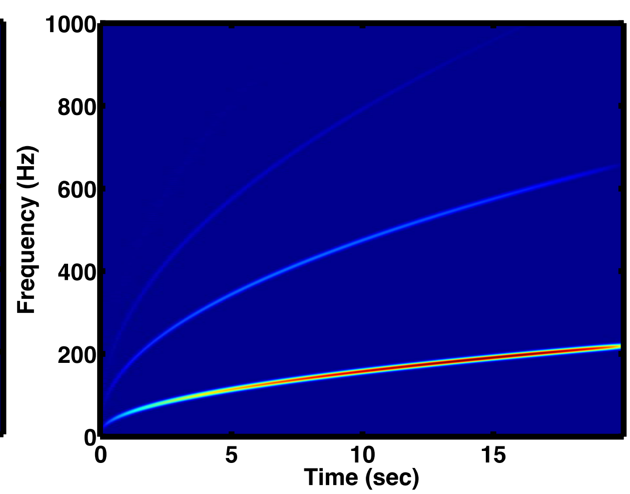

Baseplate recording, time-frequency display.	Nonlinear Vibroseis model – missing harmonics

A 3C-3D seismic survey at a new field research station near Brooks, Alberta

Don Lawton*, Malcolm Bertram, Kevin Bertram, Kevin Hall and Helen Isaac

ABSTRACT

A high-resolution 3C3D seismic survey was undertaken in May, 2014 as a baseline seismic survey for a new field research station (FRS) being developed by CMC Research Institutes, Inc. and the University of Calgary in Newell County, Alberta. The goal of this research station is to develop and calibrate various monitoring technologies for CO_2 detection thresholds at relatively shallow depths and for assessing and monitoring cap rock integrity. The specific objectives being assessed at the FRS are sensitivity of monitoring systems for early detection of loss of conformance and in mapping temporal changes in cap rock that may lead to loss of containment. The FRS is being constructed on lands southwest of Brooks, Alberta, and the 2.5 km^2 site will operate for at least 10 years. Construction has begun on an array of wells, sensing stations, and surface facilities that will be monitoring fluid injection and cap rock behaviour at depths of 300 m and 500 m below surface. Technologies being evaluated will include time-lapse surface and borehole seismic surveys, microseismic surveys, geochemical, cross well, electrical resistivity, electromagnetic, gravity, geodetic and geomechanics surveys. CREWES will have an active role in processing and undertaking research on seismic data collected at the FRS.

Figure 1a shows the layout of the 1 km x 1 km seismic survey, which comprised 1400 3-component geophones and 1434 shots (2 x Envirovibe source). This display shows PS fold for a target depth of 500 m, overlain by a projection of PS raypaths for a common conversion point near the centre of the survey area. PP data quality is excellent, as shown by the display in Figure 1b. PS data are noisier and are currently being processed.

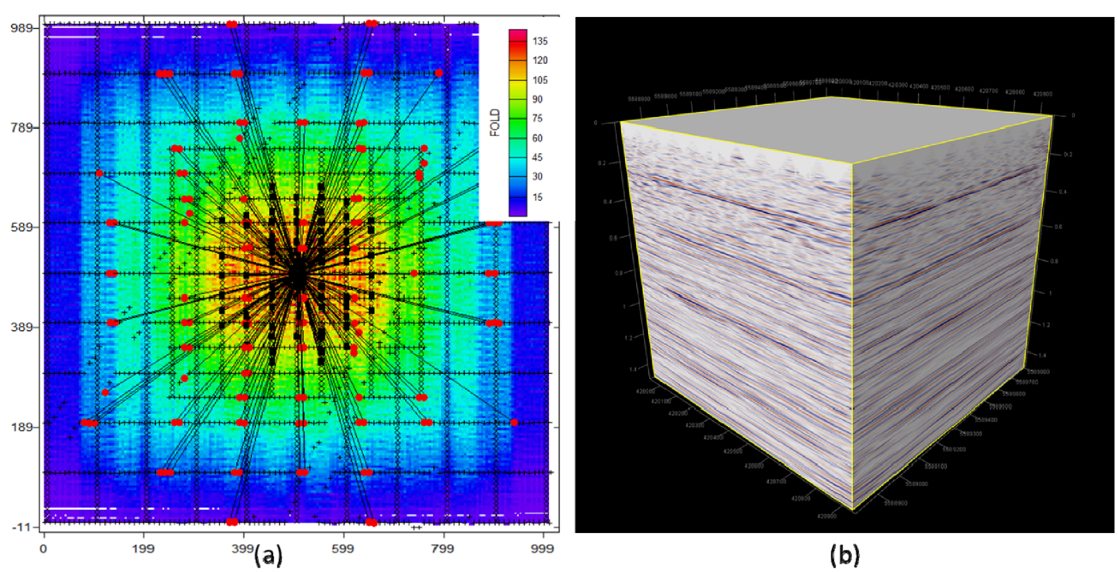

FIG. 1. PS fold and trace projection for 500 m target depth; (b) PP processed seismic volume.

FWI and the "Noise" Quandary

Laurence R. Lines*

ABSTRACT

Full waveform inversion (FWI) has been termed the most general inversion method in which we attempt to model every digital sample in the seismic trace by adjusting model parameters so that the discrepancies between data and model response are minimized – often in a least squares sense. FWI attempts to model every data sample, even though the data values be signal contaminated with "noise". This begs the question. What is noise? This paper attempts to define "noise" and how it might affect FWI.

If we consider noise as that part of the seismic data that is not related to physical properties of the Earth's interior, then noise could be due to wind, waves, traffic, instrument effects and power lines. For cases where this type of noise is random, the least-squares implementation of FWI is robust as shown in the model tests of Figure 1. Here the synthetic data has signal-to-noise (S/N) ratios of infinity (no noise), S/N=2.5, S/N=5.0. While the error of fit in each case worsens with increasing noise, the inversion estimate for seismic-Q converges to the correct solution in three iterations for each case.

If we considered multiples to be signal that can be inverted, then least-squares inversion is shown to provide reliable estimates of reflection coefficients through fitting the multiple energy. That is, through FWI, multiple energy can be used to estimate the Earth's reflectivity. Examples show FWI of multiples can be used to estimate reflectivity.

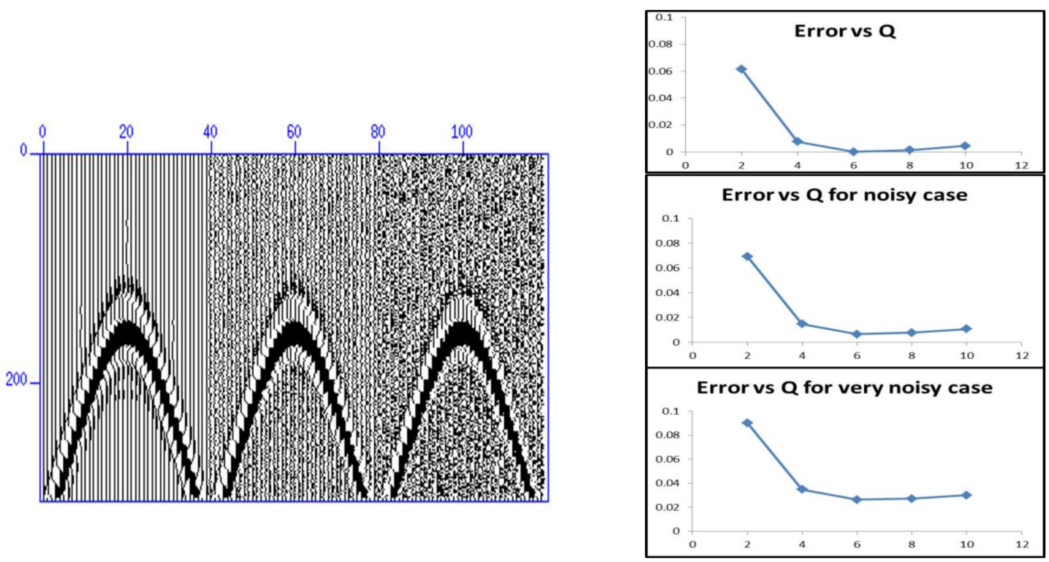

FIG. 1. Seismic model data (left) with various signal-to-noise ratios of infinity, 5.0 and 2.5 were inverted to estimate Q value of 2 pi (6.28). While the error of fit worsened with increasing noise, all inversions converged close to the correct value within 3 iterations.

Minimized energy used to determine displacements at an internal boundary (finite-difference models)

Peter M. Manning

ABSTRACT

The necessity for use of a unique calculation method for internal boundary conditions, as opposed to edge boundary conditions, is explained. The method of minimizing energy within the rigid zone below a water bottom is developed, and the matrix equations required are presented in some detail. Preliminary model results are shown.

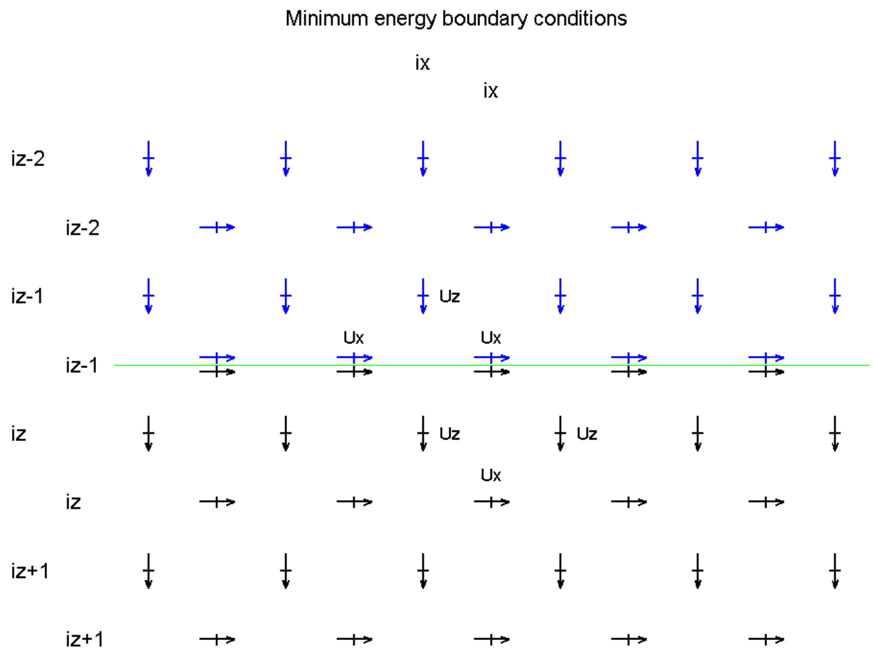

FIG 1. The displacements in the vicinity of the green line depicting the water bottom. Since there is no shear resistance within the water, displacements below and parallel to the water bottom are completely independent of those just above in the water. These lower shear displacements must be calculated directly from physical principles.

Recording seismic on geophones within ground screws

Peter M. Manning, Eric Gallant and Kevin Hall

ABSTRACT

Records were obtained from geophones installed within devices known as ground screws, normally used as bases for small buildings. The data were acquired along with other records at Priddis in November/2014. Analysis is at a preliminary stage, but comparisons may be made with surface geophones at the same recording stations. A patent on this type of recording is held by Ross Huntley.

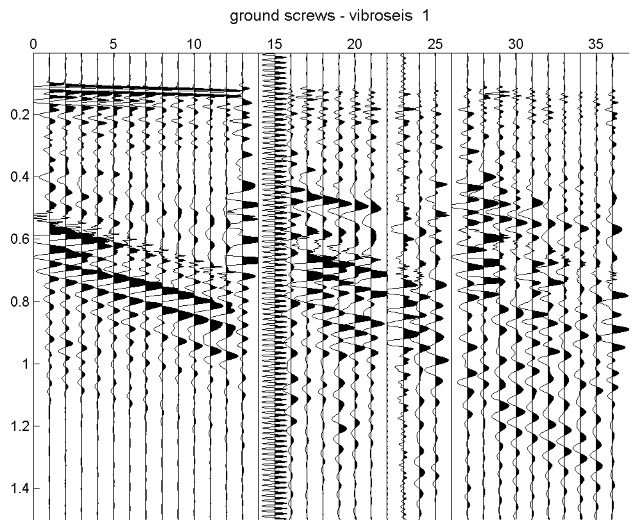

FIG 1. Data recorded from geophones installed in ground screws. There are 12 traces each of vertical data, in-line horizontal data, and cross-line horizontal data. The horizontal data show problems with element installation, but there are indications of less shallow noise.

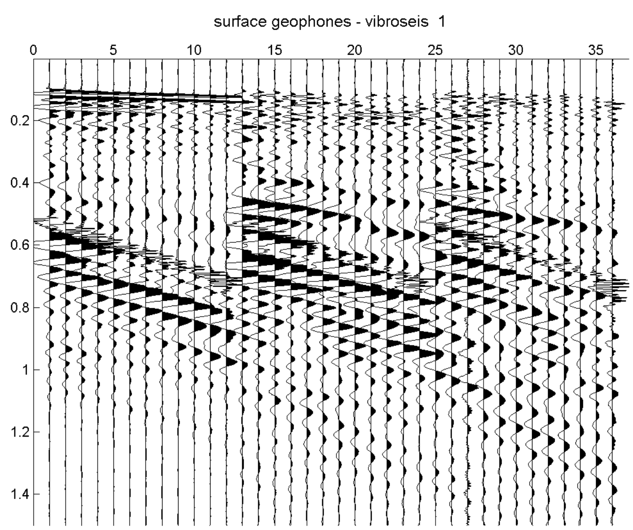

FIG 2. Data recorded from conventional surface three-component geophones with identical elements for comparison.

CREWES 5-year research plan: Towards broadband multicomponent seismology and practical iterated inversion

Gary Margrave, Kris Innanen, Don Lawton, John Bancroft, Michael Lamoureux, and Larry Lines

ABSTRACT

Seismic images provide the best possible views of the earth below its surface; but, despite an 80 year history, they are still far from optimal. Today, the computer methods used to create such images are transitioning from a standard methodology (SM), which incorporates an evolved blend of physical theory and practical experience, to the very modern full-waveform inversion (FWI) that is much more firmly rooted in mathematical physics. However, this transition is hindered by insufficient low-frequency content in seismic data, by the inherently unknown seismic source waveform, by incompletely understood physics, and by the extreme computational effort required. As a consequence, SM is the dominant approach while FWI is rarely attempted outside of dedicated research labs. SM uses a sophisticated data processing sequence to create a reflectivity image of the subsurface. Then, incorporating well information, an inversion process converts the reflectivity image to earth properties such as impedance. FWI is a fundamentally iterative process that converges on an impedance model by minimizing the difference between real and predicted seismic data. FWI never creates a reflectivity image and does not use well control; while SM does not predict synthetic data and is not iterated. We will create a new class of seismic inversion methods that combines the most robust features of SM with the most promising concepts from FWI. From SM, we will retain most of the data processing steps, the creation of a reflectivity image, and the matching to well control. In particular, matching to well control facilitates the source waveform estimation and provides the needed low frequency information. From FWI, we will incorporate the concepts of iteration, prediction of synthetic seismic data, and imaging of the data residual. The proposed approach, which we call IMMI (Iterated Modelling, Migration, and Inversion), will produce estimates of subsurface properties that both match measurements in wells and also predict most features in the recorded seismic data. Such estimates should be much more reliable than those presently achieved by SM. This will have significant benefits to resource exploration and to subsurface environmental studies.

Figure 2: The Standard Methodology (SM)

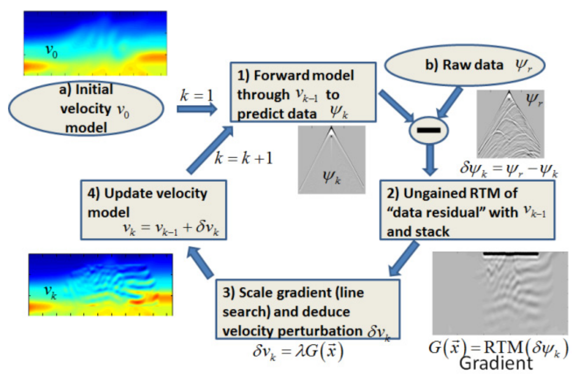

Figure 1: Full Waveform Inversion (FWI)

Stratigraphic filtering and Q estimation

Gary F. Margrave*

ABSTRACT

The long-standing prediction that a seismic wave propagating in a finely layered earth model displays an apparent attenuation is investigated. Called stratigraphic filtering, this effect looks much like constant-Q attenuation and adds to intrinsic attenuation to produce effective attenuation. Using a 1D synthetic seismogram algorithm, this paper calculates the effective attenuation in a sequence of finely layered models derived from well logs. The models all have a finely-layered Q structure, representing intrinsic attenuation, derived from measured density and sonic logs by an empirical relation. The model properties are all sampled at 0.5 m intervals and averaged into constant thickness layers. Using 1m layers, when the Q value is carefully measured using the spectral-ratio technique, the measured Q is always lower than that expected from the specified model. In a series of experiments in which various physical effects are turned off and on again, it is demonstrated conclusively that this Q bias (measured Q - model Q) is due to internal multiples. Using a series of models derived from the same logs but with progressively thicker layers (each model has constant thickness layers and each is sampled a 0.5m) it is demonstrated that there is significant Q bias for layer thicknesses less than 20m but for thicknesses greater than 20m the Q bias disappears. The feasibility of estimating stratigraphic Q from such experiments and using these measurements to correct measurements fro-m field data is discussed.

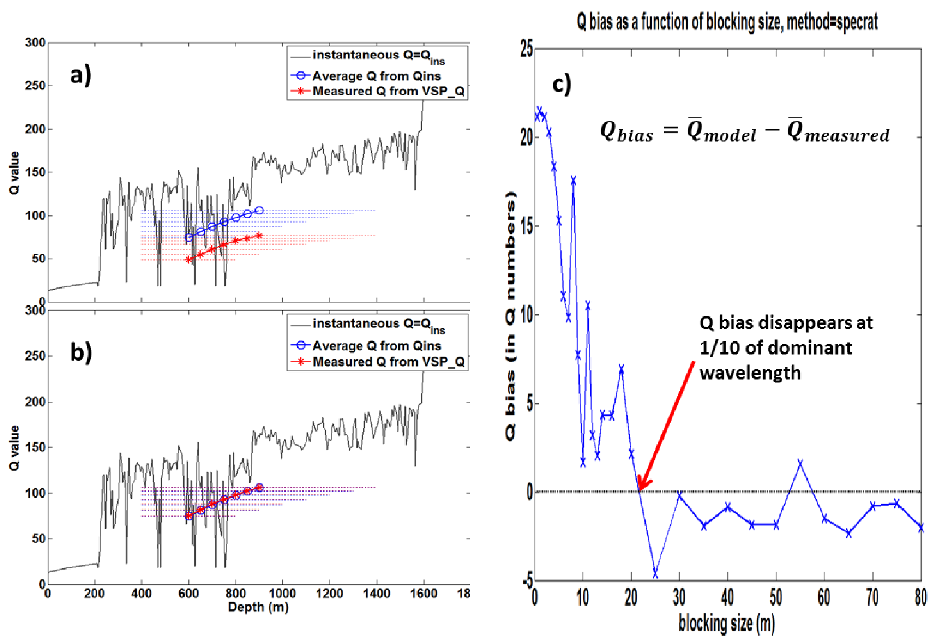

a) Measured Q (red) and modelled Q (blue) from finely layered model. b) Similar to a) except that internal multiples are turned off. c) Plot of Q bias versus model blocking (layer) size.

VSP modelling in 1D with Q and buried source

Gary F. Margrave and P.F. Daley

ABSTRACT

A published method for the calculation of 1D synthetic seismograms with constant-Q attenuation is described and extended to the case of a VSP with a buried source. Based on layer matrices (or propagator matrices) the method is very accurate for a broad frequency range from low to high and efficiently models fine layering. Each layer has unique velocity, density, and Q and can be of any thickness. Receivers can be placed at any depth and upgoing and downgoing fields are computed separately. Extensions that allow internal multiples, surface related multiples, and attenuation to be included or not, are described. The method runs rapidly (a minute or less) in native Matlab code even with thousands of layers. This is suitable to study the effect of internal multiples and attenuation on a synthetic seismogram or VSP. The method also has the ability to create both pressure and displacement responses making it suitable to studying both geophone and hydrophone recordings. Examples from a simple conceptual model and from well logs are shown.

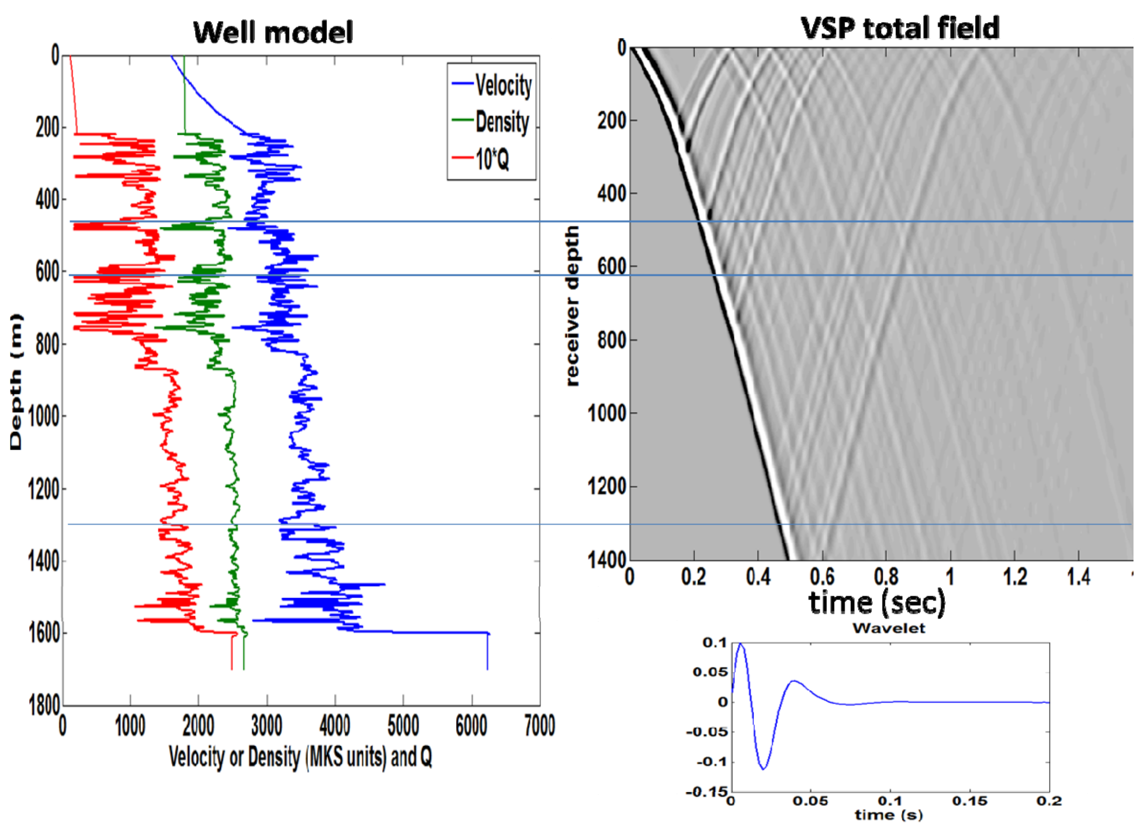

A synthetic VSP (for displacement) computed directly from well logs for a surface source is shown. The density and velocity curves are from measured logs while the Q curve is estimated from the logs by an empirical relation.

Shallow QP and QS estimation from multicomponent VSP data

Michelle C. Montano*, Don C. Lawton, and Gary F. Margrave

ABSTRACT

VSP data give us direct access to the wavelet at different receiver depths without having to include reflections. The down-going wavefield has always been the key to estimate Q and correct the effects of seismic attenuation on the data. In this study we demonstrate that we can also use the up-going wavefield to estimate Q, particularly for the shallow, near-surface layers. Q factors are estimated from synthetic VSP down-going and up-going wavefields by using the dominant frequency matching method (CREWES). We also estimated Q from real VSP data (Figure 1A) by using the spectral-ratio method (Vista software) as well as the dominant frequency matching method. We found the spectral-ratio method to be more sensitive to changes in the frequency bandwidth when we compare Q estimation from vibrator to dynamite sources. Also, we found that Q estimation for shallow layers is better using the up-going wavefield than the down-going wavefield. Combining both estimations provides the optimum understanding of Q variation with depth (Figure 1B).

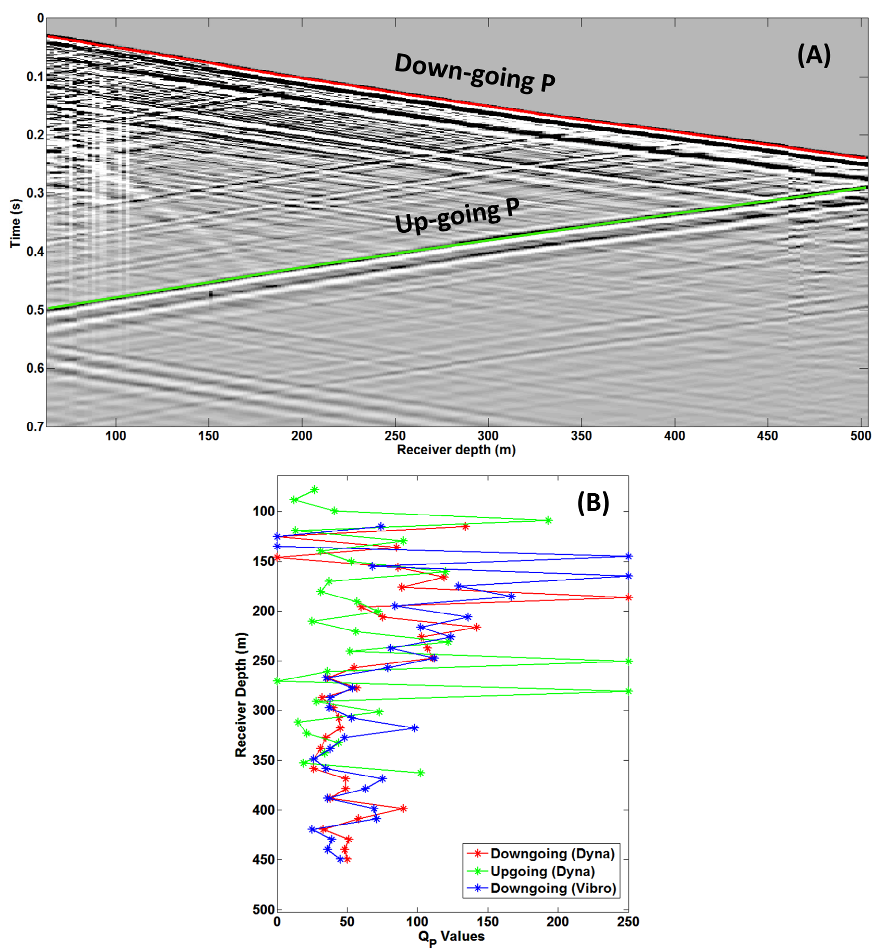

FIG. 1. (A) VSP data (Dynamite Source), (B) Q_P estimation using the dominant frequency method.

Time-lapse poroelastic modelling for a carbon capture and storage (CCS) project in Alberta

Shahin Moradi*, Edward S. Krebes and Don C. Lawton

ABSTRACT

A finite-difference algorithm was developed based on the Biot's equations of motion for modelling the wave propagation in poroelastic media. In contrast with the elastic modelling, in the poroelastic approach the properties of the pore fluid are taken into account in the algorithm. Poroelastic modelling could be useful in cases where the fluid content of the rock is of interest, i.e. Carbon Capture and Storage (CCS) projects. We examined our program using a model based on the Quest CCS project in Alberta to investigate the detectability of CO_2 after one year of injection. This was done by defining two models for baseline and monitor scenarios that represented the subsurface before and after injecting CO_2. The difference between the calculated seismic sections for the two scenarios shows that the residual amplitude is comparable with the signal amplitude (Figure 1). With this result, the injected CO_2 in the Quest project over a year could be detected providing the data have good bandwidth and a high signal-to-noise ratio. The effect of the porosity and the fluid properties on the output of the algorithm is being examined in an ongoing study.

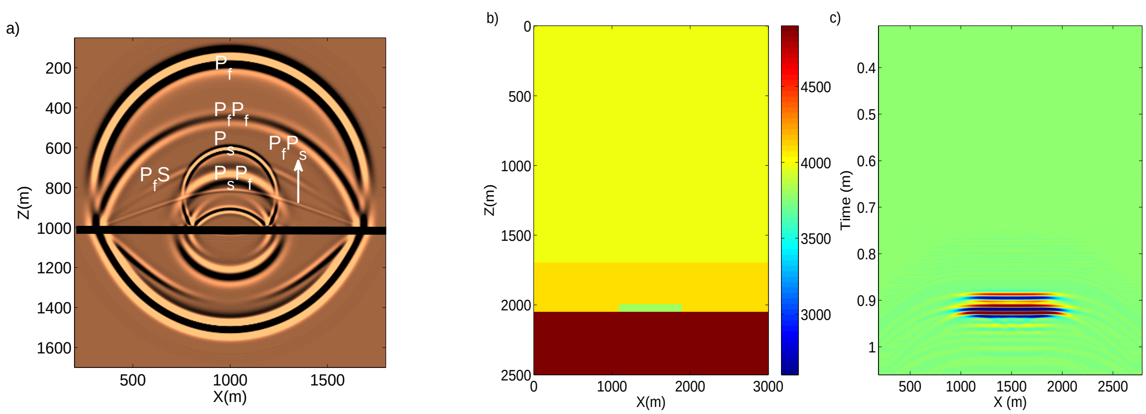

FIG. 1. a) Sample snapshot of the vertical particle velocity of the solid generated by the poroelastic algorithm for a two layer model. These layers are two sandstones with the same solid properties but different pore fluids. b) The monitor model generated based on the Quest project. The colour-bar shows the p-wave velocity of the saturated rock in meters per seconds and the green block in the depth of 2000 meters represents the CO_2 plume. c) The difference between the calculated seismic sections for the baseline and the monitor scenarios using the poroelastic finite-difference algorithm. The effect of the CO_2 appears as a residual in this section.

Numerical analysis of scattering in a viscoelastic medium

Shahpoor Moradi*, Hassan Khaniani and Kris Innanen

ABSTRACT

Recently we have developed a theoretical picture of viscoelastic scattering applicable to seismic waves propagating in arbitrary multidimensional geological volumes. The purpose of this research is to begin to integrate this theoretical analysis with numerical analysis. That combination will permit very general versions of attenuation/Q related analysis, processing, and inversion in multicomponent seismic to be formulated. Here we used the code developed by Martin and Komatitsch (2009) to simulate the reflections caused by general viscoelastic contrasts designed to be comparable to the results from the Born approximation. We apply the code to a viscoelastic geological model involving a contrast between two layers with different elastic and anelastic properties. We show that the anelastic contrasts generate reflection amplitudes which quantitatively are in agreement with those derived theoretically by Moradi and Innanen (2013).

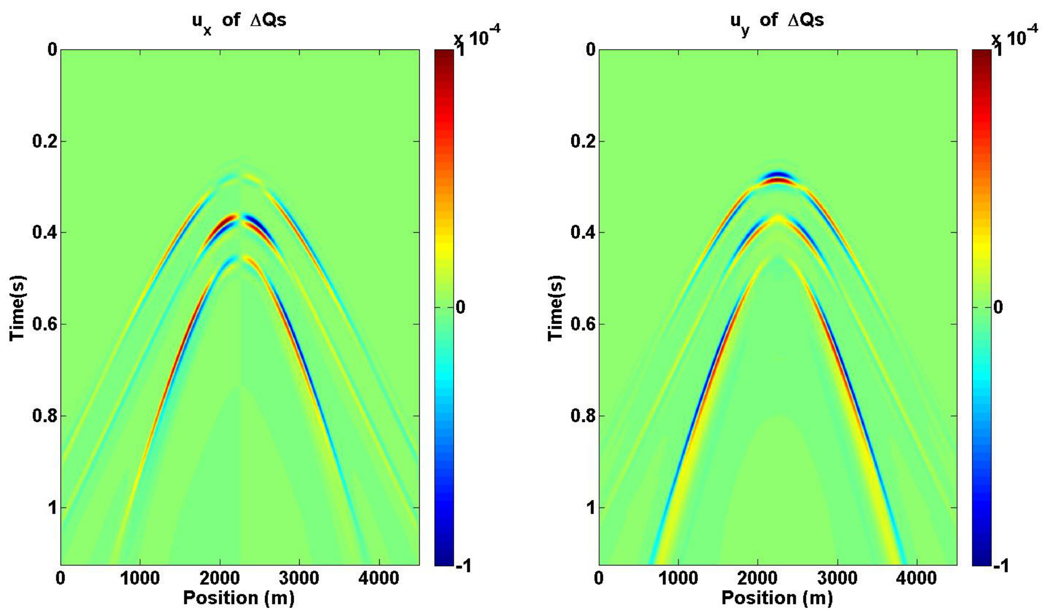

FIG. Simulated seismic data corresponding to the contrast in quality factor for S-wave velocity Q_S. The left figure is the x-component of displacement and right is the y-component of displacement.

References

Martin, R., and Komatitsch, D., 2009, An unsplit convolutional perfectly matched layer technique improved at grazing incidence for the viscoelastic wave equation: Geophysical Journal International, 179, No. 1, 333–344.

Moradi, S., and Innanen, K. A., 2013, Viscoelastic scattering potentials and inversion sensitivities: CREWES Research Report, 25.

Partial wave analysis of seismic wave scattering

Shahpoor Moradi and Kris Innanen

ABSTRACT

Developments in seismic full waveform inversion have brought a renewed interest in the scattering picture of wave propagation in recent years. Our experience has been that advances in our understanding of particular aspects of scattering has led rapidly to a concurrent advance in our understanding of how to pose and analyze practical seismic inversion methods. In this research we study the partial wave analysis of elastic wave scattering in an isotropic radially heterogenous medium in the context of Born-approximation. We show that in the presence of a scatterer there is a phase shift in the outgoing scattered spherical elastic wave. We also obtain the scattering amplitudes for scattering of P- and S-wave in terms of phase shift for P-, SV- and SH-waves. We show that the phase shifts can be calculated using the Lippman-Schwinger integral equation. A clear and consistent theory of elastic partial wave scattering will lead to better sensitivity or Jacobian matrices, a critical matter for the success of elastic seismic full waveform inversion.

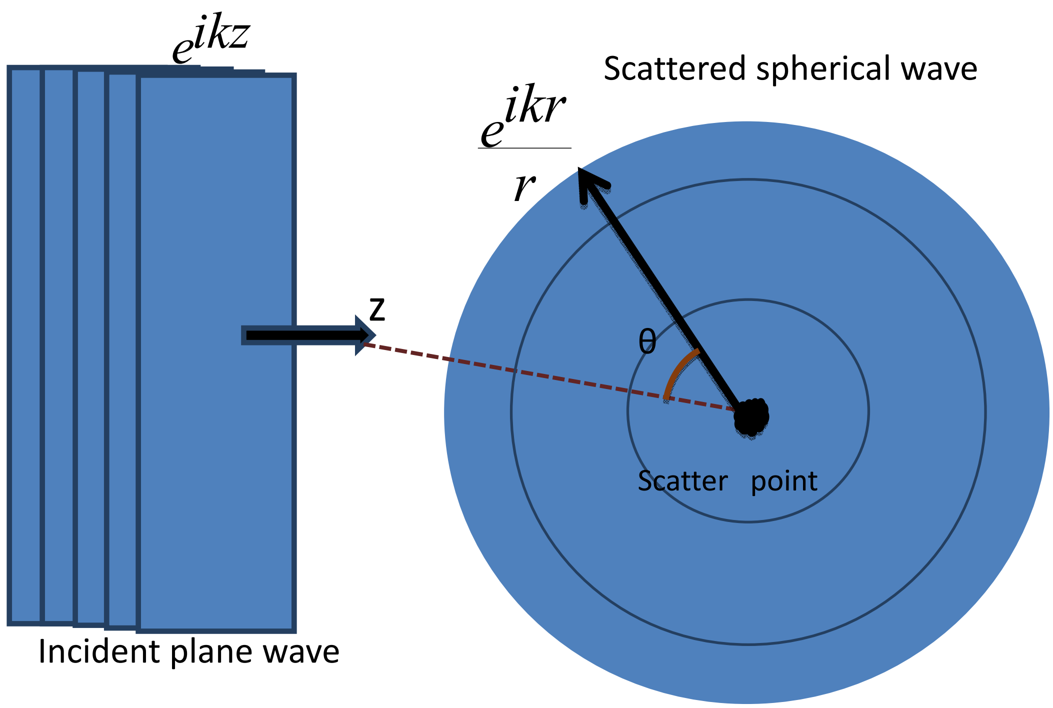

FIG. Scattering from a localized Scatterer. Incident plane wave after scattering changes to a spherical wave with an angle dependent distribution called scattering amplitude which modulates the outgoing wave according to direction. It carries all the physics information.

Scattering of homogeneous and inhomogeneous viscoelastic waves from arbitrary heterogeneities: update

Shahpoor Moradi and Kris Innanen

ABSTRACT

We consider the problem of scattering of homogeneous and inhomogeneous waves from perturbations in five viscoelastic parameters (density, P- and S-wave velocities, and P- and S-wave quality factors), as formulated in the context of the Born approximation. Within this approximation the total wave field is the superposition of an incident plane wave and a scattered wave, the latter being a spherical wave weighted by a function of solid angle called the scattering potential. In elastic media the scattering potential is real, but if dissipation is included through a viscoelastic model, the potential becomes complex and thus impacts the amplitude and phase of the outgoing wave. We show that elliptically polarized P- and SI- waves cannot to leading order be scattered into linearly polarized SI-waves. Furthermore, the elastic formulation is straightforwardly recovered in the limit as P- and S-wave quality factors tend to infinity.

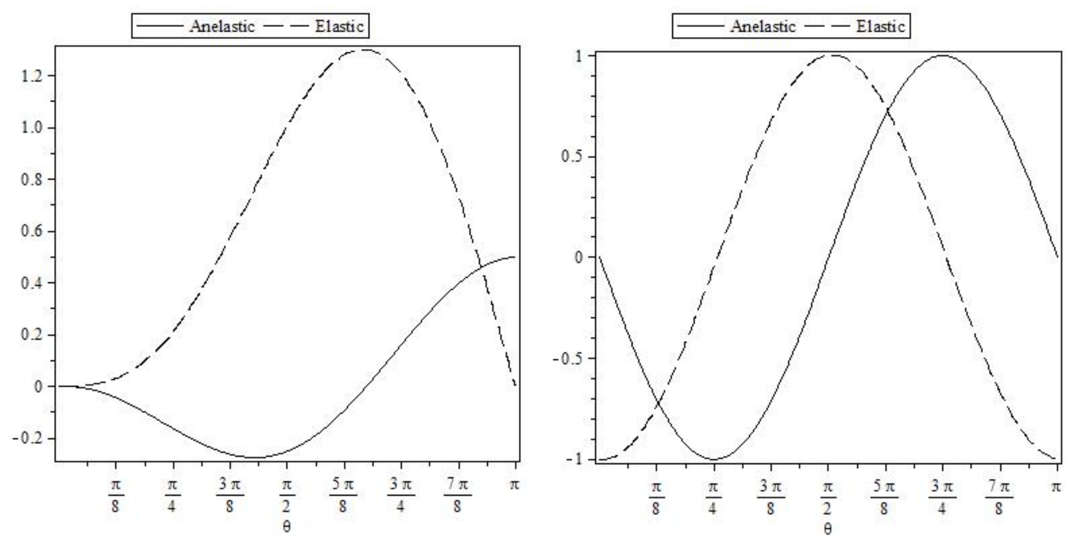

FIG. Elastic and anelastic density (left) and S-velocity(right) components of the viscoelastic potential for scattering of incident homogeneous P-wave to inhomogeneous reflected SI-wave versus of reflected wave angle, for attenuation angle $\frac{\pi}{3}$, $Q_P = 5$, $Q_S = 7$ and S-to P-velocity ratio is chosen to be 0.5. Dash line is for elastic part and solid line for anelastic part.

Some exact forms for viscoelastic reflection coefficients

Shahpoor Moradi and Kris Innanen

ABSTRACT

An explicit analytical form of the scattering matrix for Homogeneous Isotropic Linear Viscoelastic (HILV) continuum is obtained. The reflection and transmission are the complex function related to the P- and S-velocities and corresponding quality factors Q_P and Q_S. The real part is the elastic scattering potential and the imaginary part is the term induced by the anelasticity of the medium. Linearized reflection coefficients can be used for viscoelastic AVO/AVA and full waveform inversion.

$$(\downarrow PP \uparrow)_{VISCO} = (\downarrow PP \uparrow)_{ELASTIC} + i(\downarrow PP \uparrow)_{ANELASTIC}$$

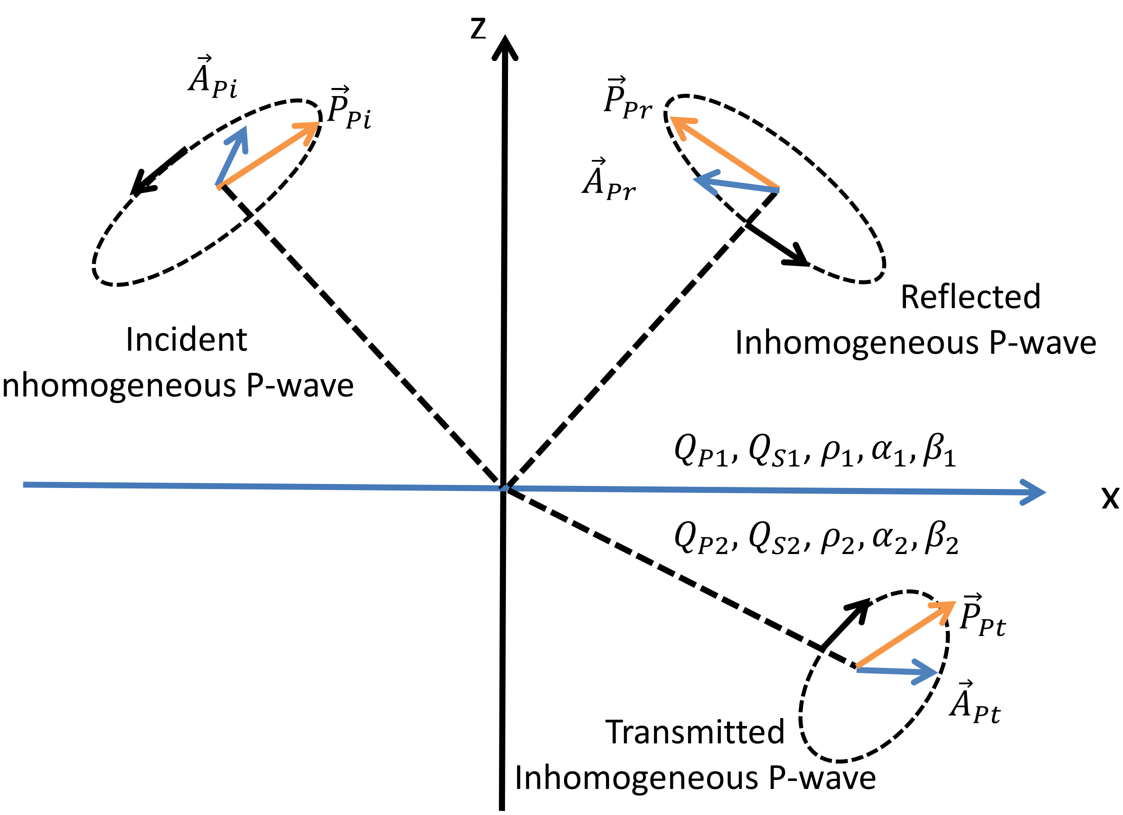

FIG. Diagram illustrating notation for directions and magnitude of propagation (P) and attenuation (A) vectors for the scattering of an inhomogeneous P-wave to an inhomogeneous P-wave.

Rock physics study of the Nisku aquifer from results of reservoir simulation

Davood Nowroozi and Donald C. Lawton

ABSTRACT

This paper is part of the comprehensive reservoir study in the Wabamun Area for CO_2 sequestration in the Nisku aquifer. Rock physics is the link between reservoir simulation and 4D seismic. The paper engages rock physics to calculate physical parameters for the solid part, fluid and jointly in the reservoir due to CO_2 injection to the Nisku aquifer in the project. The study is based on a new well drilled in the area. The density and wave velocities in the fluids are a function of the pressure and temperature. For CO_2 physical properties, the equations of state and for brine, paper were bases for the calculations. In the reservoir, the fluid is a mix of CO_2 and brine with various fractions of them, and Reuss average is used to calculate the mix fluid properties. Finally some equations are introduced for the fluid properties for the specific reservoir condition.

Gassmann's equations were used for estimating the saturated bulk modulus and the velocity in the each cell of the reservoir is available, so each cell has own physical model as a function of the pressure and the injection time as this process is isothermal. Examples of the cellular model are shown in Figure 1.

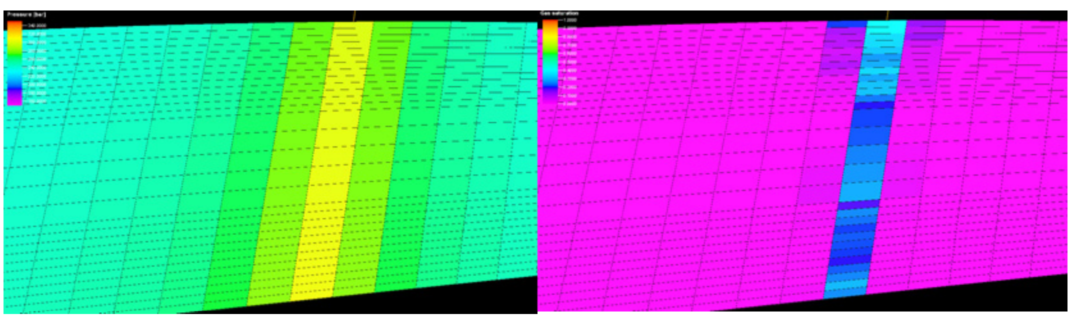

FIG. 1. Pressure (left) and CO_2 saturation (right) change around injection well after one year of injection (1 m tonnes).

Seismic parameter design for reservoir monitoring, Brooks, Alberta

Davood Nowroozi and Donald C. Lawton

ABSTRACT

The main objective of this paper is to evaluate a 3D-3C seismic survey in order to make possible 4D and reservoir studies to monitor CO_2 injection and map the underground layers and structures. A porous and permeable formation (the Medicine Hat sandstone) as a reservoir with reliable cap (low permeability) that is the Colorado shale are injection targets for CO_2 sequestration and also for the seismic survey design. The project area is a field located southwest of Brooks, Alberta. The first part is data gathering and analysis results for velocity functions and desired frequency content of targets (shallow and deep) and the second part is the parameter estimation for preventing spatial aliasing and suitable resolution for the reservoir study. For the bin size and migration aperture estimation, constant and linear velocity methods were considered. Finally, two options are introduced and their attributes (fold map for PP and PS data with different offset, offset and azimuth distribution) are compared. Some of these are shown in Figure 1.

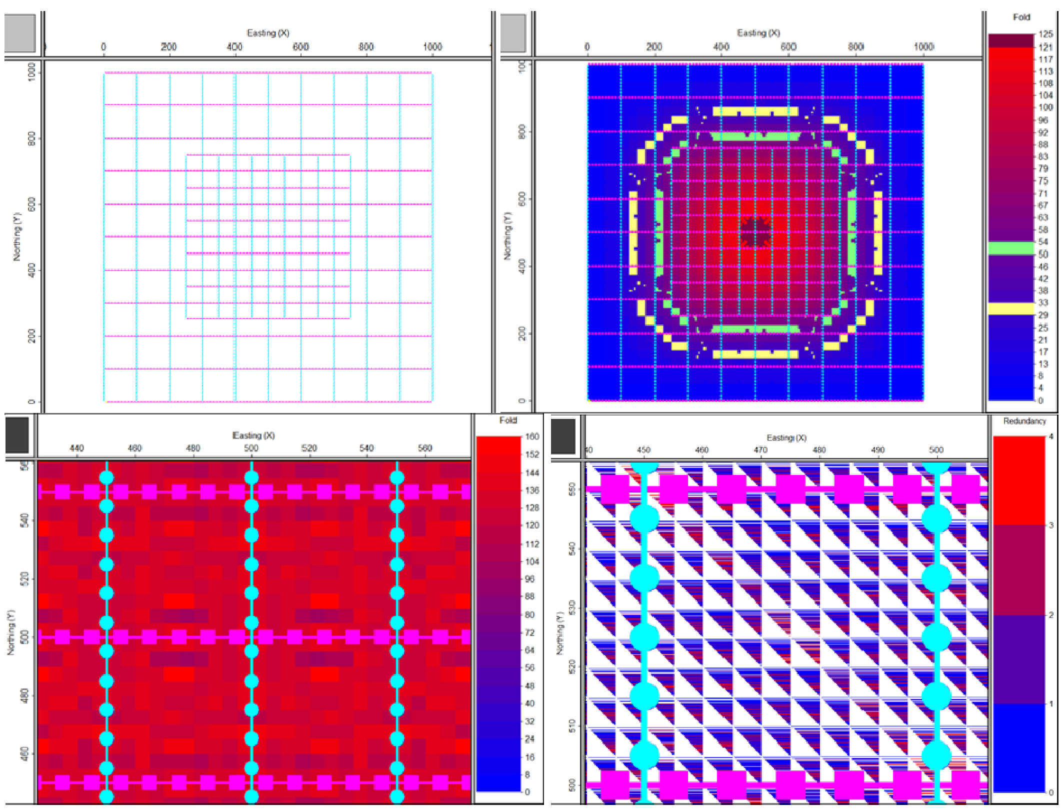

FIG. 1. Acquisition pattern, PP fold for offset 0-700 m and PS fold map (with non-asymptotic PS conversion points) for 500m depth in the central part, and PP offset distribution.

1.5D internal multiple prediction on physical modeling data

Pan Pan*, Kris Innanen and Joe Wong

ABSTRACT

Multiple attenuation is a key aspect of seismic data processing, with the completeness of multiple removal often significantly affecting final image results. In this paper, we analyze 1.5D internal multiple prediction on physical modeling data simulating a 2D marine seismic survey designed to generate significant internal multiples. We describe a processing flow appropriate for preparation of the data for input into multiple prediction. Then we examine a 1.5D (i.e., pre-stack data over a layered geology) implementation of the inverse scattering series internal multiple prediction. The results show good agreement of predictions compared against synthetic data and physical modeling data. We discuss the selection of the integral limit parameter ϵ and the influence of free-surface multiples. We also demonstrate that the beginning and ending integration points of frequencies, wavenumbers, and pseudo-depths in the code can be optimally chosen to reduce computational burden.

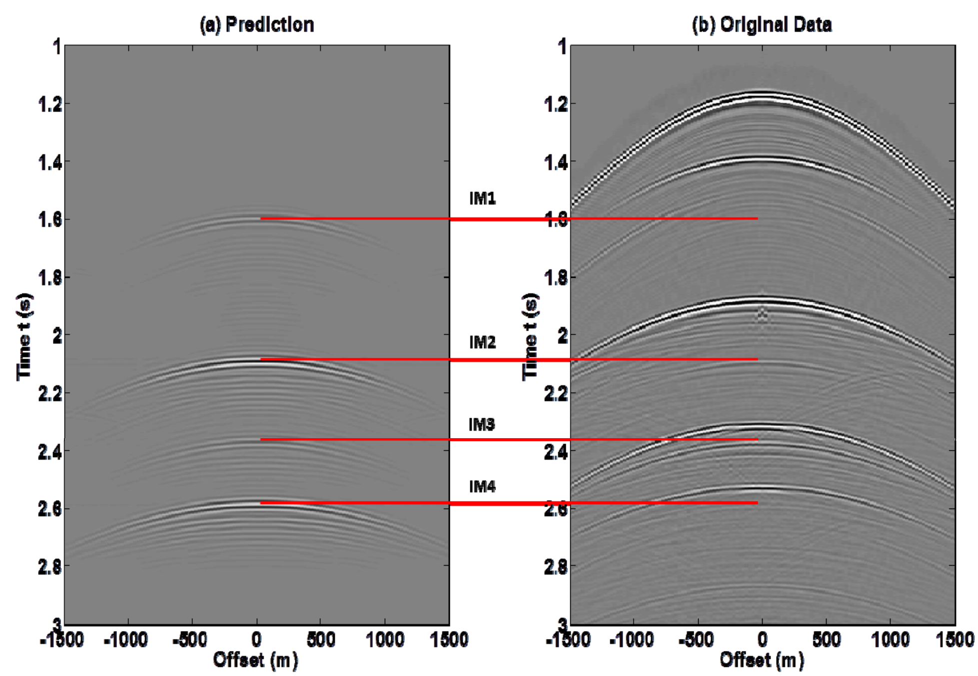

FIG. 1. Comparison of prediction output with input. (a) Prediction output; (b) input data. The red lines indicate the positions of internal multiples in both input and output data.

Internal multiple prediction on Hussar synthetics

Pan Pan and Kris Innanen

ABSTRACT

The inverse scattering series internal multiple prediction algorithm is often called upon due to its unique ability to predict internal multiples with no subsurface information and without compromising the primaries. This technology does not require velocity information from the subsurface or any advance knowledge of the multiple generators, and it predicts first-order internal multiples that are generated by all possible generators below the free surface. In this paper, we employ the 1.5D internal multiple prediction algorithm on Hussar synthetics. The synthetics are acquired by blocking the well 12-27 with different depth steps. We find that it can successfully predict internal multiples generated by the relatively thin layers of the Hussar geology (provided the interval between two primaries is larger than the optimal ϵ value). By extending the synthetic in offset, we see that certain prediction artifacts can be tied to land apertures.

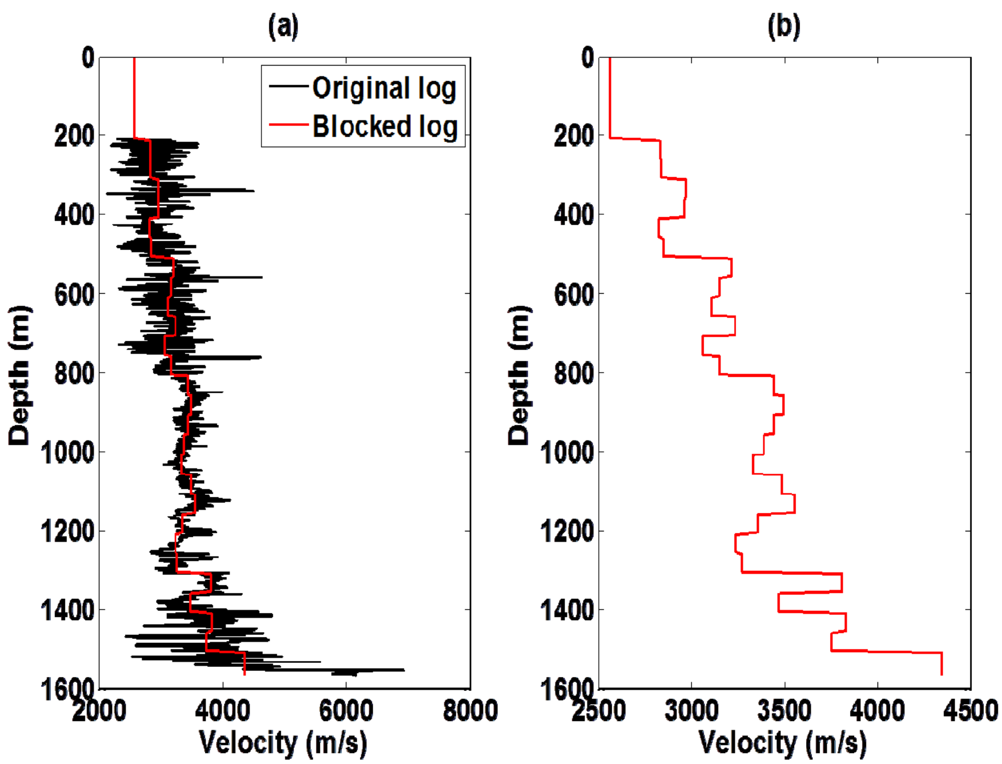

FIG. 1. A blocked v_p profile, (a) shows the original log in black and the blocked log in red; (b) shows only the blocked log. The depth step of the log being blocked is 50m.

FWI inversion sensitivities of elastic stiffness coefficients in fractured media: analytic results

Wenyong Pan, Kris Innanen, Mike Fehler, Gary Margrave and Xinding Fang

ABSTRACT

Full waveform inversion (FWI) is very powerful in estimating the subsurface properties by minimizing the difference between the modelled data and observed data iteratively. Multi-parameter FWI can also be employed to inverse the properties of the naturally fractured reservoirs, when assuming that the wavelength is much larger than the fracture size. Estimating the fracture properties using multi-parameter FWI will be challenging for several difficulties, one of which is the cross-talk problem in multi-parameter FWI. And it refers to that the seismic wavefields responses by different parameters' perturbations are coupled together. This difficulty also gives rise to the parameterization issue for multi-parameter FWI. The Fréchet derivative serves as the inversion sensitivity for the least-squares inverse problem. Furthermore, the Fréchet derivative controls the trade-off among different parameters and the amplitude variations with varying the scattering angle and azimuthal angle (in 3D) (radiation pattern) can help identify the efficiency of the parameterization and design optimal acquisition geometry. In this research, we focus on studying the inversion sensitivities of elastic constants in fractured media. We, first, review the general principle of FWI and then give the explicit Fréchet derivative for the general anisotropic media with Born approximation. The 3D Fréchet derivative with respect to different elastic constants for parallel vertical fractured media (described as HTI model) are provided. And then, we analyze the scattering characteristics due to the fractured inclusion and discuss the inversion sensitivities with varying the scattering angle and azimuthal angle.

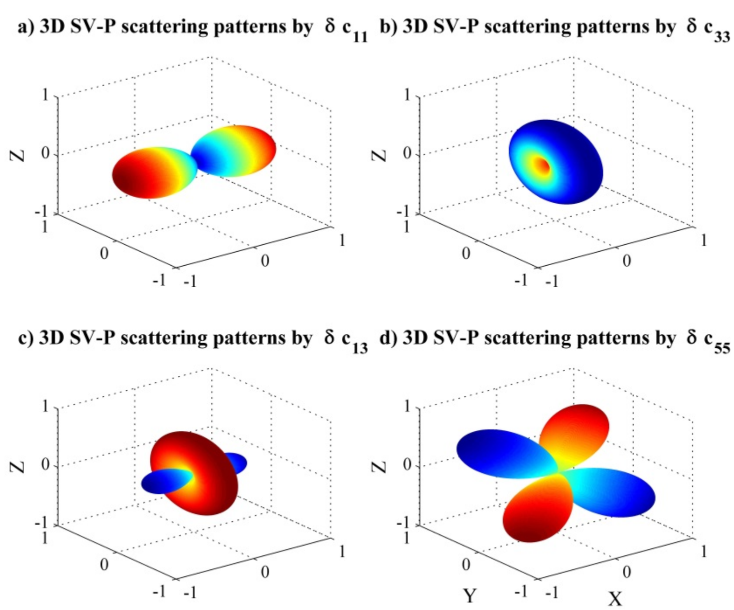

FIG. 1. 3D SV-P scattering patterns due to the perturbations of elastic constants δc_{11} (a), δc_{33} (b), δc_{13} (c) and δc_{55} (d) in transverse isotropic media respectively.

FWI inversion sensitivities of elastic stiffness coefficients in fractured media: numerical modelling

Wenyong Pan*, Kris Innanen, Gary Margrave, Junxiao Li, Xinding Fang and Mike Fehler

ABSTRACT

In the companion paper, we give the analytic expressions of the 3D scattering patterns (3D Fréchet derivative) due to the perturbations of different elastic constants. And in this paper, we perform several 2D numerical examples to verify and understand the analytic scattering patterns. Firstly, we consider an elastic and isotropic local inclusion embedded in the elastic and isotropic background. The numerical results of the scattering patterns due to the perturbations of elastic constants c_{11} and c_{44} (and Lamé constants λ and μ) are analyzed and compared to the analytic results. Then we consider a transverse isotropic (HTI or VTI) local inclusion embedded in the elastic and isotropic background. We give the numerical results of P-P and P-SV scattering patterns due to the perturbations of c_{11}, c_{13}, c_{33} and c_{44} respectively. These numerical results are consistent with the analytic results. The x and z components of the scattering patterns and the inversion sensitivity kernels in acoustic, elastic and anisotropic media (HTI or VTI) are also given for comparison.

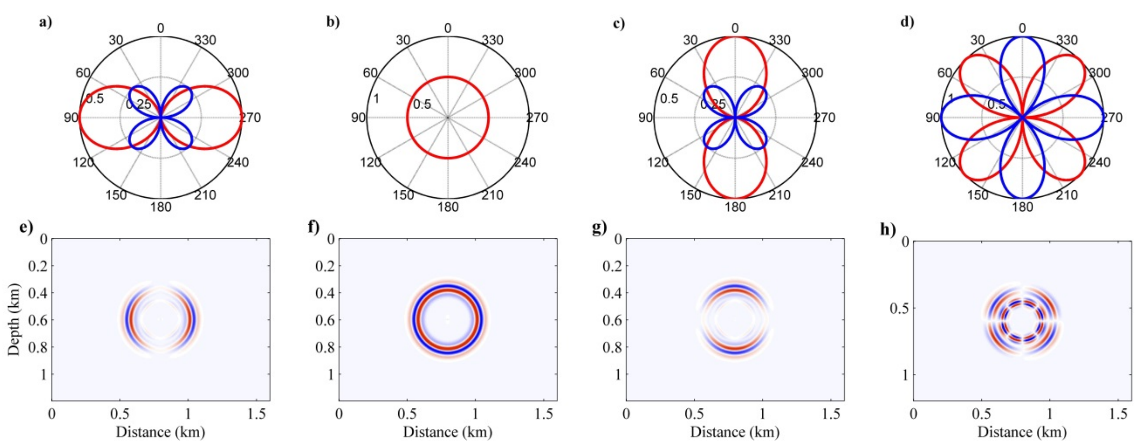

FIG. 1. (a), (b), (c) and (d) show the analytic scattering patterns (x-z plane) due to perturbations of c_{11}, c_{13}, c_{33} and c_{44} in transverse isotropic media respectively. The red lines and blue lines indicate the P-P and P-SV scattering patterns respectively. (e), (f), (g) and (h) show the numerical modelling results of the scattering patterns (x-z plane) due to the perturbations of c_{11}, c_{13}, c_{33} and c_{44}.

New Edge Detection Methods for Seismic Interpretation

Brian Russell*[1] and Claude Ribordy[1]

ABSTRACT

In this article, we will discuss a new set of edge detection methods for seismic interpretation that involve derivatives of the seismic volume in the time, inline and cross-line directions. The methods discussed in this paper were adapted from techniques that were initially applied to potential field data for edge enhancement. These methods are similar to algorithms that have already been proposed for seismic edge detection, which involve spatial differences between traces. However, the difference between these new approaches and the original methods is the way in which the vertical derivative is introduced into the computation. The edge detection methods discussed here are also very similar to coherency and semblance-based methods for seismic discontinuity detection, which in their initial form were based on cross-correlations between traces rather than derivatives. However, we can show that coherency estimates can also be implemented using temporal and spatial instantaneous attributes, which in turn depend on derivatives of the seismic volume and its Hilbert transform in the time, inline and cross-line directions. Since these methods require differentiation and multiplication of two separate seismic volumes the potential for numerical instability is greater.

The methods discussed in this article will be illustrated by a structurally complex seismic volume recorded in the North Sea. Figure 1 shows a comparison of the input data, the coherency result and several of the new methods.

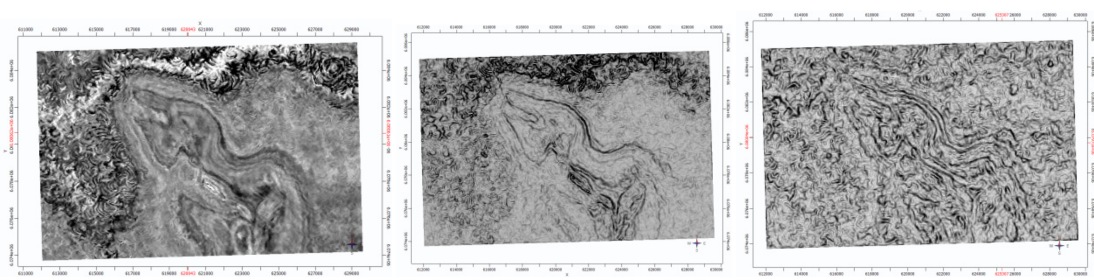

(a) (b) (c)

FIG 1: A summary of the time slices cut at 1300 ms from the North Sea volume, where (a) shows the input seismic data slice, (b) shows the total horizontal derivative filter slice, and (c) shows the total horizontal derivative of the tilt angle filter slice.

[1] Hampson-Russell, A CGG Company, Calgary, Alberta, brian.russell@cgg.com

Pre-stack (AVO) and post-stack inversion of the Hussar low frequency seismic data

A.Nassir Saeed, Gary F. Margrave and Laurence R. Lines

ABSTRACT

Post-stack and pre-stack (AVO) inversion were performed for the Hussar data to study the role of using very low frequencies seismic data and initial background models on seismic inversion. Another objective is to investigate the accuracy of the resulting acoustic and elastic properties from the inversion.

Seismic data conditioning applied to the common image gathers has improved the signal to noise ratio considerably, and enhanced angle gathers / stacks. These enhancements have facilitated extraction of source wavelets for different angle stacks. The lengths of the angle-dependant wavelets were chosen to be long enough to ensure consistent matching of source and seismic spectrums at the low-cut end of frequency band limit. The experiments proved that inverting of very low frequency seismic data is feasible and reduces the residual error between measured and inverted attributes.

The inverted elastic attributes managed to discriminate different lithologic layers. The resultant inverted sections resolved the lateral extension of the Glauconitic sand, hard shale of Ostracod, Ellerslie formations and other geological markers very well.

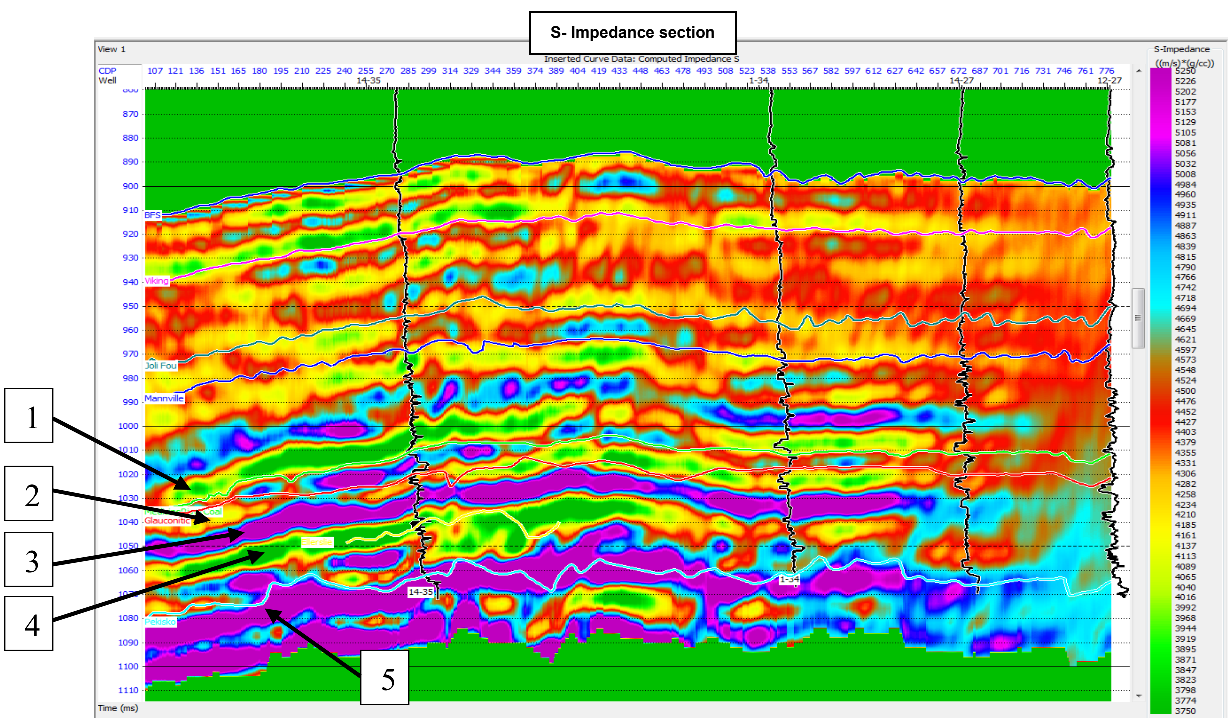

FIG. 1. S-Impedance section from the AVO inversion. (1) Medicine River Coal. (2) Glauconitic sand. (3) Hard shale Ostracod. (4) Ellerslie. (5) Pekisko.

Seismic imaging of the Hussar low frequency seismic data

A.Nassir Saeed, Gary F. Margrave, David C. Henley, J. Helen Isaac and Laurence R. Lines

ABSTRACT

We have implemented an effective seismic processing flow that meets both AVO compliant and seismic imaging objectives for the Hussar low frequency seismic data. The ground roll and pump-jack noise that poses great challenge in seismic processing and imaging of the Hussar low frequency experiments were successfully attenuated and removed via cascaded radial trace filters, while retaining reflection energy of low frequency down to 3Hz.

The resulting migrated section from the new processing shows significant imaging improvement across the entire section, and particularly in the shallow zone (100-500m) that was not clearly seen in previous processing. The zoomed pre-stack migrated sections show more stratigraphic phenomena, such as onlap and pinch-out features that were not clearly shown in the post- stack migrated section. The phase coherency of the estimated band signal show good spatial coherency down to 3Hz in the processed stacked section.

The resulting common image gathers, (CIGs) have shown good reflectivity signal at the far offset of 3450m (an increment of 57%) compared to the 1980m far offset produced by contracting processing company.

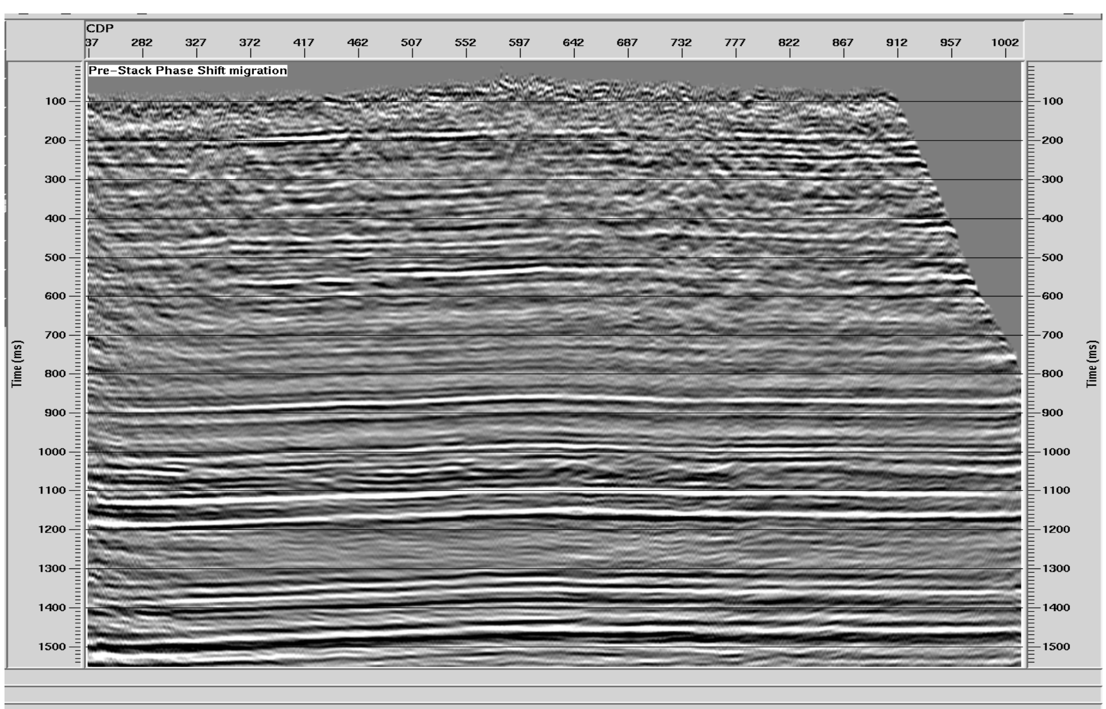

FIG. 1. Pre-stack phase-shift migrated section of the Hussar low frequency experiments recorded with 10Hz geophones and dynamite source.

Geometrical corrections for poststack image focusing velocity analysis

Adrian D. Smith and Robert J. Ferguson

ABSTRACT

Knowing the subsurface velocity structure is crucial to being able to generate accurateImages from geophysical reflection data. For seismic reflection and georadar (GPR) surveys, preliminary velocity information commonly comes from moveout analysis on shot and/or CMP gathers. In cases where we do not have offset information, we can collapse diffractions in the data through migration to obtain velocities. However, there are a number of reflection geometries where the reflection signature appears hyperbolic in shape similar to that of a point diffractor. Collapsing such hyperbolic events gives inaccurate velocity information which may distort the final image. We investigate three geometrical cases where this may occur: circular, hyperbolic, and parabolic. We derive zero-offset traveltime equations for each case, assuming a simple homogeneous media between the surface and a reflector. Generating a set of randomly distributed diffractors over a range of depths and medium velocities at georadar scale, we use a grid-search method to determine the best fitting parameters for each of the geometric cases. We find that in all three cases, observed diffractor velocities are always higher than the "true" medium velocities, and in the circular and hyperbolic cases we are able to estimate a crude velocity factor relying only on an estimate of one scale parameter. We apply a velocity correction to a georadar dataset with circular culverts, and show that it gives a more accurate final image than using just a diffractor velocity.

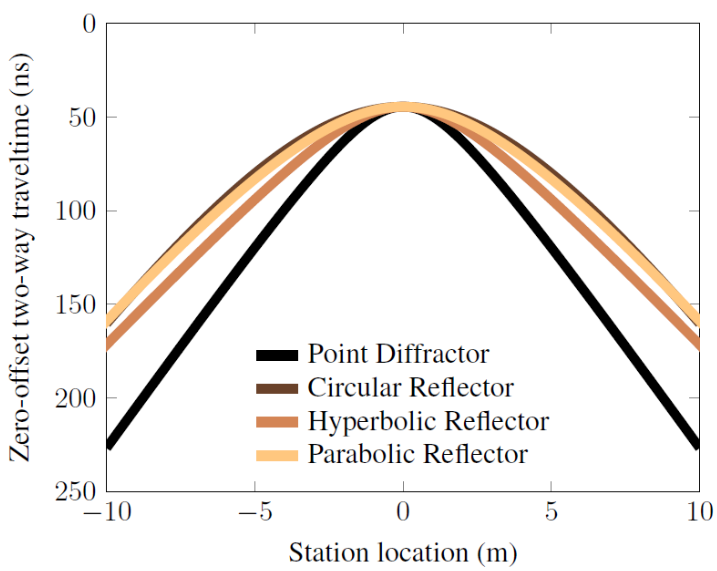

FIG. 1. Illustration of two-way georadar traveltimes from zero-offset reflections for four different geometric cases. Spatially, the point diffractor is co-located with the apexes of each geometric curve. The homogeneous medium velocity above the reflectors if $0.3c$, where c is the speed of electromagnetic radiation in a vacuum.

Georadar processing and imaging with Gabor deconvolution - Houston Coastal Center

Adrian D. Smith and Robert J. Ferguson

ABSTRACT

A 2D line from a georadar (GPR) dataset was collected at the Houston Coastal Center in 2012, aiming to image a series of culverts underneath a road bridge. We processed the dataset using a Gabor deconvolution workflow instead of traditional processing methods. We find that Gabor deconvolution is able to correct for attenuation and greatly improve resolution and signal bandwidth at late arrival times. Diffractor imaging velocities were estimated by hyperbola fitting and the dataset was imaged using zero-offset Gazdag migration to collapse the hyperbolic events of the section. We then used shot record Gazdag PSDM to improve the image. Since we are dealing with circular reflector geometry that is not a point diffractor, we apply a correction factor to the diffractor velocity to obtain a more accurate result. Certain features are visible in the deconvolved section, including the steeply dipping flanks of the edge of the bridge. In the future we hope to extend our velocity model to take into account lateral velocity variations as well to refine the velocities deeper in the subsurface.

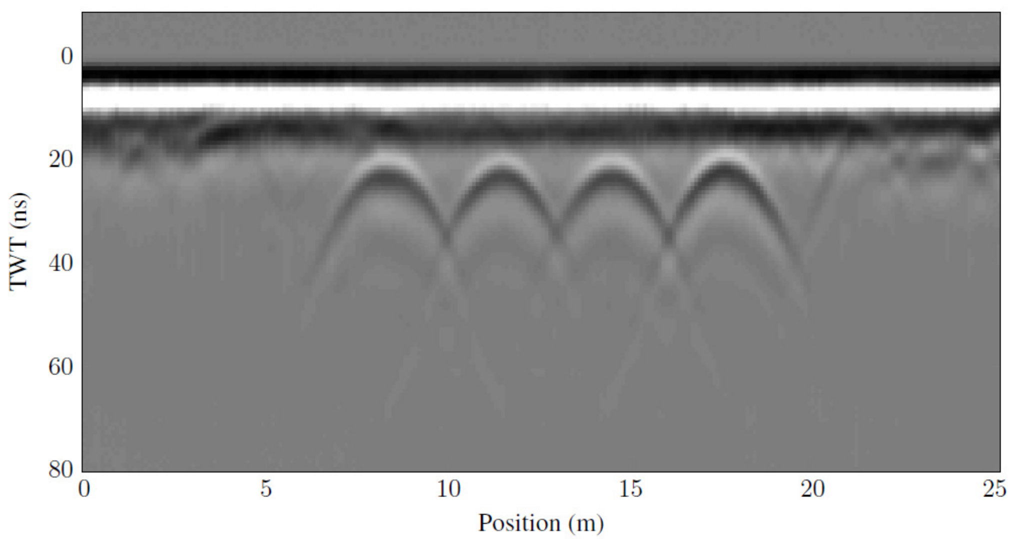

FIG. 1. Raw georadar record from the Houston Coastal Center. The four hyperbolic-shaped events originate from culverts buried beneath a bridge.

Minimum-phase signal calculation using the real cepstrum

Adrian D. Smith and Robert J. Ferguson

ABSTRACT

The concept of minimum phase in geophysics is an important one, especially for processes such as statistical deconvolution which assume the condition in the source wavelet. We wish to have an alternative method to the Hilbert transform to convert a signal of arbitrary phase to its minimum-phase equivalent, while retaining the same amplitude spectrum. We implement a minimum-phase reconstruction based on the real cepstrum developed for finite-impulse response (FIR) filters by treating the signal as a filter. We demonstrate that the algorithm is able to handle signals with ill-conditioned amplitude spectra and still give minimum-phase outputs through analysis of pole-zero plots, along with a simple deconvolution test. We also introduce two metrics: the Pole-Zero Ratio (PZR) and Pole-Zero Distance (PZD) as potential quantitative descriptions of how close a signal is to being minimum phase.

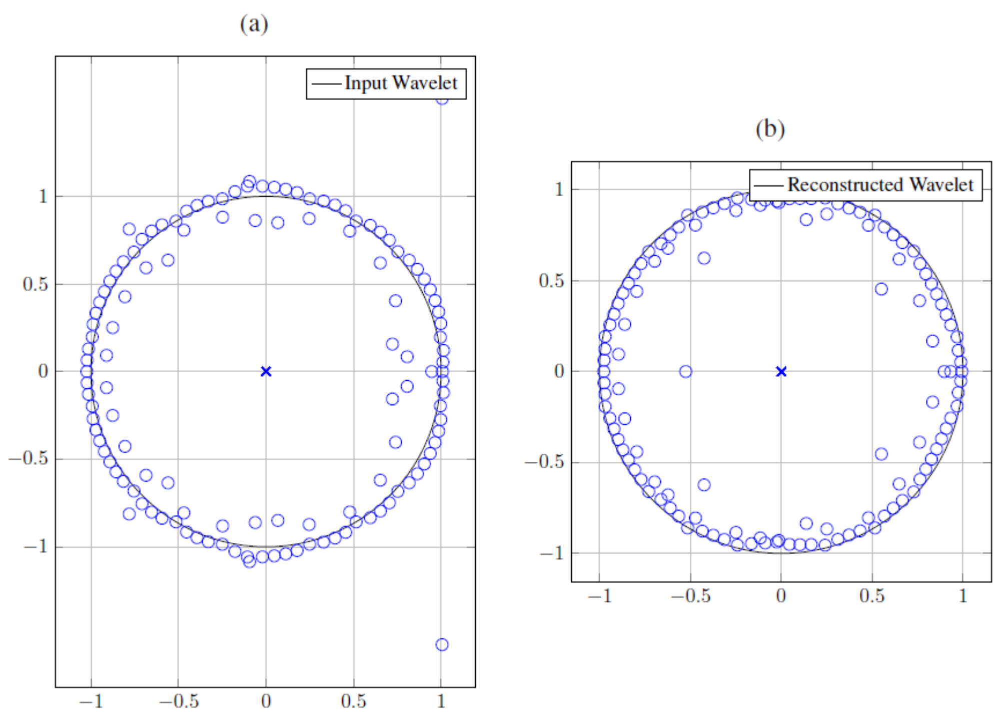

FIG. 1. Case D: Pole-zero plots showing location of poles and zeroes of signals. Poles are denoted by x's and zeros by o's. (a) Input signal. (b) Minimum phase reconstruction using the minrceps algorithm described in this report.

Subsurface imaging using reflected ground roll

Robert R. Stewart*[12] and Craig Hyslop[2]

ABSTRACT

Reflection of surface waves from lateral changes can be used to produce subsurface images. Surface waves that reflect or backscatter from lateral heterogeneities provide information about the location, depth, and the amount of subsurface variation. We first confirm the validity of forward modeling reflectivity from surface-wave phase-velocities by comparing it with a known method of determining reflectivity from shear-wave velocities. The forward model forms the basis for our method of extracting reflectivity. We use VSP-type processing as well as the undoing of dispersive effects to uncover the reflected wave. Deconvolution of the reflected wave results in reflectivity which characterizes the properties of the reflector. Mapping the corresponding wavelengths for the amplitude spectrum of reflectivity for all traces creates a lateral-reflectivity image as function of depth. The lateral-reflectivity image properly locates and determines depth to buried faults for two synthetic examples. In addition, the reflectivity image processed from the Hockley Fault system near Houston, Texas correctly highlights a major fault (Figure 1). With the correctly determined amount of change across a particular lateral location, as defined by reflectivity, an iterative inversion scheme can be used to update the surface-wave phase-velocity model. Iterative inversion improves lateral resolution of the phase-velocity model and resultant shear-wave velocity models for both synthetic and field data.

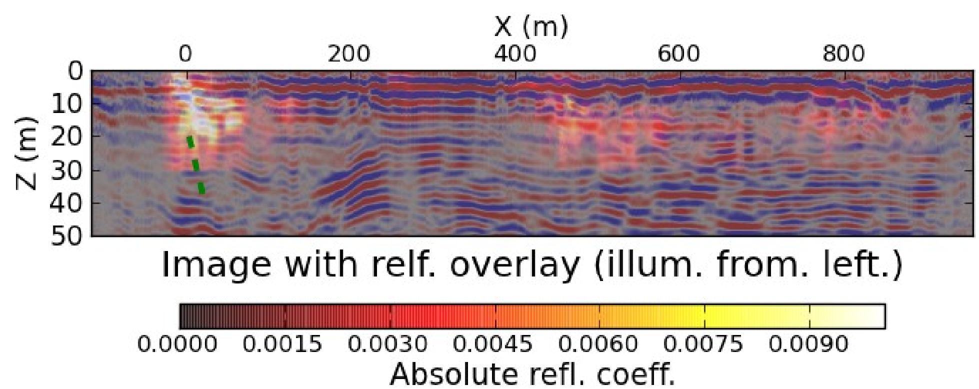

FIG 1. Seismic reflection section from the Hockley Fault System near Houston, Texas. The color overlay indicated the reflected ground roll amplitude.

[1] University of Calgary
[2] Universty of Houston

1.5D Internal multiple prediction in the plane wave domain

Jian Sun* and Kris Innanen

ABSTRACT

The inverse scattering series internal multiple attenuation algorithm was developed by Weglein and collaborators in the 1990s, based on the fact that internal multiples could be constructed from subevents satisfying the lower-higher-lower relationship in the pseudo-depth domain. Innanen (2012) implemented a 1.5D version of the algorithm in MATLAB and complemented the 1D version of the algorithm studied by Hernandez and Innanen (2012).

We present a 1.5D MATLAB implementation of this algorithm in plane wave domain, as initially formulated by Coates and Weglein (1996) and analyzed by Nita and Weglein (2009). Compared to the application in the wavenumber-pseudo depth domain, we generate improved numerical accuracy and reduced Fourier artifacts from internal multiple prediction in the plane wave domain. Furthermore, the procedure for generating the input data is greatly simplified. We believe the plane wave domain is a promising way of posing full 2D versions of the algorithm.

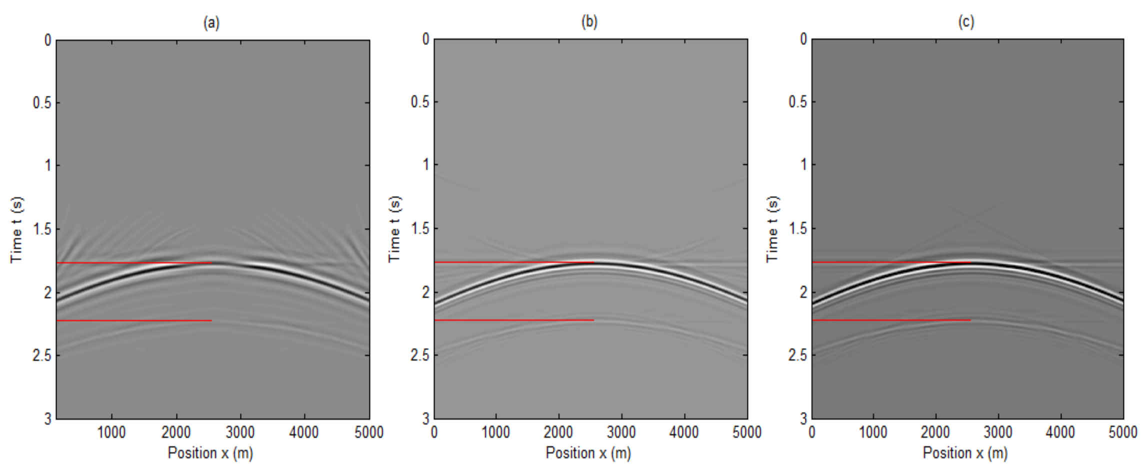

FIG. The internal multiple predictions are generated using the inverse scattering series internal multiple prediction algorithm in different domains. (a) The result is predicted using the algorithm in wavenumber-pseudo depth domain (Innanen, 2012). (b) The prediction is generated using the algorithm in horizontal slowness- pseudo depth domain. (c) The outcome is created using the algorithm in plane wave domain.

A review of converted wave AVO analysis

Jian Sun and Kris Innanen

ABSTRACT

The AVO analysis of converted wave developed rapidly since multi-component seismic data was introduced to industry. PP-PS simultaneous AVO analysis and inversion may improve estimation of rock properties by combining extracted attributes to yield fractional contrasts in P-wave and S-wave velocities and density, and discriminate between reservoir and non-productive lithology. In this paper, we review many of the milestones in the development of converted wave AVO methodology and classify those approximations of P-SV wave reflection coefficient in the light of the way of derivation and their characteristics. Although this paper covers the critical formulae and the most current technologies in AVO analysis of converted wave, it is not intended to be exhaustive.

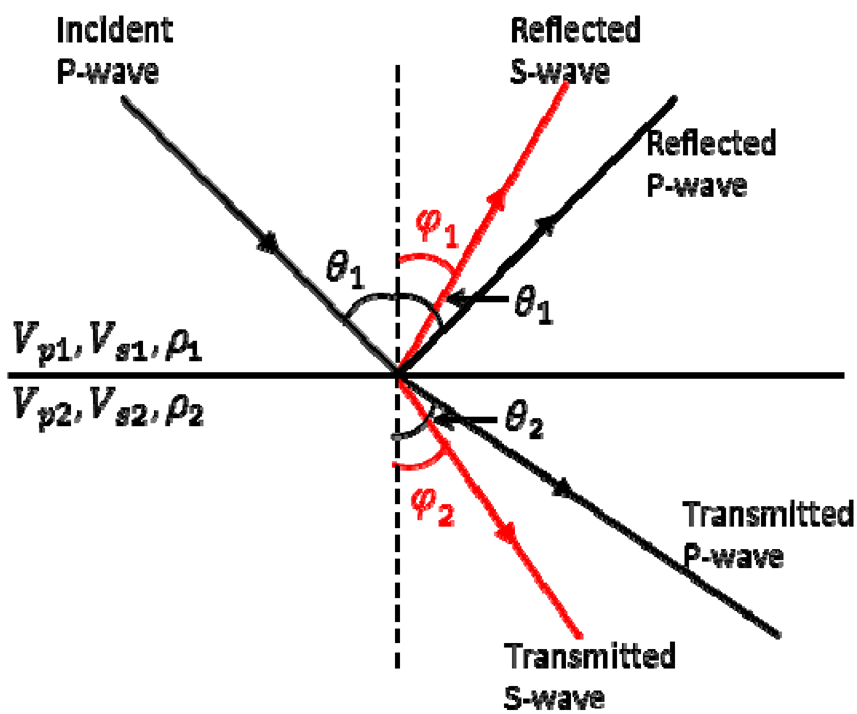

FIG. 1. Reflections and transmissions between two elastic media for an incident P-wave

Automatic first-arrival time-picking on large seismic datasets

Joe Wong

ABSTRACT

Fast, automatic procedures are required for picking first-arrival times in high-resolution 3D datasets with more than 10^8 seismograms. I present a procedure based on a modified energy ratio (MER) attribute that is effective for identifying the first-break times of arrivals with signal-to-noise ratios greater than 3. For arrivals with lower SNR values, the procedure exploits spatial coherence and trace semblance on common-source gathers to obtain reasonably reliable picked times. Running median filters are effective in removing outlier picked times. The report shows examples of first-arrival picking on common source gathers from a 3D survey.

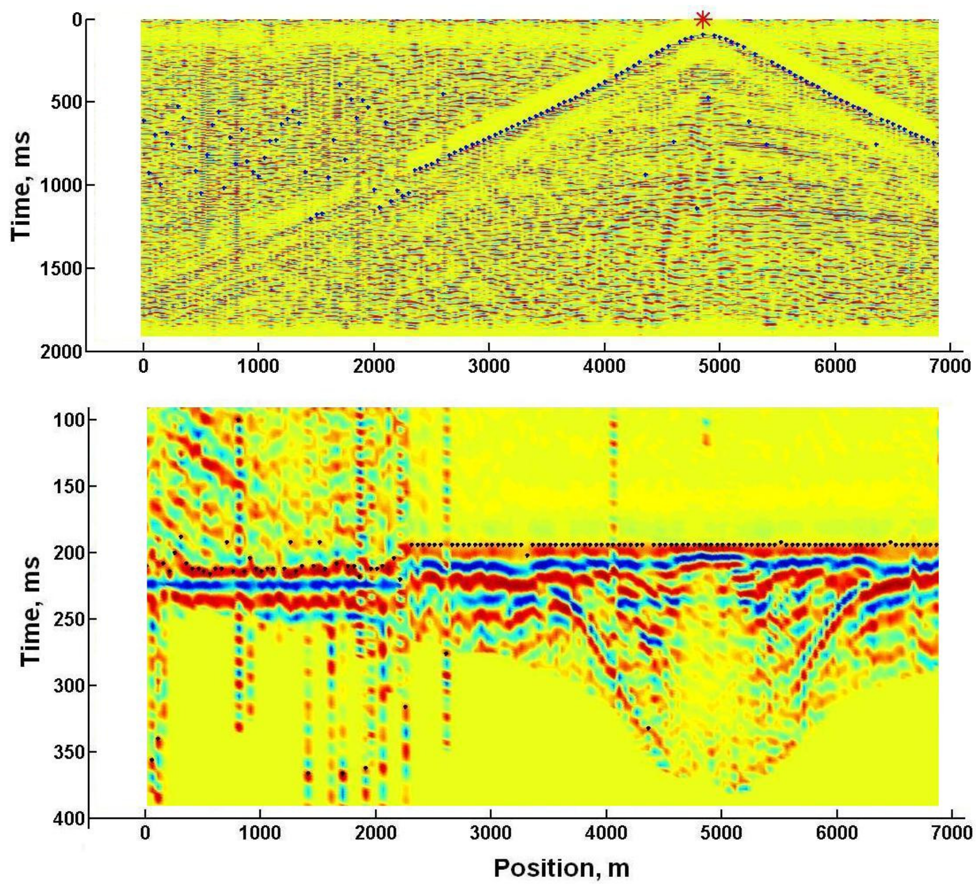

FIG. 1. Top: Common-source gather with initial first-arrival time picks displayed as small blue crosses. Between 0m and 2250m, the traces have low SNR, and first-arrival picks based only on the MER attribute are highly variable. Bottom: seismograms aligned according to improved first-arrival picks from a procedure that uses MER attributes with spatial coherence of arrival peaks and troughs. The alignment time is arbitrary, and the time shift near 2250m has been retained to emphasize its presence in the original seismograms.

Field testing of multiple simultaneous vibrator sources controlled by filtered m-sequences

Joe Wong* and David Langton

ABSTRACT

Theoretical analyses and numerical simulations predict that shifted m-sequences are suitable quasi-orthogonal pilot signals for driving multiple land vibrators in high-efficiency simultaneous source acquisition.

We conducted field tests that provided experimental confirmation for the theoretical predictions. Shifted m-sequences modified by a realizable time-domain filter were used successfully to control hydraulically-powered land vibrators. In one filed test, blended raw field data recorded with two vibrators driven simultaneously by two quasi-orthogonal filtered m-sequences were easily separated by crosscorrelation into individual common source gathers with little crosstalk.

However, in a second test involving four simultaneous vibrators driven by four quasi-orthogonal filtered m-sequences, the separation of blended raw data by crosscorrelation into ordinary common source gathers resulted in a high level of crosstalk. The crosstalk comes from strong surface-wave arrivals generated by adjacent and nearby vibrators.

Numerical simulations indicate that the performance of filtered m-sequence pilots used in simultaneous multi-sourcing is improved if the filtering process does not alter very much the spectra of the original pure m-sequences in the frequency range of 0 to 250Hz. For such cases, the ability to isolate very weak signals from very strong signals without crosstalk interference is retained.

A useful figure of merit for a quasi-orthogonal set is the ratio (expressed in decibels) of the maximum absolute value of the crosscorrelations to the autocorrelation peaks. Any set of filtered m-sequence pilots with a figure of merit less than -65dB would be suitable for simultaneous multi-sourcing.

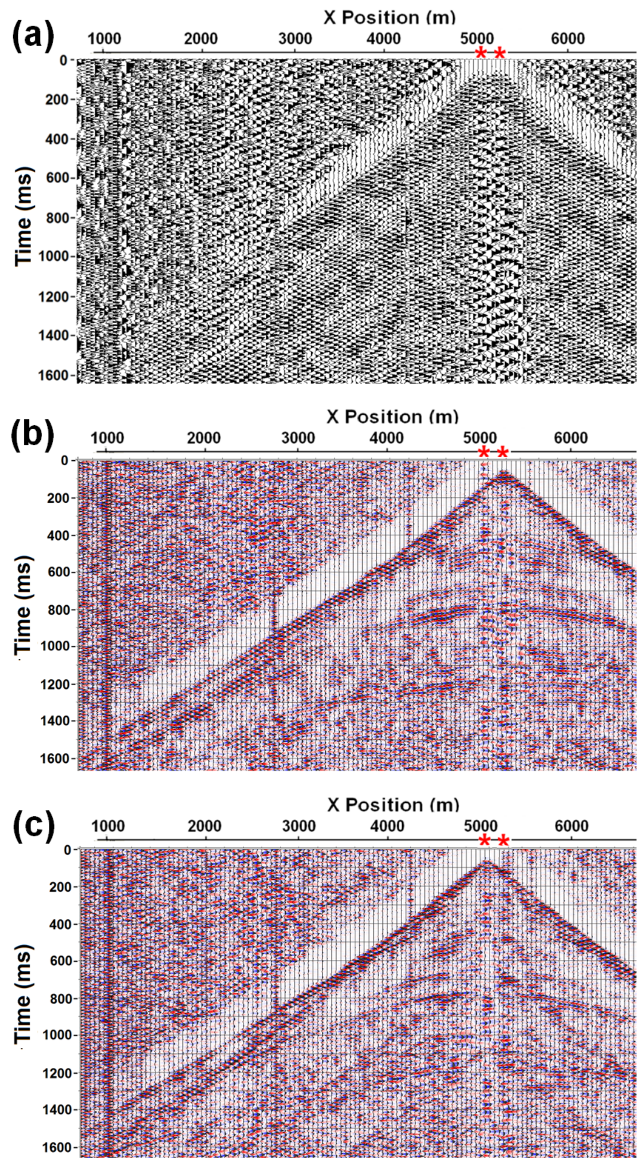

FIG. 1. Field data generated by two vibrators V1 (right red star) and V2 (left red star) controlled by two quasi-orthogonal filtered m-sequence pilots and operating simultaneously; a) Blended raw data; (b) and (c) deblended common source seismograms associated with vibrators V1 and V2, respectively..

Physically-modeled 3D marine survey over HTI targets

Joe Wong

ABSTRACT

Using the University of Calgary Seismic Physical modeling Facility with a scale factor of 10^4, we conducted a high-resolution 3D marine survey over layered media containing HTI targets overlying a water-filled channel. The survey covered a scaled-up area of about 6000m by 6000m. Sources were placed on a rectangular grid with $\Delta X = \Delta Y = 100$m. Receivers were placed on a rectangular grid with ΔX and $\Delta Y = 50$m. Source and receiver lines both were aligned in the Y direction. The minimum separation between source and receiver lines was 100m. The data were digitized with 2ms sampling and 14-bit precision. Seismograms with length of 2000ms were recorded with vertical stacking of 200 repeated waveforms and stored in SEG-Y files. To reduce survey time, acquisition was conducted using eight simultaneous sources. The resulting supergathers of seismic traces must be deblended or separated into ordinary common source gathers before further post-survey processing and imaging.

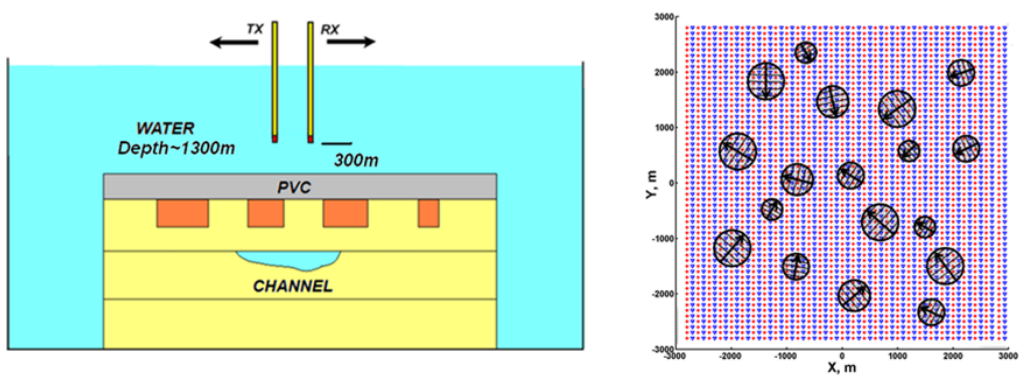

FIG. 1. Schematic side and top views of the marine 3D survey over the model. The HTI cylinders or "pucks" are shown in light-brown. The yellow material is Plexiglas (PLX).

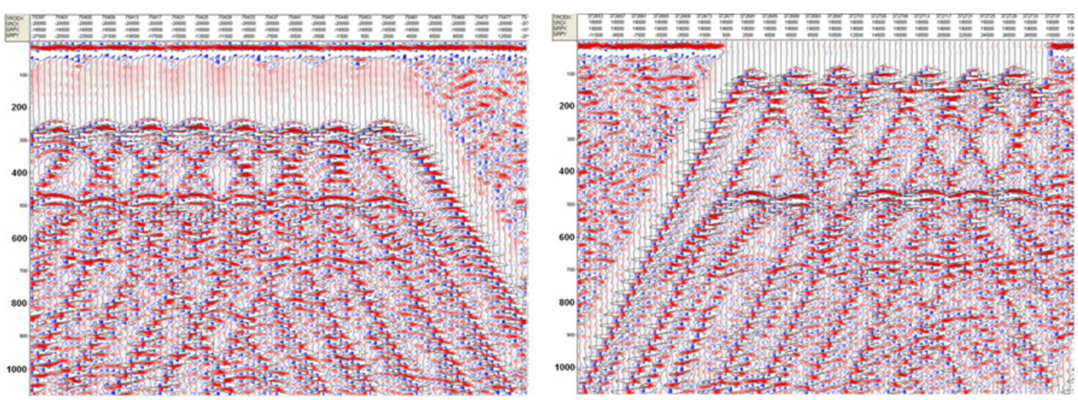

FIG. 2. Two examples of supergathers from the 3D marine survey. Traces are separated by ΔY=50m. Separation of source line from receiver line = 350m (left) and 100m (right). The apexes of the hyperbolas give the Y coordinates of the simultaneous sources.

Analysis of multicomponent walkaway vertical seismic profile data

Bona Wu*, Don C. Lawton and Kevin W. Hall

ABSTRACT

A multicomponent walkaway VSP data processed to for PP and PS imaging as well to study the AVO response. To date, a PP wave corridor stack and VSP-CDP mapping have been completed and are correlated to synthetic seismograms (Figure 1). Overall, we see a good correlation between VSP and synthetic data, and observed changes inside the reservoir, interpreted to be due to production. A common shot stack reflectivity gather was produced for AVO analysis. At the top and bottom of target reservoir, the AVO responses of VSP PP wave data and synthetic gathers show similar trends (Figure 2). The results give us promise for inverting walkaway VSP data for reservoir properties.

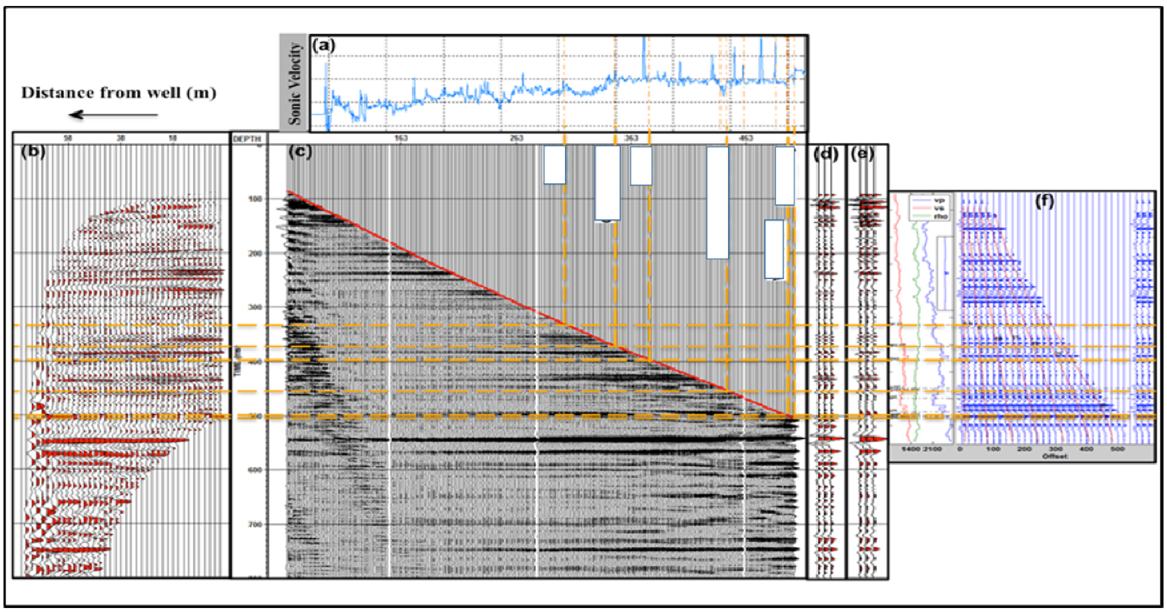

FIG.1 Composite plot of sonic log, VSP data and synthetic seismogram. (a) sonic log, (b) VSP-CDP mapping of far-offset VSP data, (c) upgoing P wave gather of zero-offset VSP, (d) corridor stack, (e) non-corridor stack, (f) synthetic offset gather and stack.

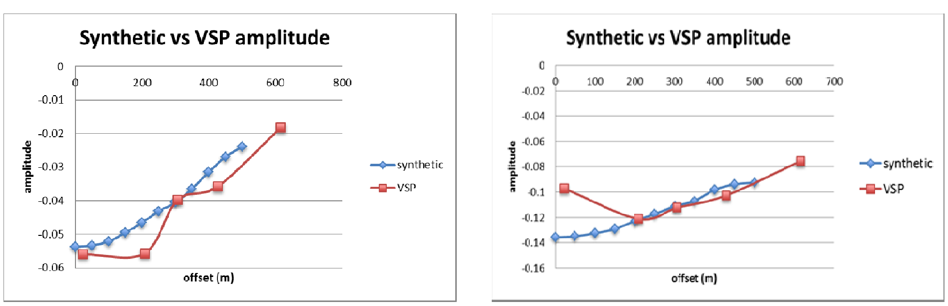

FIG.2 Comparison of AVO responses. Left, amplitude response of top reservoir; Right, amplitude response of base reservoir.

Tikhonov regularization of instantaneous frequency attribute computations

Matt Yedlin[1], Gary F. Margrave[2], Daryl Van Vorst[1] and Yochai Ben Horin[3]

ABSTRACT

We present a brief review of the concept of instantaneous frequency, obtained by differentiating the instantaneous phase, computed using the Hilbert Transform. This computation is recast as a Tikhonov regularized linear inverse problem and is compared with the alternative Fomel smoothing regularization . Both smoothing methods, and an equivalent frequency measure obtained via the normalized first moment of the spectrum of the Gabor Transform are applied to synthetic data, an earthquake and a quarry blast. From analysis, a new measure, the local frequency, emerges. The local frequency concept arises directly from the smoothing apparent in all the three algorithms utilized.

Local Frequency Comparison for a Gulf of Suez Earthquake

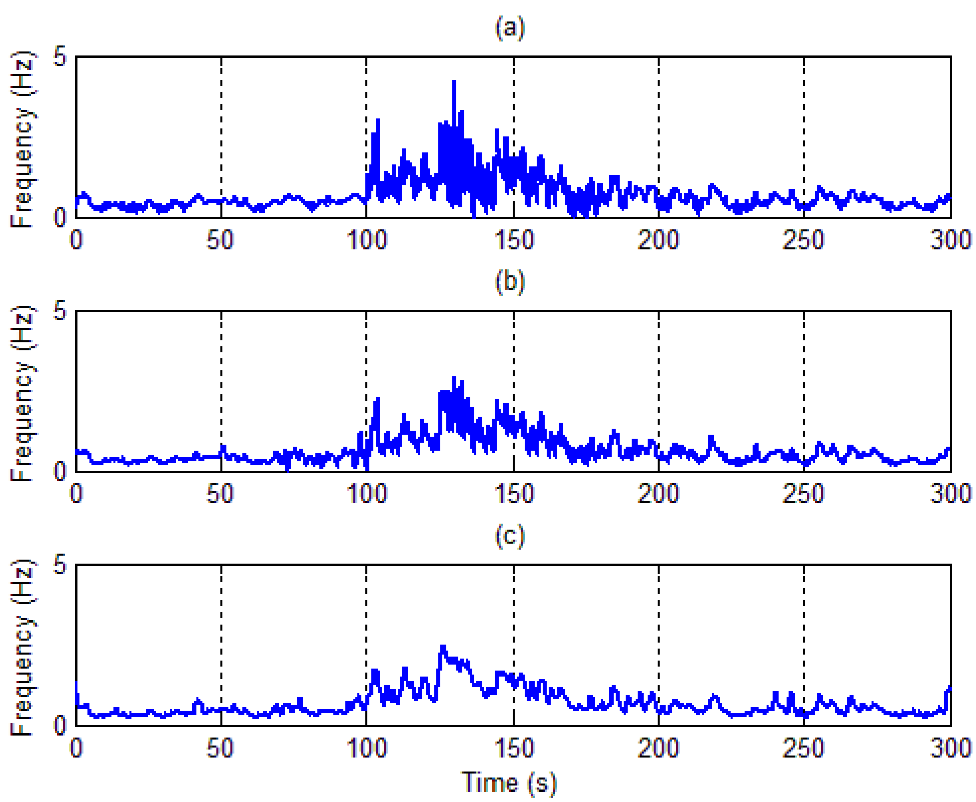

a) Local frequency computed using Tikhonov regularization. b) Local frequency computed using Fomel smoothing. c) Local frequency computed using Gabor transform first moment.

[1] Department of Electrical and Computer Engineering, UBC
[2] Geoscience, University of Calgary
[3] SOREQ, Yavneh, Israel